ISSN 0915-6364

NATIONAL INSTITUTE FOR FUSION SCIENCE

Cross Section Database for Carbon Atoms and Ions: Electron-impact Ionization, Excitation, and Charge Exchange in Collisions with Hydrogen Atoms

H. Suno and T. Kato

(Received - Jan. 21, 2005)

NIFS-DATA-91 Feb. 2004

RESEARCH REPORT
NIFS-DATA Series

TOKI, JAPAN

Cross Section Database for Carbon Atoms and Ions: Electron-impact Ionization, Excitation, and Charge Exchange in Collisions with Hydrogen Atoms

Hiroya Suno and Takako Kato

National Institute for Fusion Science, Toki, Gifu 509-5292, Japan

(Dated: February 1, 2005)

Abstract

A database have been constructed for the recommended cross sections on electron-impact excitation and ionization of carbon atoms and ions C, C^{+}-C^{5+} , as well as charge-exchange processes between carbon ions C^{+}-C^{6+} and hydrogen atoms. We have collected a large amount of theoretical and experimental cross section data from the litterature, and have critically assessed their accuracy. The recommended cross sections, the best values for use, are expressed in a form of simple analytical functions. These are also presented in graphical form.

Keywords: Electron-impact excitation, electron-impact ionization, charge exchange

I. INTRODUCTION

The interactions among electrons, ions and hydrogen atoms are the most important processes which occur in laboratory and astrophysical plasmas. The understanding of these collision processes is essential for diagnosing and modeling plasmas in controlled fusion experiments, plasmas processing, and astrophysics. In addition to the application of studying plasma dynamics, collision processes such as electron-impact excitation, ionization, and charge transfer processes are interesting from the view of fundamental physics, like many-body collision dynamics.

In this paper, we shall be interested in carbon atoms and ions C^{n+} $(n = 0 - 6)$. The carbon atoms and ions are abundant in various astrophysical environments, fusion reactors, and plasma-chemistry atmospheres. We treat electron-impact excitation and ionization of these atoms and ions, as well as charge transfer processes in collisions between carbon ions and hydrogen atoms. Therefore, we have collected the data for cross sections from the litterature and have critically assessed their accuracy to obtain the recommended data. The recommended data have been fitted to simple analytical fit functions. For electron-impact excitation processes, rate coefficients have also been derived. The fit coefficients are presented in Tables. The values derived from fitted functions are presented as the recommended data in Graphs, together with the original data from the litterature. We have taken into account the important transitions for excitation, ionization and charge transfer processes. For these data and the processes which are not shown in this paper, the original data can be found at NIFS Database webpage `http://dbshino.nifs.ac.jp`, AMDIS for excitation and ionization, and CHART for charge transfer.

This Report is organized as follows. In Sec. II, we deal with electron-impact excitation of C^{n+} $(n = 0 - 5)$ atoms and ions. Electron-impact ionization processes of these atoms and ions are treated in Sec. III. The double-ionization of C^+ is also presented. In Sec. IV, charge exchange cross sections between carbon ions C^{n+} $(n = 1 - 6)$ and hydrogen atoms are presented. State-selective cross sections are also taken into account. A brief summary of the work is given in Sec. V.

II. ELECTRON-IMPACT EXCITATION OF CARBON IONS AND ATOMS

There exist numerous theoretical cross section data for electron-impact excitation of carbon ions. Previously, Itikawa et al. [1] compiled cross sections reported until 1985 for carbon ions (C^+-C^{5+}) as well as oxygen ions (O^+-O^{12+}), critically evaluated the data, and fitted the recommended values to analytical formulae. Before 1985, cross sections were calculated by the distorted-wave method, Coulomb-Born approximation, Coulomb-Born Oppenheimer method, and close-coupling method. These are reported for various excitation processes of all ions C^+-C^{5+} in Los Alamos Scientific Report (1977) [2–5]. McDowell et al. [6] had calculated electron-impact excitation cross sections for C^{5+} and C^{4+} ions using the distorted-wave method. Close-coupling calculations had been carried out for C^{4+} by Foster et al. [7]. Berrington et al. [8, 9] had reported cross sections calculated by the R-matrix method. In the following, we have compiled cross section and rate coefficient data for electron-impact excitation of carbon atoms and ions reported after 1985 and have given the recommended data. These recommended data are fitted to analytical functions. The references for the data which we adopted as recommended data are shown in Tables I-VI.

For C^{5+}, Aggarwal and Kingston [10] have reported their R-matrix calculations of cross sections (collision strengths) and rate coefficients (effective collision strengths) for numerous excitation processes up to $n = 5$, where n is the principal quantum number. The energy region of their calculations is below 50 Ryd. All of their data can be found in the NIFS AMDIS Database. Zou and Shirai [11] have calculated cross sections for the 1s→2s and 1s→2p processes using the close-coupling method with exchange 3-levels, while Fisher et al. [12] have carried out cross section calculations using the convergent close-coupling method for the same transitions. Callaway et al. [13] have reported rate coefficient data calculated by the close-coupling method for 1s→2s and 1s→2p excitation processes.

For C^{4+} ion, Badnell [14] have reported cross section calculations using the distorted-wave method for several excitation processes among $n = 1$ and $n = 2$ states, where n indicates the principal quantum number of the most excited electron in the initial and final electonic configurations. Cross section calculations have been carried out also with a combination of the distorted-wave method with exchange and the configuration interaction method by Srivastava et al. [15] for the $1s^2\ ^1S$→$1s2s\ ^1S$ and $1s^2\ ^1S$→$1s2p\ ^1P$ excitations. Kato and Nakazaki [16] evaluated the data for excitation of He-like ions.

For C^{3+}, experimental cross sections measured by Bannister et al. [17], Greenwood et al. [18], and Janzen et al. [19] were reported for the 2s ^{2}S→2p ^{2}P excitation. Burke [20] and Griffin et al. [21] calculated rate coefficients by using the close-coupling method and the R-matrix method, respectively for several transitions among $n = 1$ to $n = 4$ states.

For C^{2+}, Berrington et al. [22] reported cross sections calculated by the R-matrix method for several excitation processes among $n = 2$ and $n = 3$ states. Itikawa and Sakimoto [23] calculated cross sections by using the distorted-wave method for the $2s^2$ ^{1}S→2s2p ^{3}P and $2s^2$ ^{1}S→2s2p ^{1}P transitions. Rate coefficients were calculated using the R-matrix method by Berrington et al. [24] for transitions among $n = 2$ and $n = 3$ states.

Unfortunately, we found no new theoretical cross section data published for C^+ since 1985. However, Blum and Pradhan [25] calculated rate coefficients for fine structure transitions among $n = 2$ and $n = 3$ configurations. Experimental measurement by Williams et al. [26] have been reported for the $2s^22p$ ^{2}P→$2s2p^2$ ^{4}P process.

For the C atom, Dunseath et al. [27] reported cross sections calculated by the R-matrix method for a large number of excitation processes among $n = 2$ and $n = 3$ states. All of their numerical data can be found on the NIFS AMDIS Database. Cross sections calculated using the close-coupling methode were reported by Henry et al. [28] for the $2s^22p^2$ ^{3}P→$2s^22p^2$ ^{1}D and $2s^22p^2$ ^{3}P→$2s^22p^2$ ^{1}S excitation processes. Pindzola et al. [29] calculated cross sections by using the distorted-wave method with exchange for the $2s^22p^2$ ^{3}P→$2s^22p^2$ ^{1}D process. Thomas et al. [30] reported their matrix variational calculations for the $2s^22p^2$ ^{3}P→$2s^22p^2$ ^{1}S and $2s^22p^2$ ^{1}D→$2s^22p^2$ ^{1}S transitions.

In general, electron-impact excitation cross sections calculated by different theoretical method do not agree well, especially for optically forbidden transitions. Our recommended cross sections are chosen following the criterions: the close-coupling method and R-matrix method can lead to more reliable results at lower collision energies, so can the distorted-wave method and Coulomb-Born method at high energies. Experimental measurements are considered as more reliable than theoretical calculations. For certain transitions we have not find any new cross section data published since Ref. [1]. In such cases, we only used the fitted formula given in Ref. [1].

In this paper, we fit the collision strength Ω by a fitting formula. The electron-impact excitation cross sections Q_{if} are related in terms of collision strengths Ω_{if} as follows, where i and f indicate respectively the initial and final states. For the excitation from a state i to

f, the cross section is given by

$$Q_{if}[\pi a_0^2] = \frac{\Omega_{if}}{\omega_i E_e[Ry]} = \frac{1}{\omega_i V_{if}[Ry]} \frac{\Omega_{if}}{X}, \tag{1}$$

where E_e is the energy of the incident electron, ω_i the statistical weight of the initial state, V_{if} the excitation energy, and Ω_{if} the collision strength. Here, the cross section is in units of πa_0^2, where a_0 is the Bohr radius and X is the reduced electron energy defined by

$$X = E_e/V_{if}. \tag{2}$$

When the cross section and energy are given respectively in units of cm^2 and eV, we have

$$Q_{if}[\mathrm{cm}^2] = 1.1969 \times 10^{-15} \times \frac{\Omega_{if}}{\omega_i E_e[eV]} = 1.1969 \times 10^{-15} \times \frac{\Omega_{if}}{\omega_i V_{if}[eV] X}. \tag{3}$$

With the Maxwellian distribution of electron velocity for temperature T_e, the rate coefficient is calculated by

$$R_{if}[\mathrm{cm}^3\mathrm{s}^{-1}] = \frac{8.010 \times 10^{-8}}{\omega_i \sqrt{T_e[eV]}} y \int_1^\infty dX \Omega_{if}(X) e^{-yX}, \tag{4}$$

where

$$y = V_{if}/T_e. \tag{5}$$

We have carefully chosen the reliable data from the references. Once the recommended values of cross sections were determined, a fit was made in terms of collision strengths, which facilitates more the fit procedure than the cross section because of their energy dependence. Two types of formulae have been used for the fit procedures. The formula of Type 1 is defined by

$$\Omega_{if}(X) = A + \frac{B}{X} + \frac{C}{X^2} + \frac{D}{X^3} + E \ln X, \tag{6}$$

whereas for Type 2 we have

$$\Omega_{if}(X) = \frac{A}{X^2} + Be^{-FX} + Ce^{-2FX} + De^{-3FX} + Ee^{-4FX}. \tag{7}$$

Here, A, B, C, D, E and F are adjustable coefficients. Note that, for Type 1, we have $E = 0$ in the case of a optically forbidden transition. For optically allowed transitions, we can drop the term D/X^3 in Eq. (7) since the remaining four terms are sufficient to fit the electron-impact excitation cross sections. With the use of these formulae, the rate coefficients can be calculated in the form:

$$R[\mathrm{cm}^3\mathrm{s}^{-1}] = \frac{8.010 \times 10^{-8}}{\omega_i \sqrt{T_e[eV]}} e^{-y} \gamma. \tag{8}$$

Here, γ is the effective collision strength and is defined by

$$\gamma = ye^y \int_1^\infty \Omega_{if} e^{-yX} dX. \tag{9}$$

We have

$$\gamma = y\left\{\left(\frac{A}{y}+C\right)+\frac{D}{2}(1-y)+e^y E_1(y)\left(B-Cy+\frac{D}{2}y^2+\frac{E}{y}\right)\right\} \tag{10}$$

for Type 1 and by

$$\gamma = Ay\{1-e^y E_1(y)y\}+\left(\frac{Be^{-F}}{F+y}+\frac{Ce^{-2F}}{2F+y}+\frac{De^{-3F}}{3F+y}+\frac{Ee^{-4F}}{4F+y}\right)y \tag{11}$$

for Type 2, with

$$E_1(y) = \int_y^\infty \frac{e^{-t}}{t} dt. \tag{12}$$

Most of the cases, the cross section (or collision strength) data are fitted by using the formula in Eq. (6). If Eq. (6) is not good to fit the collision strength, we use Eq. (7). If both of these formulae fail to fit and rate coefficient data are available, we use Eq. (10) or Eq. (11).

When the resonant effects are included in the data and their effects are large, we devide the collision strength into two parts,

$$\Omega = \Omega_{NR}(X) \quad \text{for } X > X_1 \tag{13}$$

$$\Omega_R(X) \quad \text{for } 1 \le X \le X_1, \tag{14}$$

where Ω_R and Ω_{NR} indicate the collision strengths with and without resonance effects, respectively. The reduced energy X_1 defines the boundary of the region where the resonance effects dominate. Note that $\Omega_R(X_1)$ is not necessarily equal to $\Omega_{NR}(X_1)$. Since Ω_R has a complicated structure as a function of X, it is almost impossible to fit it to any simple formula. Instead, we assume the collision strentgh in the following

$$\Omega_R(X) = PX + Q \quad \text{for } 1 \le X \le X_1. \tag{15}$$

The quantities P, Q, and X_1 are determined as fit parameters by equating the rate coefficients calculated with the use of Eqs. (14) and (15) to the rate coefficients given in the litterature.

The values of fit parameters A, B, C, D, E and F for each excitation process are given in Tables I-VI, together with the excitation energies, the references of the adopted data, and

the rms percent error (for the definition, see below). When resonance effects are included, the parameters P, Q, and X_1 are also tabulated for $\Omega_R(X)$ in Eq. (15).

For most of the excitation processes, the recommended values of collision strengths and rate coefficients, which can be reproduced with the fit parameters, are shown graphically in Fig. 1-124, together with the original data from the litterature. The boundary between the resonance and non-resonance regions is also indicated as a dashed line.

In our work, the quality of the fit function is expressed in terms of the rms percent error, which is defined by

$$\text{rms percent error} = \sqrt{\frac{1}{N}\sum_{i=1}^{N}\left(\frac{\Omega_i^{\text{Fit}} - \Omega_i^{\text{Data}}}{\Omega_i^{\text{Data}}}\right)^2}, \tag{16}$$

where N is the number of data points, Ω_i^{Fit} the fitted collision strengths, and Ω_i^{Data} the collision strengths in the original data. For most of the transitions, the rms percent errors are less than 0.1 and in difficult cases, they are at most 1.46. The rms percent errors are missing for the coefficients that were directly taken from Ref. [1].

III. ELECTRON-IMPACT IONIZATION OF CARBON IONS AND ATOMS

Electron-impact ionization of carbon ions has been extensively studied both experimentally and theoretically. We selected the data considered to be reliable and they are shown in Graphs. 125-137. Experimental measurements of C^{n+} were carried out by Donets and Ovsyamnikov [34] for the ions C^{n+} with $n = 1, 2, 3, 4$ and 5, in the electron energies between 1 and 10 keV.

For electron-impact ionization of the C^{5+} ion, experimental measurements were reported by Aichele et al. [35]. Theoretical cross sections calculated by using a semi-empirical method, the distorted-wave method with exchange, relativistic distorted-wave method, and distorted-wave Born method with exchange, were reported respectively by Pattard and Rost [36], Younger et al. [37], Kao et al. [38], Fang et al. [39]. For C^{5+} as well as the other ions, the experimental data by Donets et al. [34] are larger than the other data.

For C^{4+}, experimental measurements were carried out by Crandall et al. [40]. Theoretical calculations using the binary encounter approximation and distorted-wave Born method with exchange were reported respectively by Salop [41] and Fang et al. [39]. We selected the data by [39] as recommended data.

For C^{3+}, experimental measurements were performed by Knopp et al. [42], Crandall et al. [43]. Theoretical calculations using the distorted-wave method with exchange and R-matrix method were carried out respectively by Jakubowicz and Moores [44] and Knopp et al. [42]. The Coulomb-Born method with exchange was employed by Sampson et al. [45]. Scott et al. [46] and Badnell and Griffin [47] used the R-matrix method with pseudodtates. We have selected the data by [42] as the recommended data. Because of the excitation-autoionization, there are two peaks in the cross section. We fit the cross sections with a sum of two different equations in the form of Eq. (17) (see below for the definition).

For C^{2+}, experimental measurements were reported by Woodruff et al. [48] and Falk et al. [49]. Theoretical calculations using the binary encounter approximation and Coulomb-Born method were carried out by Salop [41] and Moores [50]. Jakubowicz and Moores [44] and Younger [37] reported cross sections calculated by the distorted-wave method with exchange and the distorted-wave Born method with exchange respectively. We recommend the data by [48].

For C^{+}, experiments were carried out by Yamada et al. [51]. Qian and Pan [52] reported theoretical results obtained by R-matrix calculations using the single-channel approximation and the 3-state close coupling approximation. For C^{+}, the cross section measurements by Westermann et al. [53] are reported for the double ionization process $C^{+}+e \rightarrow C^{3+}$.

For the C atom, we found the measurements by Brook et al. [54] and the theoretical calculations using the Born approximation by Omidvar et al. [55]. We choose the data by [54] as recommendation.

Most of experimental and theoretical cross sections from different authors agree fairly well with each other. However, the experimental electron-impact ionization cross sections reported by Donets et al. [34] are always larger than the other ones except for C^{3+}. In general, we have chosen the most recent results as the recommended data. The rms percent errors are at most 1.07 (C^{4+}).

The recommended cross section for electron-impact ionization is parametrized by the expression

$$\sigma[\mathrm{cm}^2] = \frac{10^{-13}}{IE}\left\{A_1 \ln(E/I) + \sum_{i=2}^{N} A_i \left(1 - \frac{I}{E}\right)^{i-1}\right\}, \tag{17}$$

where the collision energy E and ionization potential I are expressed in eV units and A_i are fitting coefficients. Note that the coefficient A_1 can be related to the continuum oscillator

strength $df/d\epsilon$ by

$$A_1 = 8.39 \times 10^{-2} I[\text{eV}] \int_0^\infty \frac{1}{E+\epsilon} \frac{df}{d\epsilon} d\epsilon \tag{18}$$

where ϵ is the energy of ejected electrons. However we do not use this equation to derive A_1 value. The values of A_i in Eq. (17) are given in Table VII, together with the ionization enrgy, the references of the adopted data, and the rms percent error. The fitted cross sections are graphically presented as a solid curve from Fig. 125 to Fig. 137.

IV. CHARGE EXCHANGE IN COLLISIONS BETWEEN CARBON IONS AND HYDROGEN ATOMS

There exist numerous theoretical and experimental results for charge exchange processes in collisions of carbon ions with hydrogen atoms. The references for the recommended data are listed in Table VIII for each process. These data are fitted to analytical functions and the fitting parameters are listed in Tables.

The C^{6+}+H collisions are the processes the most extensively studied: state-selective cross sections were calculated by Toshima and Tawara (using the close-coupling method) [56], Belkic et al. (classical distorted-wave method) [57, 58], Ryufuku (unitarized distorted-wave approximation) [59], Olson and Schultz (classical trajectory Monte Carlo method) [60], Green et al. (close-coupling method) [61], Harel et al. (molecular orbital approach) [62], Kazanskii and Komarov (molecular orbital approach) [63], Fritsch and Lin (atomic orbital close-coupling method) [64], Fritsch (atomic orbital method) [65], Kimura and Lin (atomic orbital and molecular orbital methods) [66], Das et al. (classical distorted-wave method) [67]. These authors also obtained the total cross sections for the C^{6+}+H$\rightarrow C^{5+}$+H^+ process. Meaurements of total cross sections were performed by Panov et al. [68]. Janev et al. [69] gave the recommended total charge exchange cross sections.

For the C^{5+}+H collisions, state-selective charge transfer cross sections were calculated using the molecular orbital close-coupling method by Shimakura et al. [70] as shown in Fig. 159. Since their energy region is limited to fit the cross sections, only their data are shown in graphs. Total charge transfer cross sections were calculated by Shimakura et al. (molecular orbital close-coupling method) [70] and Shipsey et al. (perturbed-stationary method and classical trajectory Monte Carlo method) [71]. Experimental measurements of total cross sections were carried out by Goffe et al. [72], Panov et al. [68], and Phaneuf et

al. [73].

For the C^{4+}+H collisions, state-selective charge transfer cross sections were calculated by Errea et al. (using the molecular orbital close-coupling method) [74], Gargaud et al. (molecular orbital approach) [75], and Fritsch and Lin (atomic orbital close-coupling method) [64]. Experimental measurements of state-selective cross sections were carried out by Hoekstra et al. [77]. Total charge transfer cross sections were calculated by Errea et al. [74], Gargaud et al. [75], and Tseng et al. [76]. Experimental measurements of total charge transfer cross sections were performed by Hoesktra et al. [77], Phaneuf et al. [73, 78], Crandall et al. [79], Goffe et al. [72], Dijkkamp et al. [80], and Bliek et al. [81]. Since the structures of the state-selective cross sections are too complicated to fit in a formula, we just show their data in graphs.

For the C^{3+}+H collisions, state-selective charge transfer cross sections were calculated by Opradolce et al.(using the molecular orbital method) [82] and Bienstock et al.(molecular orbital close-coupling method) [83]. Experimental measurements of state-selective cross sections were carried out by Ciric et al. [84] and McCullough et al. [85]. Total charge transfer cross sections were calculated by Errea et al. (using the molecular orbital close-coupling method) [86], Tseng and Lin (atomic orbital close-coupling method) [87], Heil (molecular orbital close-coupling method) [88], and Bienstock et al. (molecular orbital close-coupling method) [83]. Experimental measurements of total charge transfer cross sections were carried out by Phaneuf et al. [73, 78], Goffe et al. [72], Sant'Anna et al. [89], McCullough et al. [85], Ciric et al. [84].

For C^{2+}+H collisions, total charge transfer cross sections were calculated by Gu et al. (using the classical trajectory Monte Carlo method) [90], Errea et al.(molecular orbital close-coupling method) [91]. Experimental measurements of total charge transfer cross sections were carried out by Goffe et al. [72], Nutt et al. [92], Phaneuf et al. [78], and Gardner et al. [93]. We have selected the data by [72] and [92] as the recommended data.

For the C^{+}+H collisions, total charge transfer cross sections were calculated using the classical trajectory Monte Carlo method by Stancil et al. [94]. Experimental measurements of total charge transfer cross sections were carried out by Phaneuf et al. [78], Nutt et al. [92], Goffe et al. [72], and Stancil et al. [94]. Stancil et al. [94] gave also the recommended values of total charge transfer cross sections.

The recommended (total and state selective) cross sections are fitted to the following

analytic functions:

$$\sigma[\mathrm{cm}^2] = 10^{-16} \times \begin{cases} \dfrac{a_1 \exp[-(a_2/E)^{a_3}]}{1+(E/a_4)^{a_5}+(E/a_6)^{a_7}+(E/a_8)^{a_9}} \\ \dfrac{a_1 \exp[-(a_2/E)^{a_3}]}{1+(E/a_4)^{a_5}+(E/a_6)^{a_7}+(E/a_8)^{a_9}} + \dfrac{a_{10} \exp[-(a_{11}/E)^{a_{12}}]}{1+(E/a_{13})^{a_{14}}} \\ \dfrac{a_1 \exp[-(a_2/E)^{a_3}]}{1+(E/a_4)^{a_5}+(E/a_6)^{a_7}+(E/a_8)^{a_9}} + \dfrac{a_{10} \exp[-(a_{11}/E)^{a_{12}}]}{1+(E/a_{13})^{a_{14}}+(E/a_{15})^{a_{16}}} \end{cases}, \tag{19}$$

where the collision energy E is expressed in eV/amu units and a_i, i =1-14 are fitting parameters. The values of a_i in Eq. (19) are given in Tables VIII and IX, together with the references of the adopted data and the rms percent error. The recommended cross sections are shown graphically in Figs. 139-174. Unfortunately, we did not find enough data for fitting for certain state-selective charge transfer processes. In such cases, we show only the original data in figures. This is the case for Figs. 159, 161-167, 169-171. The rms percent errors are at most 1.33 in our fitting.

V. SUMMARY

We have compiled and have critically assessed cross sections for electron-impact excitation and ionization of atomic carbon ions, as well as charge exchange in collisions between carbon ions and hydrogen atoms. The recommended cross sections are expressed in terms of simple analytic functions. These can immediately lead to applications in fusion science.

Acknowledgments

We thank Prof. Hiroshi Sato for providing us the code for fitting the cross sections to analytic fit functions. Useful dicussions with Profs. Mineo Kimura, Akinori Igarashi and Prof. Ratko Janev are also appreciated.

---

[1] Itikawa, Y., Hara, S., Kato, T., Nakazaki, S., Pindzola, M.S., Crandall, D.H., Atomic Data Nucl. Data Tables **33**, 149 (1985).

[2] Peak, J.M., quoted in Los Alamos Scientific Laboratory Report, edited by LA-6691-MS, Magee, N.H., Mann, J.B., Merts, A.L., and Robb, W.D. (1977DW).

[3] Mann, J.B., quoted in Los Alamos Scientific Laboratory Report, edited by LA-6691-MS, Magee, N.H., Mann, J.B., Merts, A.L., and Robb, W.D. (1977CB).

[4] Mann, J.B., quoted in Los Alamos Scientific Laboratory Report, edited by LA-6691-MS, Magee, N.H., Mann, J.B., Merts, A.L., and Robb, W.D. (1977CBO).

[5] Rob, W.D., quoted in Los Alamos Scientific Laboratory Report, edited by LA-6691-MS, Magee, N.H., Mann, J.B., Merts, A.L., and Robb, W.D. (1977CC).

[6] McDowell, M.R.C., Morgan, L.A., Myerscough, V.P., and Scott, T., J. Phys. B: At. Mol. Opt. Phys. **10**, 2727 (1977).

[7] Foster, G., Hummer, D.G., Norcross, D.W. Information quarterly No.6 (1977).

[8] Berrington, K.A., Burke, P.G., Dufton, P.L., and Kingston, A.E., J. Phys. B:At. Mol. Opt. Phys. **10**, 1465 (1977).

[9] Berrington, K.A., Burke, P.G., Dufton, P.L., and Kingston, A.E., Atomic Data Nucl. Data Tables **26**, 1 (1981).

[10] Aggarwal and K. M., Kingston, A. E., J. Phys. B: At. Mol. Opt. Phys. **24**, 4583 (1991).

[11] Zou, Y. and Shirai, T., Phys. Rev. A **45**, 6902 (1992).

[12] Fisher, V.I., Ralchenko, Y.V., Bernshtam, V.A., Goldgirsh, A., Maron, Y., Vainshtein, L.A., Bray, I., and Golten, H., Phys. Rev. A **55**, 329 (1997).

[13] Callaway, J., Atom. Data Nucl. Data Tables **57**, 9 (1994).

[14] Badnell, N.R., J. Phys. B: At. Mol. Opt. Phys. **18**, 955 (1985).

[15] Srivastava, R. and Katiyar, Phys. Rev. A **35**, 1080 (1987).

[16] Kato, T. and Nakazaki, S., Atom. Data Nucl. Data Tables **42** 313 (1989).

[17] Bannister, M.E., Chung, Y.-S., Djuric, N., Wallbank, B. , Woitke, O., Zhou, S., Dunn, G.H., and Smith, A.C.H., Phys. Rev. A **57**, 278 (1998).

[18] Greenwood, J.B., Simth, S.J., and Chutjian, A., Phys. Rev. A **59**, 1348 (1999).

[19] Janzen, P.H., Gardner, L.D., Reisenfeld, D.B., Savin, D.W., Kohl, J.L., and Bartschat, K., Phys. Rev. A **59**, 4821 (1999).

[20] Burke, V.M., J. Phys. B: At. Mol. Opt. Phys. **25**, 4917 (1992).

[21] Griffin, D.C., Badnell, N.R., and Pindzola, M.S., J. Phys. B: At. Mol. Opt. Phys. **33**, 1013 (2000).

[22] Berrington, K.A., Burke, P.G., Dufton, P.L., and Kingston, A.E., Atomic Data Nucl. Data Tables **33**, 195 (1985).

[23] Itikawa, Y. and Sakimoto K., Phys. Rev A **31**, 1319 (1985).

[24] Berrington, K.A., Burke, V.M., Burke, P.G., and Scialla, S., J. Phys. B: At. Mol. Opt. Phys. **22**, 665 (1989).

[25] Blum, R.D. and Pradhan, A., Astrophys. J. Suppl. **80**, 425 (1992).

[26] Williams, I.D., Greenwood, J.B., and McGuiness, P.J., J. Phys. B: At. Mol. Opt. Phys. **28**, L555 (1995).

[27] Dunseath, K.M., Burke, V.M., Burke, P.G., Kingston, A.E., Reid, R.H.G., and Tait, J.H., JET Order No.JP2/11566 (1993).

[28] Henry, R.J.W., Burke, P.G., and Sinfailam, A.-L., Phys. Rev. **178**, 218 (1969).

[29] Pindzola, M.S., Bhatia, A.K., and Temkin, A., Phys. Rev. A **15**, 35 (1977).

[30] Thomas, L.D. and Nesbet, R.K., Phys. Rev. A **12**, 2378 (1975).

[31] Mann, J.B., private communication (1981).

[32] Flower, D.R. and Launay, J.M., Astron. Astrophys., **29**, 321 (1973).

[33] Savin, D.W., Gardner, L.D., Reisenfeld, D.B., Young, A.R. and Kohl, J.L., Phys. Rev. A **51**, 2162 (1995).

[34] Donets, E.D. and Ovsyannikov, V.P., Sov. Phys.-JETP **53**, 466 (1981).

[35] Aichele, K., Hartenfeller, U., Hathiramani, D., Hofmann, G.,

[36] Pattard, T. and Rost, J.M., Physica Scripta **T80**, 295 (1999). Schafer, V., Steidl, M., Stenke, M., Salzborn, E., Pattard, T., and Rost, J.M., J. Phys. B: At. Mol. Opt. Phys. **31**, 2369 (1998).

[37] Younger, S.M., Phys. Rev. A **22**, 111 (1980).

[38] Kao, H.C., Kuo, T.Y., Yen, H.P., Wei, C.M., and Huang, K.N., Phys. Rev. A **45**, 4646 (1992).

[39] Fang, D., Hu, W., Chen, C., Wang, Y., Lu, F., Tang, J., and Yang, F., Atomic Data Nucl. Data Tables **61**, 91 (1995).

[40] Crandall, D.H., Phaneuf, R.A., and Gregory, D.C., ORNL/TM 7029 (1979).

[41] Salop, A., Phys. Rev. A **14**, 2095 (1976).

[42] Knopp, H., Teng, H., Ricz, S., Schippers, S., and Müller, A., Physica Scripta **T92**, 379 (2001).

[43] Crandall, D.H., Phaneuf, R.A., and Gregory, D.C., ORNL/TM 9501 (1985).

[44] Jakubowicz, H and Moores, D.H., J. Phys. B: At. Mol. Opt. Phys. **14**, 3733 (1981).

[45] Sampson, D.H. and Golden, L.B., J. Phys. B: At. Mol. Opt. Phys., **12**, L785 (1979).

[46] Scott, M.P., Teng, H., and Burke, P.G., J. Phys. B: At. Mol. Opt. Phys., **33**, L63 (2000).

[47] Badnell, N.R. and Griffin, D.C., J. Phys. B: At. Mol. Opt. Phys. **33**, 2955 (2000).

[48] Woodruff, P.R., Hublet, M.-C., Harrison, M.F.A., and Brook, E., J. Phys. B: At. Mol. Opt. Phys., **11**, 679 (1978).

[49] Falk, R.A., Stefani, G., Camilloni, R., Dunn, G.H., Phaneuf, R.A., Gregory, D.C., and Crandall, D.H., Phys. Rev. A **28**, 91 (1983).

[50] Moores, D.L., J. Phys. B: At. Mol. Opt. Phys., **11**, L403 (1978).

[51] Yamada, I, Danjo, A., Hirayama, T., Matsumoto, A., Ohtani, S., Suzuki, H., Takayanagi, T., Tawara, H., Wakita, K., Yoshino, M. J., Phys. Soc. Jpn

[52] Qian, X.Z. and Pan, S.F., Phys. Lett. A **239**, 363 (1988).

[53] Westermann, M., Scheuermann, F., Aichele, K., Hartenfeller, U., Hathiramani, D., Steidl, M. and Salzborn, E., Physica Scripta **T80**, 285 (1999).

[54] Brook, E., Harrison, M.F.A., and Smith, A.C.H., J. Phys. B: At. Mol. Opt. Phys. **11**, 3115 (1978).

[55] Omidvar, K. and Kyle H.L., and Sullivan E.C., Phys. Rev. A **5**, 1174 (1972). **58**, 1585 (1989).

[56] Toshima, N. and Tawara, H., NIFS-DATA, **26** (1995).

[57] Belkic, D., Gayet, R. and Salin, A., Atomic Data Nucl. Data Tables **51**, 59 (1992).

[58] Belkic, D., private communication.

[59] Ryufuku, H. JAERI-M **82-031**, 42 (1982).

[60] Olson, R.E. and Schultz, D.R., Physica Scripta, **T28**, 71 (1989).

[61] Green, T., Shipsey, E.J. and Browne, J.C., Phys. Rev. A **25**, 1364 (1982).

[62] Harel, C., Jouin, H. and Pons, B., Atomic Data Nucl. Tables **68**, 279 (1998).

[63] Kazanskii, A.K. and Komarov, I.V., Sov. Phys. - Techn. Phys. **27**, 1064 (1982).

[64] Fritsch, W. and Lin, C.D., J. Phys. B: At. Mol. Opt. Phys. **17**, 3271 (1984).

[65] Fritsch, W., J. de Phys. **C1**, 87 (1989).

[66] Kimura, M. and Lin, C.D., Phys. Rev. A **32**, 1357 (1985).

[67] Das, M., Deb, N.C., and Mukherjee, S.C., Physica Scripta **54**, 44 (1996).

[68] Panov, M.N., Baselaev, A.A., and Lozhkin, K.O., Physica Sctipta **T3**, 124 (1983).

[69] Janev, R.K., Phaneuf, R.A. and Tawara, H., Atomic Data Nucl. Data Tables **55**, 201 (1993).

[70] Shimakura, N., Koizumi, S., Suzuki, S., Kimura, M., Phys. Rev. A **45**, 7876 (1992).

[71] Shipsey, E.J., Browne, J.C., and Olson, R.E., J. Phys. B: At. Mol. Opt. Phys. **14**, 869 (1981).

[72] Goffe, T.V., Shah, M.B., and Gilbody, H.B., J. Phys. B: At. Mol. Opt. Phys. **12**, 3763 (1979).

[73] Phaneuf, R.A., Alvarez, I., Meyer, F.W., and Crandall, D.H., Phys. Rev. A **26**, 1892 (1982)

[74] Errea, L.F., Gorfinkiel, J.D., Harel, C., Jouin, H., Macias, A, Mendez, L., Pons, B., and Riera, A., J. Phys. B: At. Mol. Opt. Phys. **32**, L673 (1999).

[75] Gargaud, M., McCarroll, R., and Valion, P., J. Phys. B: At. Mol. Opt. Phys. **20**, 1555 (1987).

[76] Tseng, H.C. and Lin, C.D., Phys. Rev. A **58**, 1966 (1998).

[77] Hoekstra, R., Beijers, J.P.M., Schlatmann, A.R., and Morgenstern, R., Phys. Rev. A **41**, 4800 (1990).

[78] Phaneuf, R.A., Meyer, F.W., and McKnight, R.H., Phys. Rev. A **17**, 534 (1978).

[79] Crandall, D.H., Phaneuf, R.A., Meyer, F.W., Phys. Rev. A **19** 504 (1979).

[80] Dijkkamp,D., Ciric, D., Flieg, E., de Boer, A., and de heer, F.J., J. Phys. B: At. Mol. Opt. Phys. **18**, 4763 (1985).

[81] Bliek, F.W., Hoekstra, R., Bannister, M.E., and Havener, C.C., Phys. Rev. A **56**, 426 (1997).

[82] Opradolce, L., Benmeuraiem, L., McCarroll, R., and Piacentini, R.D., J. Phys. B: At. Mol. Opt. Phys. **21**, 503 (1988).

[83] Bienstock, S., Heil, T.G., Bottcher, C., and Dalgarno, A., Phys. Rev. A **25**, 2850 (1982).

[84] Ciric, D., Brazuk, A., Dijkkamp, D., de Heer, F.J., and Winter, H., J. Phys. B: At. Mol. Opt. Phys. **18**, 3629 (1985).

[85] McCullough, R.W., Wilkie, F.G., and Gilbody, H.B., J. Phys. B: At. Mol. Opt. Phys. **17**, 1373 (1984).

[86] Errea, L.F., Herrero, B., Mendez, L., and Riera, A., J. Phys. B: At. Mol. Opt. Phys. **24**, 4061 (1991).

[87] Tseng, H.C. and Lin, C.D., J. Phys. B: At. Mol. Opt. Phys. **32**, 5271 (1999).

[88] Heil, T.G., Butler, S.E., and Dalgarno, A., Phys. Rev. A **23**, 1100 (1981).

[89] Sant'Anna, M.M., Melo, W.S., Santos, A.C.F., Shah, M.B., and Montenegro, E.C., J. Phys. B: At. Mol. Opt. Phys. **33**, 353 (2000).

[90] Gu, J.P., Hirsch, G., Buenker, R.J., Kimura, M., Dutta, C.M., and Nordlander, P., Phys. Rev. A **57**, 4483 (1998).

[91] Errea, L.F., Macias, A., Mendez, L., and Riera, A., J. Phys. B: At. Mol. Opt. Phys. **33**, 1369 (2000).

[92] Nutt, W.L., McCullough, R.W., and Gilbody, H.B., J. Phys. B: At. Mol. Opt. Phys. **12**, L157 (1979).

[93] Gardner, L.D., Bayfield, J.E., Koch, P.M., Sellin, I.A., Pegg, D.J., Peterson, R.S., and Crandall, D.H., Phys. Rev. A **21**, 1397 (1980).

[94] Stancil, P.C., Gu, J.-P., Havener, C.C., Krstić, P.S., Schultz, D.R., Kimura, M., Zygelman, B., Hirsch, G., Buenker, R.J., and Bannister, M.E., J. Phys. B: At. Mol. Opt. Phys. **31**, 3647 (1998).

TABLE I: Values of the fit parameters for electron-impact excitation of the C^{5+} ion.

Transition	V_{if}[eV]	Fitting Eq.	Fit parameters	rms	ref.
C^{5+} (H like)					
1s-2s	367	(6)	A =2.446(-2)[a], B =-1.567(-2), C =1.010(-2), D =0.0, E =0.0	0.004	[6, 11]
1s-2p	367	(6)	A =1.040(-2), B =1.720(-2), C =4.370(-2), D =0.0, E =1.259(-1)	—[b]	[1]
1s-3s	435	(6)	A =4.866(-3), B =-2.522(-3), C =3.158(-3), D =-1.765(-3), E =0.0	—	[1]
1s-3p	435	(6)	A =4.248(-3), B =8.978(-3), C =4.082(-3), D =0.0, E =2.130(-2)	0.01	[2, 10]
1s-3d	435	(6)	A =3.874(-3), B =-6.100(-3), C =3.909(-3), D =2.143(-3), E =0.0	0.01	[3, 10]
1s-4s	459	(6)	A =1.814(-3), B =-1.035(-3), C =1.515(-3), D =-9.157(-4), E =0.0	0.001	[4]
1s-4p	459	(6)	A =1.106(-3), B =2.965(-3), C =3.247(-3), D =0.0, E =7.915(-3)	0.02	[4, 10]
1s-5p	470	(6)	A =6.869(-4), B =1.166(-3), C =2.120(-3), D =0.0, E =3.711(-3)	0.02	[4, 10]

[a] $x(\pm y) = x \times 10^{\pm y}$

[b] Rms is missing for the coefficients taken from Ref. [1].

TABLE II: Values of the fit parameters for electron-impact excitation of the C^{4+} ion.

Transition	V_{if}[eV]	Fitting Eq.	Fit parameters	rms	ref.
C^{4+} (He like)					
$1s^2\ ^1S$-$1s2s\ ^3S$	299	(6)	A =-1.820(-5)[a], B =1.093(-3), C =1.675(-2), D =-8.788(-3), E =0.0,	—[b]	[1]
			[P =-1.777, Q =1.826, X_1=1.02]		
$1s^2\ ^1S$-$1s2s\ ^1S$	304	(6)	A =2.830(-2), B =-3.159(-2), C =2.694(-2), D =-1.063(-2), E =0.0	—	[1]
$1s^2\ ^1S$-$1s2p\ ^3P$	304	(6)	A =8.926(-5), B =-2.824(-3), C =7.379(-2), D =-2.670(-2), E =0.0	0.70	[2, 7, 14]
$1s^2\ ^1S$-$1s2p\ ^1P$	308	(6)	A =1.642(-2), B =-7.345(-2), C =9.320(-2), D =0.0, E =1.247(-1)	0.06	[2, 5]
$1s^2\ ^1S$-$1s3d\ ^3D$	354	(6)	A =5.061(-5), B =-5.619(-4), C =2.116(-3), D =7.710(-4), E =0.0	—	[1]
$1s^2\ ^1S$-$1s3p\ ^1P$	355	(6)	A =1.286(-2), B =-2.133(-2), C =1.656(-2), D =0.0, E =2.107(-2)	—	[1]
$1s2s\ ^3S$-$1s2s\ ^1S$	5.4	(6)	A =-3.821(-3), B =7.199(-1), C =-1.671, D =1.393, E =0.0	1.46	[14]
$1s2s\ ^3S$-$1s2p\ ^3P$	5.4	(6)	A =9.507, B =1.195(1), C =-7.559, D =0.0, E =4.417	0.008	[5, 14]
$1s2s\ ^3S$-$1s2p\ ^1P$	8.94	(6)	A =-5.935(-3), B =6.629(-1), C =-7.935(-1), D =2.695(-1), E =0.0	—	[1]
$1s2s\ ^3S$-$1s3p\ ^3P$	54.5	(6)	A =-7.449(-1), B =1.335, C =-3.423(-1), D =0.0, F =1.011	—	[1]
$1s2s\ ^1S$-$1s2p\ ^3P$	0.022	(7)	A =1.187(-2), B =4.767(-2), C =-3.971(-2), D =3.753(-2), E =1.534(-1), F =6(-4)	—	[1]
$1s2s\ ^1S$-$1s2p\ ^1P$	3.5	(6)	A =1.508, B =3.987, C =-1.245, D =0.0, E =1.652	0.004	[14]
$1s2p\ ^3P$-$1s2p\ ^1P$	3.2	(7)	A =2.487(-2), B =1.042, C =-3.304, D =0.0, E =1.758(-1), F =2(-2)	—	[1]
$1s2p\ ^3P$-$1s3s\ ^3S$	47.7	(6)	A =-1.091(-1), B =2.359(-1), C =-5.644(-2), D =0.0, F =1.758(-1)	—	[1]

[a] $x(\pm y) = x \times 10^{\pm y}$

[b] Rms is missing for the coefficients taken from Ref. [1].

TABLE III: Values of the fit parameters for electron-impact excitation of the C^{3+} ion.

Transition	V_{if}[eV]	Fitting Eq.	Fit parameters	rms	ref.
C^{3+} (Li like)					
2s ^{2}S-2p ^{2}P	8.0	(6)	A =4.744[a], B =4.440, C =5.971(-1), D =0.0, E =4.519	0.01	[4]
2s ^{2}S-3s ^{2}S	37.6	(6)	A =4.846(-1), B =-2.743(-1), C =4.768(-1), D =-3.971(-1), E =0.0,	—[b]	[1]
			X_1=1.072, P =7.390(-1), Q =2.460(-1)		
2s ^{2}S-3p ^{2}P	40.0	(6)	A =-5.731(-1), B =9.548(-1), C =-8.931(-2), D =0.0, E =5.638(-1)	—	[1]
			X_1=1.019, P =-3.412, Q =9.141		
2s ^{2}S-3d ^{2}D	40.0	(6)	A =1.252, B =-1.243, C =4.93(-1), D =1.326(-1), E =0.0	—	[1]
2s ^{2}S-4p ^{2}P	50.6	(10)	A =2.775(-1), B =-6.663(-1), C =4.959(-1), D =0, E =3.530(-6)	0.02	[21]
2p ^{2}P-3s ^{2}S	29.4	(10)	A =1.273, B =-5.038, C =5.374, D =0, E =2.270(-3)	0.05	[21]
2p ^{2}P-3d ^{2}D	32.1	(10)	A =1.899(+1), B =-4.193(+1), C =2.857(+1), D =0, E =4.027(-3)	0.04	[21]
2p ^{2}P-4s ^{2}S	41.8	(10)	A =1.964(-1), B =-6.743(-1), C =7.166(-1), D =0, E =2.411(-4)	0.04	[21]

[a] $x(\pm y) = x \times 10^{\pm y}$

[b] Rms is missing for the coefficients taken from Ref. [1].

TABLE IV: Values of the fit parameters for electron-impact excitation of the C^{2+} ion.

Transition	V_{if}[eV]	Fitting Eq.	Fit parameters	rms	ref.
C^{2+} (Be like)					
$2s^2\ ^1S$-$2s2p\ ^3P$	6.5	(6)	A =-4.024(-2)[a], B =2.914, C =-4.344, D =2.121, E =0.0	—[b]	[1]
			X_1=2.0, P =5.434(-1), Q =3.453(-1)		
$2s^2\ ^1S$-$2s2p\ ^1P$	12.7	(6)	A =6.261(-1), B =3.044, C =5.384(-1), D =0.0, E =4.364	0.04	[8, 22, 31]
$2s^2\ ^1S$-$2p^2\ ^3P$	17.2	(6)	A =-5.732(-3), B =8.467(-2), C =-1.676(-1), D =1.307(-1), E =0.0	0.01	[22]
			X_1=2.0,P =5.389(-3), Q =7.167(-3)		
$2s^2\ ^1S$-$2p^2\ ^1D$	18.2	(6)	A =2.915(-1), B =1.655(-1), C =-3.445(-1), D =3.720(-1), E =0.0	0.03	[22, 32]
$2s^2\ ^1S$-$2p^2\ ^1S$	22.9	(6)	A =2.092(-2), B =2.289(-1), C =-4.268(-1), D =2.137(-1), E =0.0	0.01	[9, 22]
$2s^2\ ^1S$-$2s3s\ ^3S$	29.5	(6)	A =3.910(-3), B =2.740(-1), C =1.120, D =1.110, E =0	0.36	[24]
$2s^2\ ^1S$-$2s3s\ ^1S$	30.6	(6)	A =4.260(-1), B =4.350(-1), C =-2.280, D =1.760, E =0	0.0004	[24]
$2s^2\ ^1S$-$2s3p\ ^1P$	32.1	(6)	A =-1.140(-1), B =-5.230(-1), C =8.110(-1), D =0, E =3.730(-1)	0.0005	[24]
$2s^2\ ^1S$-$2s3p\ ^3P$	32.2	(6)	A =-2.190(-2), B =3.660(-1), C =-1.030, D =8.240(-1), E =0	0.20	[24]
$2s^2\ ^1S$-$2s3d\ ^3D$	33.5	(6)	A =4.190(-2), B =6.490(-2), C =1.100(-2), D =1.050(-1), E =0	0.0005	[24]
$2s^2\ ^1S$-$2s3d\ ^1D$	34.3	(6)	A =7.330(-1), B =5.400(-2), C =-2.110, D =1.490, E =0	0.0005	[24]
$2s2p\ ^3P$-$2p^2\ ^3P$	10.6	(6)	A =9.842, B =-8.660, C =2.184(+1), D =0.0, E =1.631	—	[1]
$2s2p\ ^3P$-$2p^2\ ^1D$	11.7	(6)	A =-1.822(-1), B =4.490, C =-4.889, D =2.056, E =0.0	0.06	[5, 9]
$2s2p\ ^3P$-$2p^2\ ^1S$	16.5	(6)	A =3.280(-4), B =1.676(-1), C =2.778(-1), D =-4.524(-1), E =0.0	0.02	[9]

[a] $x(\pm y) = x \times 10^{\pm y}$

[b] Rms is missing for the coefficients taken from Ref. [1].

TABLE IV: Values of the fit parameters for electron-impact excitation of the C^{2+} ion (continued).

Transition	V_{if}[eV]	Fitting Eq.	Fit parameters	rms	ref.
C^{2+} (Be like)					
2s2p ^{3}P-2s3s ^{1}S	24.1	(6)	A =-1.200(-2), B =1.310, C =-4.030, D =3.590, E =0	0.88	[24]
2s2p ^{3}P-2s3p ^{1}P	25.6	(6)	A =-1.310(-2), B =1.580, C =-4.800, D =4.270, E =0	0.0004	[24]
2s2p ^{3}P-2s3p ^{3}P	25.7	(6)	A =1.980, B =1.490(+1), C =-4.330(+1), D =3.170(+1), E =0	0.0004	[24]
2s2p ^{3}P-2s3d ^{3}D	27.0	(6)	A =-2.900(-1), B =2.090, C =7.110, D =0, E =1.010(+1)	0.80	[24]
2s2p ^{3}P-2s3s ^{1}D	27.8	(6)	A =9.840(-3), B =5.080(-1), C =-7.040(-1), D =9.550(-1), E =0	0.0004	[24]
2s2p ^{1}P-2p^2 ^{3}P	4.3	(6)	A =-8.624(-3), B =4.141, C =-7.089, D =3.824, E =0.0	—	[1]
			X_1=1.85, P =7.072(-1), Q =2.899(-1)		
2s2p ^{1}P-2p^2 ^{1}D	4.3	(6)	A =3.762, B =9.351, C =-3.004, D =0.0, E =7.320	—	[1]
2s2p ^{1}P-2p^2 ^{1}S	10.1	(6)	A =3.032, B =-2.375, C =2.675, D =0.0, E =2.991	—	[1]
2p^2 ^{3}P-2p^2 ^{1}D	1.01	(6)	A =1.925, B =1.440(+1), C =-3.560(+1), D =2.727(+1), E =0.0	—	[1]
2p^2 ^{3}P-2p^2 ^{1}S	5.8	(6)	A =4.319(-2), B =1.004, C =-1.037, D =3.630(-1), E =0.0	—	[1]
2p^2 ^{1}D-2p^2 ^{1}S	4.79	(6)	A =8.948(-1), B =-8.607(-1), C =1.007, D =-4.136(-1), E =0.0	—	[1]

TABLE V: Values of the fit parameters for electron-impact excitation of the C^+ ion.

Transition	V_{if}[eV]	Fitting Eq.	Fit parameters	rms	ref.
C^+ (B like)					
$2s^22p\ ^2P$-$2s2p^2\ ^4P$	4.74	(7)	A =4.360(-1)[a], B =1.627, C =-2.923, D =1.094(+1), E =-6.580, F =5.769(-2)	—[b]	[1]
$2s^22p\ ^2P$-$2s2p^2\ ^2D$	9.27	(6)	A =-2.155, B =1.374(+1), C =-6.562, D =0.0, E =4.136	—	[1]
$2s^22p\ ^2P$-$2s2p^2\ ^2S$	12.0	(6)	A =8.572(-1), B =2.079(-1), C =7.058(-1), D =0.0, E =4.136	—	[1]
$2s^22p\ ^2P$-$2s2p^2\ ^2P$	13.7	(6)	A =-6.883(-1), B =4.106, C =3.435(-1), D =0.0, E =1.631(+1)	—	[1]
$2s^22p\ ^2P$-$2s^23s\ ^2S$	14.4	(6)	A =-9.843(-1), B =2.983, C =-9.975(-1), D =0.0, E =8.910(-1)	—	[1]
$2s^22p\ ^2P$-$2s^23p\ ^2P$	16.3	(6)	A =1.678, B =-2.238, C =4.829, D =0.0, E =0.0	—	[1]
$2s^22p\ ^2P$-$2s^23d\ ^2D$	18.0	(6)	A =-1.703, B =2.675, C =1.165, D =0.0, E =5.791	—	[1]

[a] $x(\pm y) = x \times 10^{\pm y}$

[b] Rms is missing for the coefficients taken from Ref. [1].

TABLE VI: Values of the fit parameters for electron-impact excitation of the C atom.

Transition	V_{if}[eV]	Fitting Eq.	Fit parameters	rms	ref.
C					
$2s^22p^2\ ^3P$-$2s^22p^2\ ^1D$	1.26	(11)	A =1.277, B =1.304(+1), C =-3.314(+1), D =6.357(+1), E =-4.621(+1), F =4(-2)	0.01	[27]
$2s^22p^2\ ^3P$-$2s^22p^2\ ^1S$	2.68	(10)	A =1.598(-1), B =2.836, C =-9.813, D =-1.012(+1), E =1.233(-1)	0.01	[27]
$2s^22p^2\ ^3P$-$2s2p^3\ ^5S$	4.18	(11)	A =-2.302, B =8.923, C =-2.873(+1), D =4.555(+1), E =-2.431(+1), F =1.323(-1)	0.003	[27]
$2s^22p^2\ ^3P$-$2s^22p3s\ ^3P$	7.48	(6)	A =-6.117, B =2.989, C =4.148, D =0, E =1.222(+1)	0.07	[27]
$2s^22p^2\ ^3P$-$2s^22p3s\ ^1P$	7.68	(11)	A =2.423, B =7.590(-1), C =-6.486, D =3.143, E =-2.074(+1), F=6.744(-1)	0.01	[27]
$2s^22p^2\ ^3P$-$2s2p^3\ ^3D$	7.94	(6)	A =1.307(+1), B =-3.052(+1), C =1.835(+1), D =0, E =1.001(+1)	0.20	[27]
$2s^22p^2\ ^3P$-$2s^22p3p\ ^1P$	8.53	(7)	A =1.909, B =-6.101(-1), C =-2.336, D =-3.093(+2), E =7.450(+2), F =1.491	0.06	[27]
$2s^22p^2\ ^3P$-$2s^22p3p\ ^3D$	8.64	(10)	A =9.753(-1), B =1.908, C =2.161, D =-4.891, E =0	0.01	[27]
$2s^22p^2\ ^3P$-$2s^22p3p\ ^3S$	8.77	(10)	A =1.886(-3), B =2.263(-1), C =8.836(-1), D =-1.031, E =0	0.001	[27]
$2s^22p^2\ ^3P$-$2s^22p3p\ ^3P$	8.85	(6)	A =7.728, B =8.661(-1), C =-1.640(+1), D =7.754, E =0	0.22	[27]
$2s^22p^2\ ^3P$-$2s^22p3p\ ^1D$	9.00	(7)	A =-1.389, B =1.062, C =-3.742(-1), D =4.786, E =-4.126, F =2.606(-1)	0.18	[27]
$2s^22p^2\ ^3P$-$2s^22p3p\ ^1S$	9.20	(7)	A =3.567(-2), B =5.081(-1), C =-7.062(-1), D =1.463, E =-2.569, F =4.101(-1)	0.33	[27]
$2s^22p^2\ ^3P$-$2s2p^3\ ^3P$	9.33	(6)	A =1.146(+1), B =-2.477(+1), C =1.281(+1), D =0, E =6.328	0.11	[27]
$2s^22p^2\ ^3P$-$2s^22p3d\ ^1D$	9.63	(6)	A =5.747(-2), B =-1.444(-1), C =1.793, D =-1.719, E =0	0.52	[27]
$2s^22p^2\ ^3P$-$2s^22p3d\ ^3F$	9.69	(11)	A =-3.067, B =2.352, C =-3.127, D =-9.123, E =1.656(+1), F =1.476(-1)	0.007	[27]
$2s^22p^2\ ^3P$-$2s^22p3d\ ^3D$	9.71	(6)	A =4.081, B =-9.274, C =5.423, D =0, E =4.970	0.02	[27]

TABLE VI: Values of the fit parameters for electron-impact excitation of the C atom (continued).

Transition	V_{if}[eV]	Fitting Eq.	Fit parameters	rms	ref.
C					
$2s^22p^2\ ^3P$-$2s^22p3d\ ^1F$	9.73	(11)	A =1.183, B =-8.798(-1), C =7.839, D =-1.718(+1), E =-8.149(-1), F =5.66(-1)	0.01	[27]
$2s^22p^2\ ^3P$-$2s^22p3d\ ^3P$	9.83	(6)	A =1.247, B =-5.247, C =3.983, D =0, E =3.876	0.02	[27]
$2s^22p^2\ ^3P$-$2s2p^3\ ^1D$	12.2	(7)	A =-3.820, B =2.082, C =2.801, D =-9.506, E =1.552(+1), F =2.937(-1)	0.16	[27]
$2s^22p^2\ ^3P$-$2s2p^3\ ^3S$	13.1	(6)	A =8.801(-1), B =-9.630, C =8.179, D =0, E =1.199(+1)	1.95	[27]
$2s^22p^2\ ^3P$-$2s2p^3\ ^1P$	14.9	(11)	A =2.975, B =-4.065, C =-2.943(-1), D =7.361(+1), E =-3.359(+2), F =1.40	0.10	[27]
$2s^22p^2\ ^1D$-$2s^22p^2\ ^1S$	1.42	(10)	A =2.029, B =-1.093(+1), C =2.049(+1), D =-1.221(+1), E =0.0	0.01	[27]
$2s^22p^2\ ^1D$-$2s2p^3\ ^3D$	6.68	(7)	A =1.003(+2),B =-5.439(+1),C =-1260(+2),D =1.861(+2),E =-9.357(+2),F =6.9(-1)	0.09	[27]
$2s^22p^2\ ^1D$-$2s^22p3s\ ^3P$	6.22	(7)	A =9.576, B =-6.855(-1), C =2.121, D =3.983, E =-7.383(+1), F =4.750(-1)	0.19	[27]
$2s^22p^2\ ^1D$-$2s^22p3s\ ^1P$	6.42	(6)	A =-1.795, B =-1.134, C =2.995, D =0, E =4.794	0.20	[27]

TABLE VII: Values of the fitting parameters for electron-impact ionization in Eq. (17)

	I	A_1	A_2	A_3	A_4	A_5	rms	ref.
$C^{5+} \rightarrow C^{6+}$	490	2.489(-1)[a]	1.847(-1)	4.475(-2)	-9.432(-2)	5.122(-1)	0.02	[36]
$C^{4+} \rightarrow C^{5+}$	392	9.205(-1)	-6.297(-1)	1.316	-9.156(-2)	0.0	1.07	[39]
$C^{3+} \rightarrow C^{4+}$ [b]	64.5	1.350	-8.748(-1)	-1.444	2.330	-2.730	0.11	[42]
	285	-2.777	5.376	-8.748	1.766(+1)	-9.086		
$C^{2+} \rightarrow C^{3+}$	41.4	4.009(-1)	-3.518(-1)	2.375	-3.992	2.794	0.08	[48]
$C^{+} \rightarrow C^{2+}$	24.4	8.390(-1)	-7.950(-1)	3.263	-5.382	3.476	0.24	[51]
$C^{+} \rightarrow C^{3+}$ [b]	70.0	1.674(-1)	-1.583(-1)	1.941(-2)	1.200(-1)	-3.559(-1)	0.430	[53]
	320	-7.904(-1)	1.315	7.235(-1)	-7.621(-1)	2.485		
$C \rightarrow C^{+}$	10.6	1.829	-1.975	1.149	-3.583	2.451	0.61	[54]

[a] $x(\pm y) = x \times 10^{\pm y}$

[b] A sum of two sets of Eq. (17) were needed to fit these cross sections.

TABLE VIII: Values of the fitting parameters in Eq. (19) for charge transfer in C^{6+}+H collisions.

Transition	Parameters							rms and ref.
C^{6+}+H	a_1=8.775(+3)[a]	a_2=2.203(+6)	a_3=7.199(-1)	a_4=4.031(+3)	a_5=-3.389	a_6=3.785(+2)	a_7=2.211	rms=1.33
$\rightarrow C^{5+}$(1s)+H^+	a_8=4.927(+4)	a_9=5.159	a_{10}=5.556(+1)	a_{11}=1.362(+4)	a_{12}=5.824(-1)	a_{13}=2.211(-9)	a_{14}=7.417(-1)	[56, 57]
C^{6+}+H	a_1=6.077(+1)	a_2=1.203(+6)	a_3=4.784(-1)	a_4=3.421(+3)	a_5=1.388	a_6=9.320(+3)	a_7=1.093	rms=0.44
$\rightarrow C^{5+}$(2s)+H^+	a_8=4.930(+4)	a_9=4.448	a_{10}=1.120(+2)	a_{11}=2.781(+3)	a_{12}=1.194	a_{13}=1.732(+2)	a_{14}=8.134	[56, 57]
C^{6+}+H	a_1=4.400(+4)	a_2=4.203(+6)	a_3=4.630(-1)	a_4=4.108(+3)	a_5=2.529	a_6=9.326(+3)	a_7=2.430	rms=2.18
$\rightarrow C^{5+}$(2p)+H^+	a_8=4.929(+4)	a_9=5.889	a_{10}=4.900(-2)	a_{11}=1.360(+2)	a_{12}=6.767(-1)	a_{13}=2.132(+1)	a_{14}=2.553	[56, 57]
C^{6+}+H	a_1=7.553(+1)	a_2=1.203(+6)	a_3=4.747(-1)	a_4=3.766(+3)	a_5=9.873(-1)	a_6=9.294(+3)	a_7=8.192(-1)	rms=0.24
$\rightarrow C^{5+}$(n=2)+H^+	a_8=4.928(+4)	a_9=3.779	a_{10}=4.900(-2)	a_{11}=1.360(+2)	a_{12}=6.760(-1)	a_{13}=2.132(+1)	a_{14}=2.010	[56]
C^{6+}+H	a_1=9.197(-1)	a_2=1.203(+6)	a_3=-7.438(-2)	a_4=5.026(+3)	a_5=-3.446	a_6=4.364(+4)	a_7=2.946	rms=0.28
$\rightarrow C^{5+}$(3s)+H^+	a_8=2.290(+5)	a_9=5.395						[56, 57]
C^{6+}+H	a_1=1.606	a_2=1.267(+6)	a_3=-3.948(-1)	a_4=6.026(+3)	a_5=-3.064	a_6=4.684(+4)	a_7=2.461	rms=0.17
$\rightarrow C^{5+}$(3p)+H^+	a_8=1.941(+5)	a_9=5.264						[57, 62, 69]
C^{6+}+H	a_1=8.680	a_2=1.192(+6)	a_3=1.436(-1)	a_4=7.064(+4)	a_5=2.995	a_6=6.849(+3)	a_7=-2.652	rms=0.21
$\rightarrow C^{5+}$(3d)+H^+	a_8=1.545(+5)	a_9=5.895						[57, 62, 69]
C^{6+}+H	a_1=1.121(+1)	a_2=1.195(+6)	a_3=6.029(-2)	a_4=6.088(+4)	a_5=2.798	a_6=5.994(+3)	a_7=-2.943	rms=0.16
$\rightarrow C^{5+}$(n=3)+H^+	a_8=1.547(+5)	a_9=5.436						[62, 62, 69]

[a] $x(\pm y) = x \times 10^{\pm y}$

TABLE VIII: Values of the fitting parameters in Eq. (19) for charge transfer in C^{6+}+H collisions (continued).

Transition	Parameters							ref.
C^{6+}+H	a_1=2.570(+1)	a_2=1.334(+6)	a_3=-4.311(-1)	a_4=9.667(+4)	a_5=-8.384(-1)	a_6=3.104(+3)	a_7=7.322(-1)	rms=0.20
→C^{5+}(4s)+H^+	a_8=2.051(+5)	a_9=2.951						[57, 62, 69]
C^{6+}+H	a_1=3.654(+2)	a_2=2.932(+6)	a_3=1.646(-1)	a_4=1.328(+4)	a_5=3.086	a_6=2.879(+3)	a_7=1.233	rms=0.10
→C^{5+}(4p)+H^+	a_8=9.395(+4)	a_9=6.076						[57, 62, 69]
C^{6+}+H	a_1=9.718(+2)	a_2=2.930(+6)	a_3=1.749(-1)	a_4=1.481(+4)	a_5=3.120	a_6=2.204(+3)	a_7=1.038	rms=0.17
→C^{5+}(4d)+H^+	a_8=8.098(+4)	a_9=6.391						[57, 61, 69]
C^{6+}+H	a_1=3.705(+1)	a_2=3.080(+5)	a_3=1.880(-1)	a_4=7.779(+4)	a_5=1.992	a_6=6.461(+4)	a_7=5.695	rms=0.18
→C^{5+}(4f)+H^+	a_8=9.590(+4)	a_9=1.631	a_{10}=7.417(+1)	a_{11}=4.791(+3)	a_{12}=-5.261(-1)	a_{13}=1.515(+3)	a_{14}=-1.121	
	a_{15}=7.601(+3)	a_{16}=-6.016(-2)						[57, 62, 69]
C^{6+}+H	a_1=4.570(+3)	a_2=1.201(+6)	a_3=1.936(-1)	a_4=6.222(+2)	a_5=8.580(-1)	a_6=1.683(+4)	a_7=3.534	rms=0.08
→C^{5+}(n=4)+H^+	a_8=5.590(+4)	a_9=5.735						[57, 61, 69]
C^{6+}+H	a_1=3.960(+4)	a_2=8690(+5)	a_3=-1.380	a_4=6.004(+3)	a_5=4.215	a_6=5.845(+2)	a_7=2.676	rms=0.38
→C^{5+}(5s)+H^+	a_8=1.968(+4)	a_9=5.396	a_{10}=8.126(-1)	a_{11}=4.121(+4)	a_{12}=4.196(-1)	a_{13}=1.656(+3)	a_{14}=1.956(+3)	
	a_{15}=6.126(+4)	a_{16}=3.048						[57, 62, 69]
C^{6+}+H	a_1=3.230(+1)	a_2=5.615(+3)	a_3=-3.934(-1)	a_4=1.302(+4)	a_5=-1.240	a_6=2.084(+4)	a_7=-1.240	rms=0.22
→C^{5+}(5p)+H^+	a_8=2.084(+4)	a_9=1.625	a_{10}=9.971(+1)	a_{11}=1.800(+5)	a_{12}=2.287(-1)	a_{13}=1.142(+3)	a_{14}=3.097	[57, 62, 69]

TABLE VIII: Values of the fitting parameters in Eq. (19) for charge transfer in C^{6+}+H collisions (continued).

Transition	Parameters							ref.
C^{6+}+H	a_1=3.960(+4)	a_2=8690(+5)	a_3=4.461(-1)	a_4=6.140(+3)	a_5=-5.379(-1)	a_6=4.690(+2)	a_7=1.793	rms=0.24
$\rightarrow C^{5+}$(5d)+H^+	a_8=1.960(+4)	a_9=5.644	a_{10}=2.906	a_{11}=4.120(+4)	a_{12}=-6.217(-1)	a_{13}=1.311(+3)	a_{14}=-4.244(-2)	
	a_{15}=6.110(+4)	a_{16}=1.688						[57, 62, 69]
C^{6+}+H	a_1=3.965(+4)	a_2=8690(+5)	a_3=0.3591(-1)	a_4=6.133(+3)	a_5=-1.572	a_6=4.456(+2)	a_7=1.662	rms=0.14
$\rightarrow C^{5+}$(5f)+H^+	a_8=2.022(+4)	a_9=5.796	a_{10}=3.904	a_{11}=4.129(+4)	a_{12}=-7.814(-1)	a_{13}=1.550(+3)	a_{14}=-2.499(-2)	
	a_{15}=6.113(+4)	a_{16}=1.070						[57, 61, 69]
C^{6+}+H	a_1=3.960(+4)	a_2=8690(+5)	a_3=3.379(-1)	a_4=6.141(+3)	a_5=-3.628	a_6=4.376(+2)	a_7=1.392	rms=1.90
$\rightarrow C^{5+}$(5g)+H^+	a_8=1.963(+4)	a_9=5.969	a_{10}=7.954	a_{11}=4.120(+4)	a_{12}=9.565(-2)	a_{13}=1.296(+3)	a_{14}=-4.248(-2)	
	a_{15}=6.111(+4)	a_{16}=5.873						[57, 61, 69]
C^{6+}+H	a_1=5.196(+1)	a_2=1.870(+4)	a_3=3.448(-1)	a_4=5.788(+4)	a_5=4.234	a_6=2.991(+4)	a_7=1.498	rms=0.11
$\rightarrow C^{5+}$(n=5)+H^+	a_8=9.741(+4)	a_9=4.707	a_{10}=2.709(+1)	a_{11}=2.119(+3)	a_{12}=1.947(-1)	a_{13}=8.518(+2)	a_{14}=3.159	[56, 57, 62]
C^{6+}+H	a_1=2.301(+2)	a_2=5.983(+3)	a_3=3.117(-1)	a_4=1.300(+4)	a_5=6.613(-1)	a_6=7.299(+4)	a_7=4.895	rms=0.20
$\rightarrow C^{5+}$+H^+	a_8=2.100(+41)	a_9=1.557	a_{10}=3.355(-2)	a_{11}=1.800(+5)	a_{12}=-9.768(-2)	a_{13}=4.500(+3)	a_{14}=3.584	[58, 69]

TABLE IX: Values of the fitting parameters in Eq. (19) for charge transfer in C^{n+}+H collisions.

Transition	Parameters							ref.
C^{5+}+H	a_1=1.397(+2)	a_2=1.897(+4)	a_3=2.697(-1)	a_4=5.814(+4)	a_5=3.761	a_6=3.211(+4)	a_7=1.477	rms=0.02
→C^{4+}+H^+	a_8=9.750(+4)	a_9=5.583	a_{10}=9.227(+2)	a_{11}=5.496(+2)	a_{12}=-4.044(-1)	a_{13}=7.590(-7)	a_{14}=1.755(-1)	[70, 72, 78]
C^{4+}+H	a_1=9.600(+1)	a_2=3.088(+5)	a_3=1.218(-1)	a_4=7.784(+4)	a_5=2.059	a_6=6.458(+4)	a_7=5.498	rms=0.09
→C^{3+}+H^+	a_8=9.596(+4)	a_9=1.690	a_{10}=1.270(+2)	a_{11}=2.080(+2)	a_{12}=-2.589(-1)	a_{13}=2.830(+2)	a_{14}=-3.554(-1)	
	a_{15}=7.157(+1)	a_{16}=-1.956						[72, 78]
C^{3+}+H	a_1=6.239(+1)	a_2=1.873(+4)	a_3=2.589(-1)	a_4=5.783(+4)	a_5=4.767	a_6=3.026(+4)	a_7=1.492	rms=0.09
→C^{2+}+H^+	a_8=9.744(+4)	a_9=4.254	a_{10}=3.847(+2)	a_{11}=1.946(+2)	a_{12}=-1.814(-1)	a_{13}=4.743(-3)	a_{14}=3.457(-1)	[72, 78]
C^{2+}+H	a_1=3.719(+1)	a_2=1.086(+4)	a_3=3.514(-1)	a_4=3.785(+4)	a_5=9.584(-1)	a_6=3.462(+4)	a_7=3.442	rms=0.08
→C^{+}+H^+	a_8=4.597(+4)	a_9=8.611(-1)						[72, 92]
C^{+}+H	a_1=3.016(+3)	a_2=2.941(+6)	a_3=2.283(-1)	a_4=9.976(+3)	a_5=2.911	a_6=2.497(+3)	a_7=1.604	rms=0.24
→C+H^+	a_8=4.969(+4)	a_9=4.980						[94]

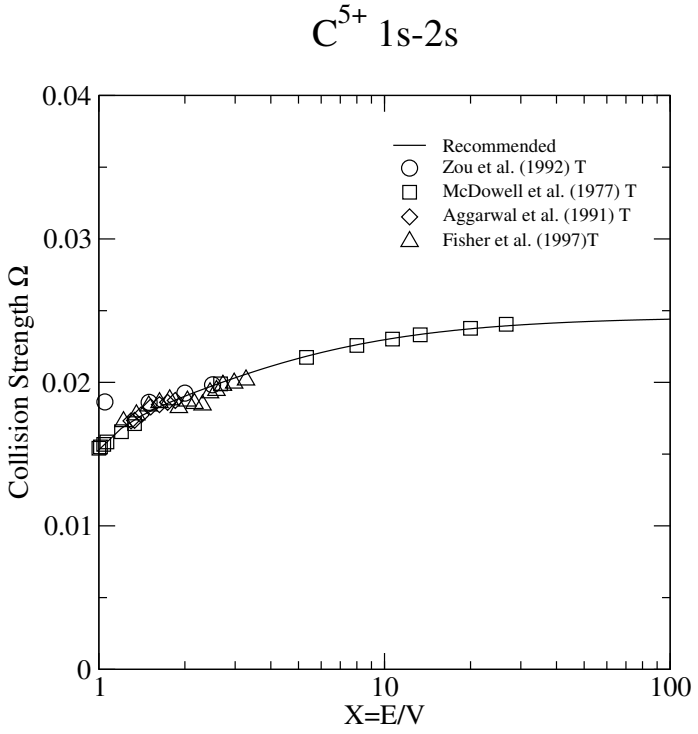

FIG. 1: Collision strength for electron-impact excitation.

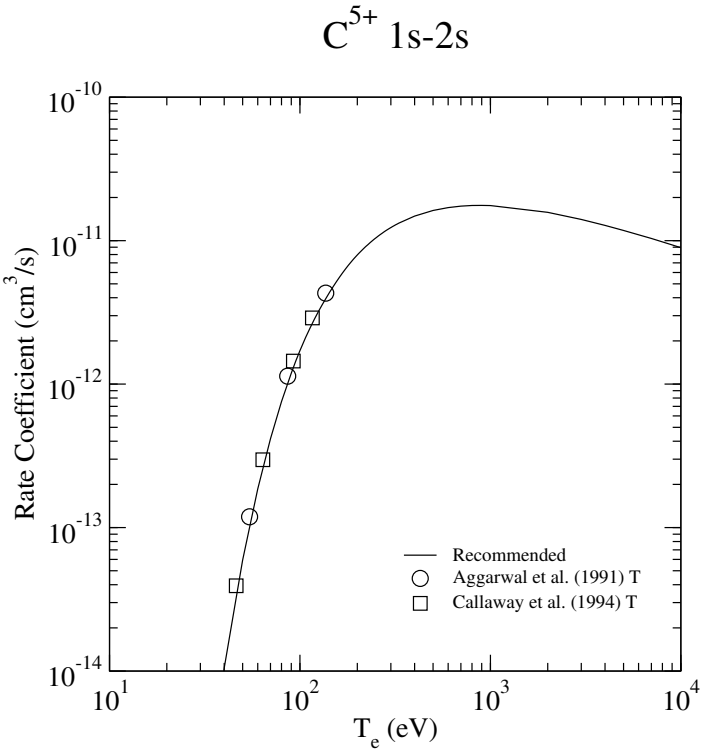

FIG. 2: Rate coefficient for electron-impact excitation.

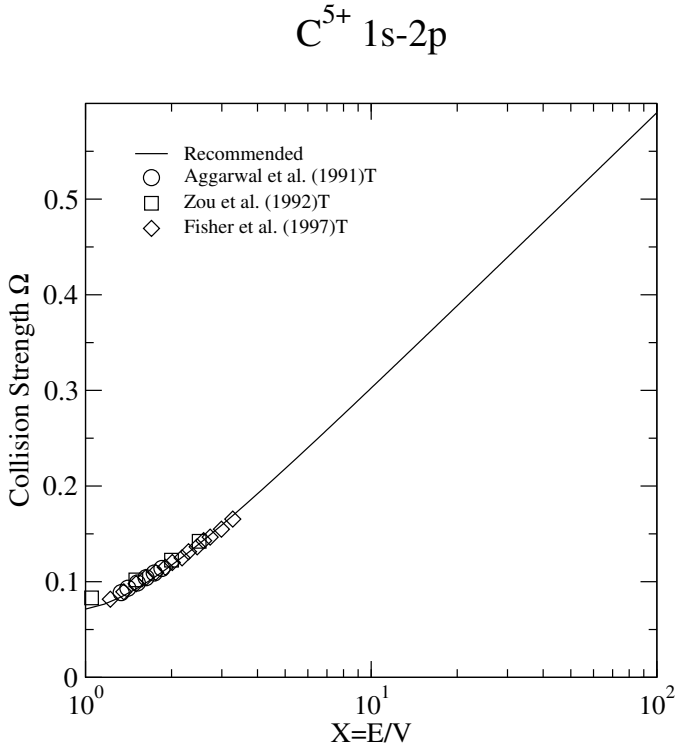

FIG. 3: Collision strength for electron-impact excitation.

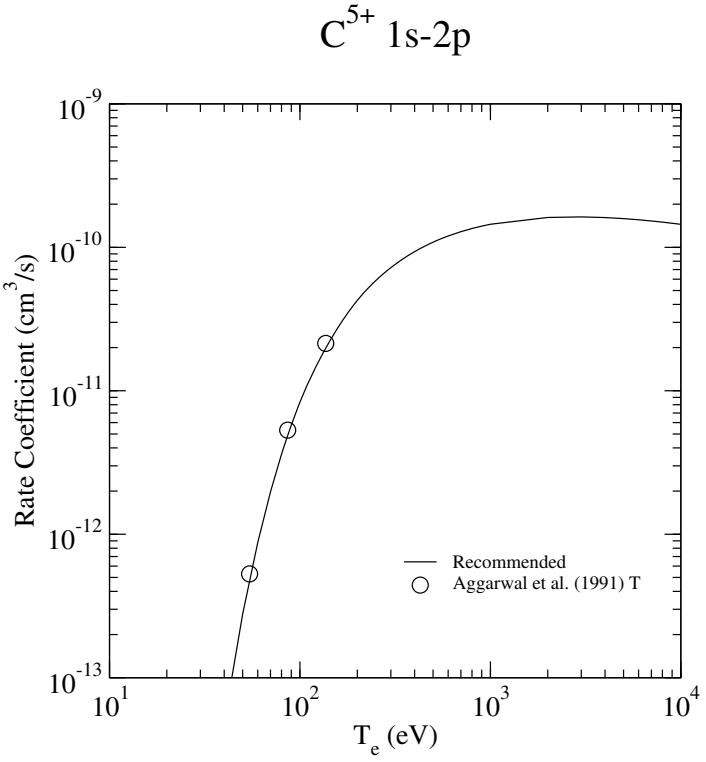

FIG. 4: Rate coefficient for electron-impact excitation.

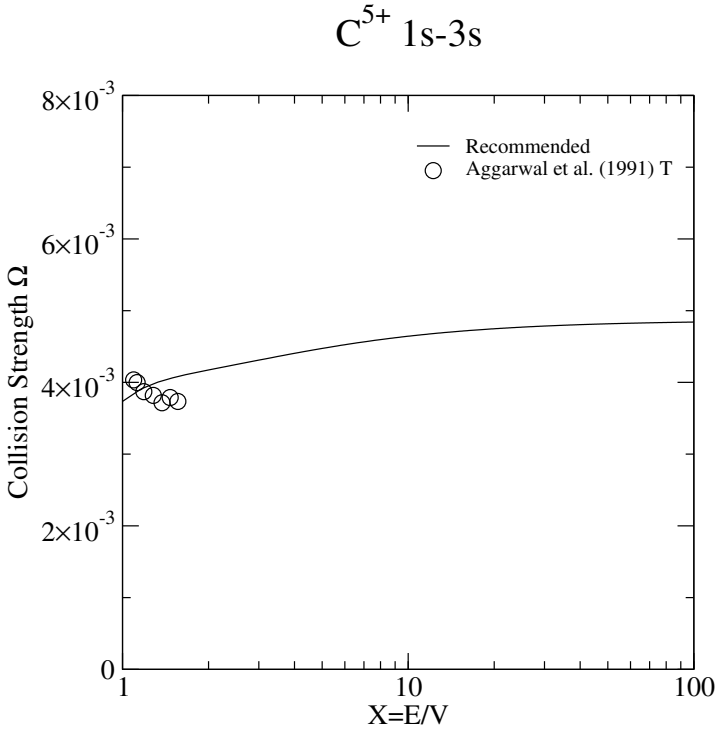

FIG. 5: Collision strength for electron-impact excitation.

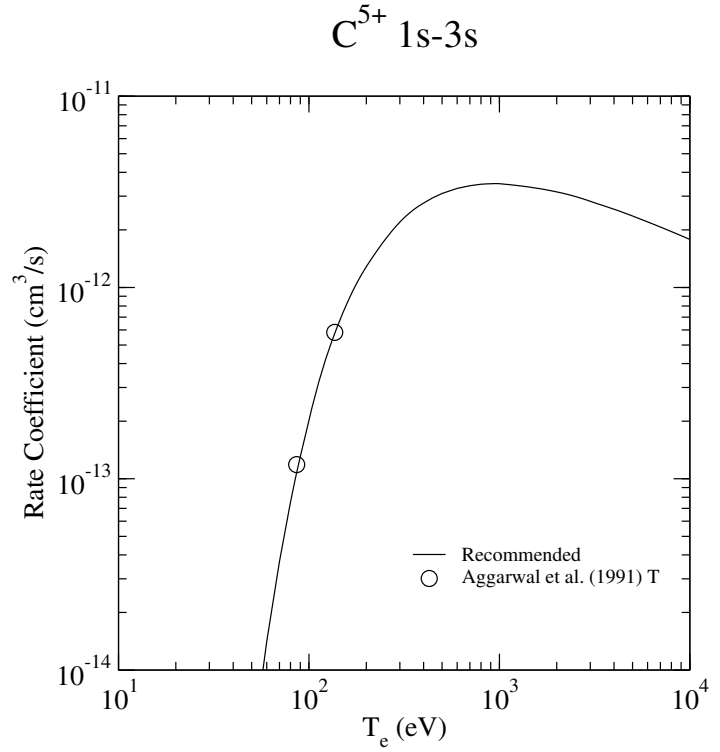

FIG. 6: Rate coefficient for electron-impact excitation.

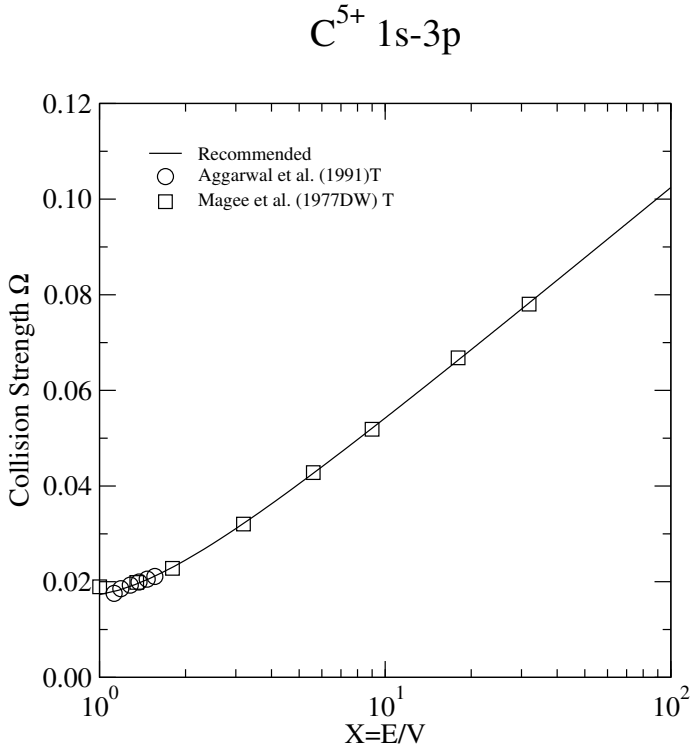

FIG. 7: Collision strength for electron-impact excitation.

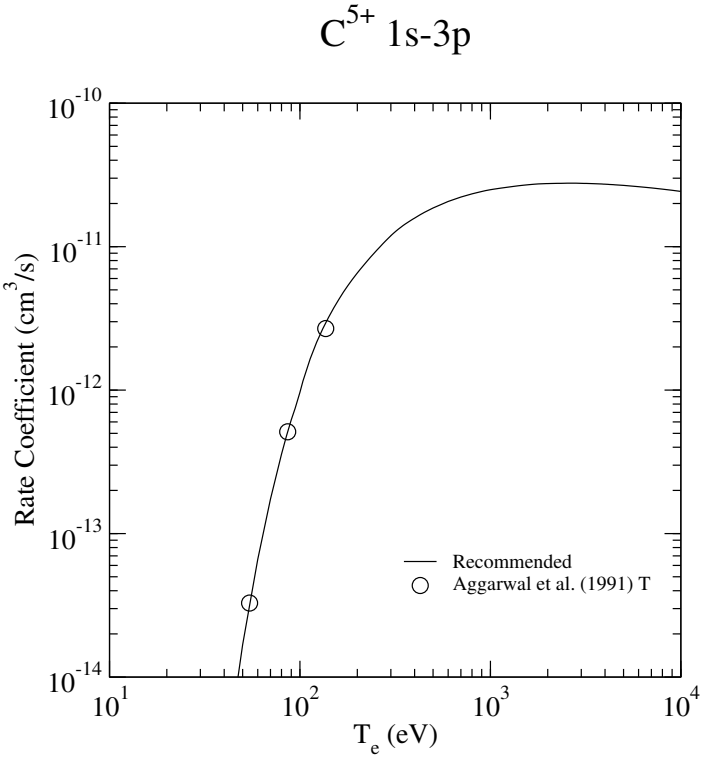

FIG. 8: Rate coefficient for electron-impact excitation.

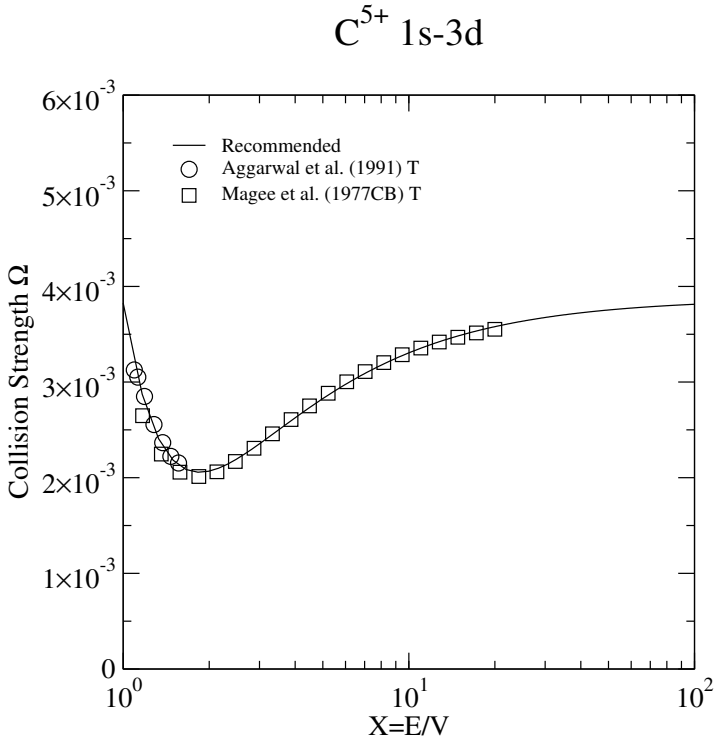

FIG. 9: Collision strength for electron-impact excitation.

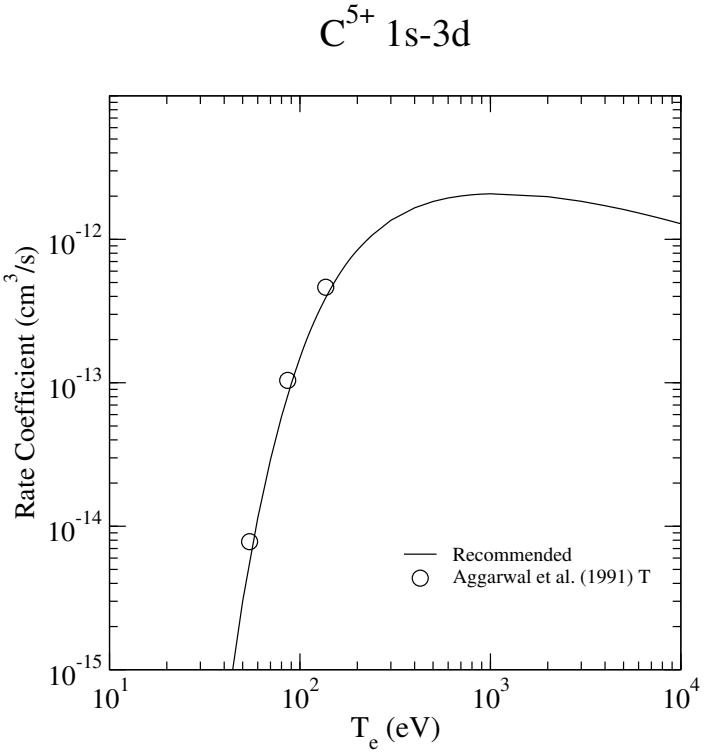

FIG. 10: Rate coefficient for electron-impact excitation.

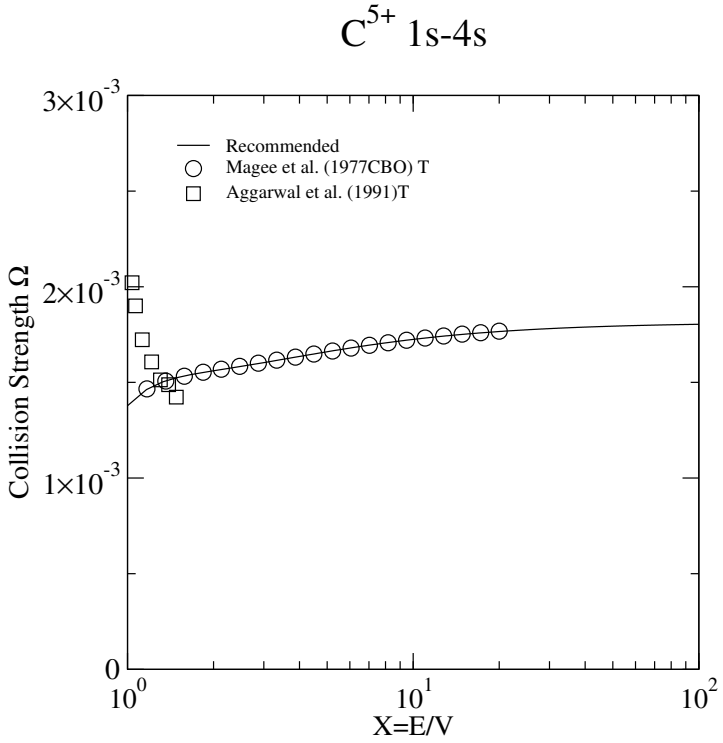

FIG. 11: Collision strength for electron-impact excitation.

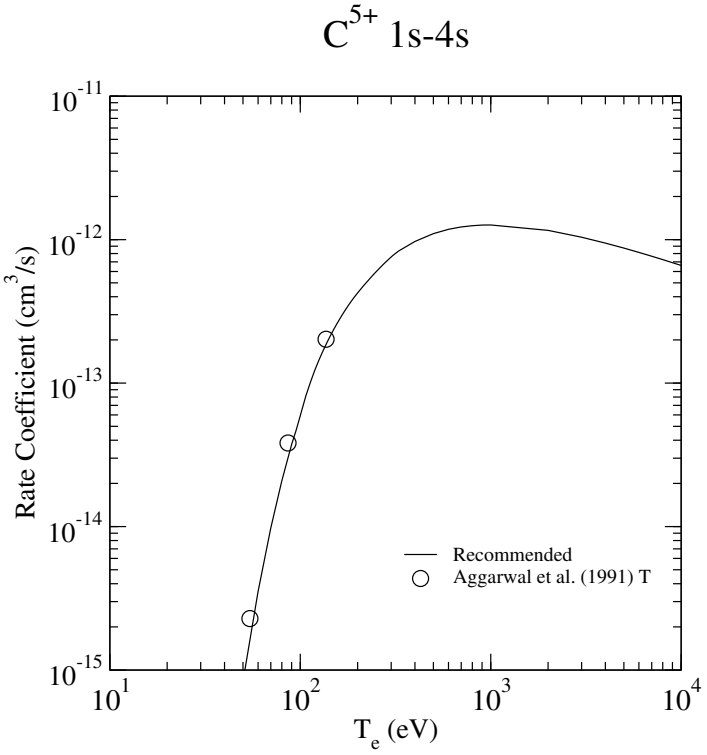

FIG. 12: Rate coefficient for electron-impact excitation.

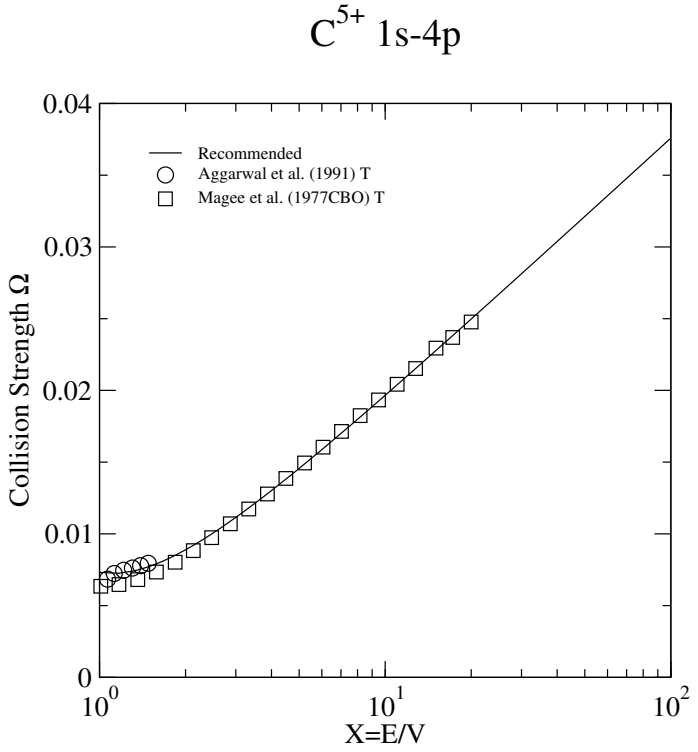

FIG. 13: Collision strength for electron-impact excitation.

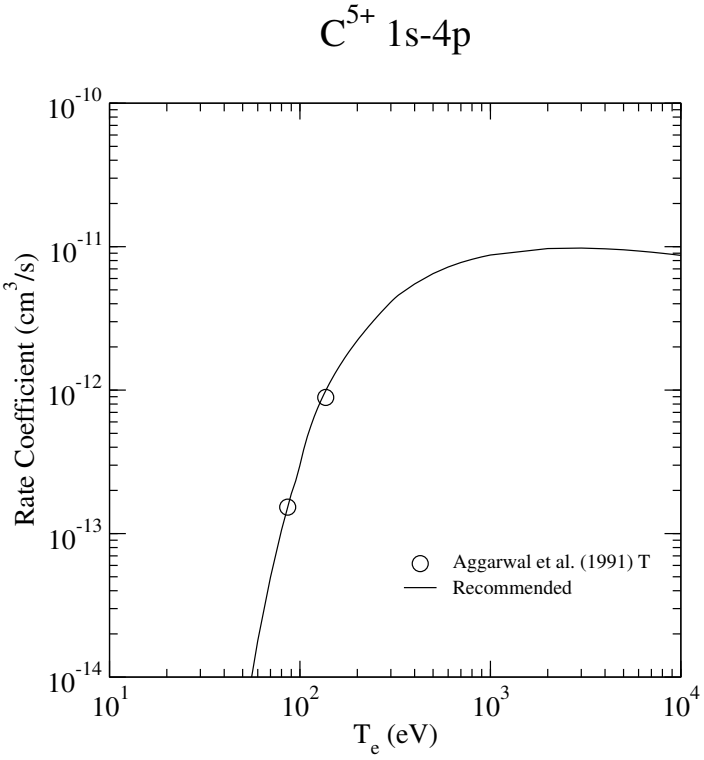

FIG. 14: Rate coefficient for electron-impact excitation.

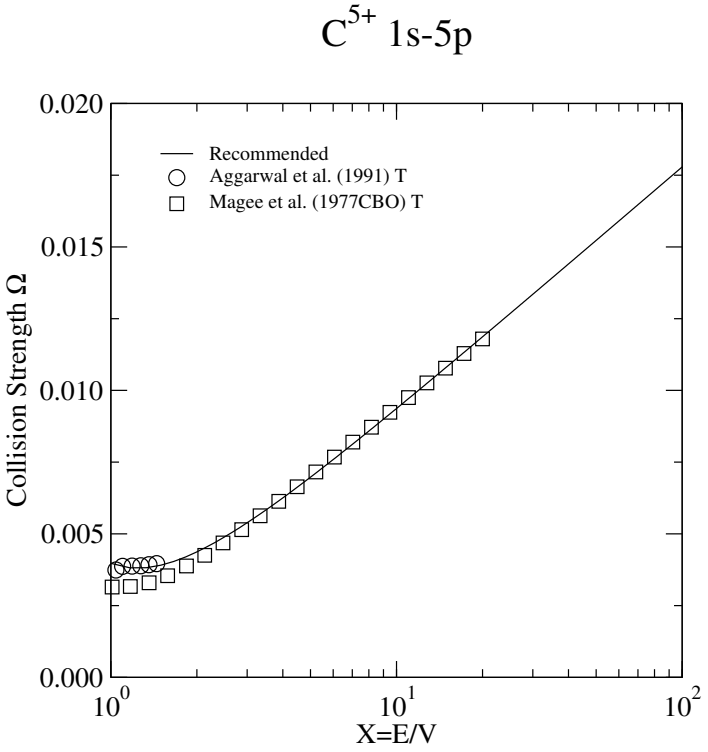

FIG. 15: Collision strength for electron-impact excitation.

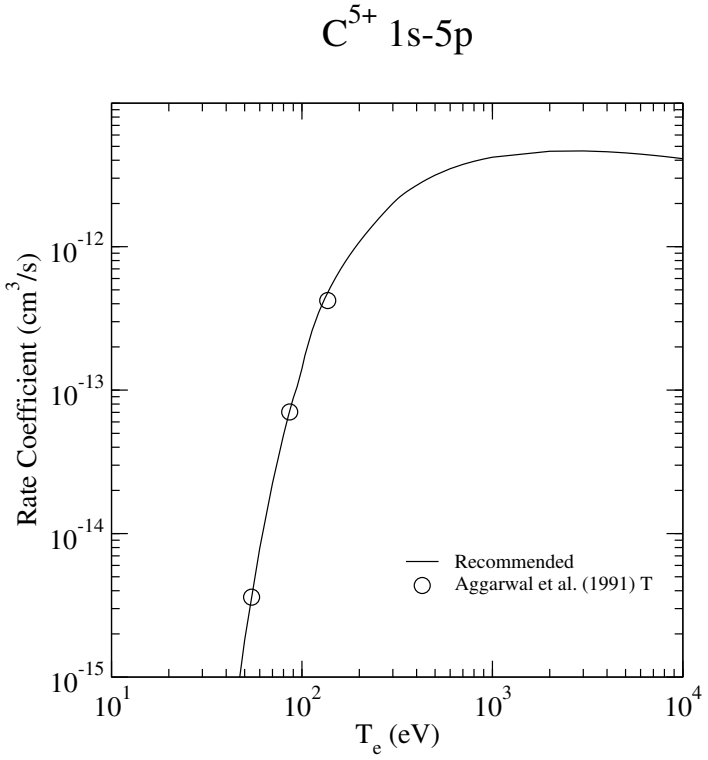

FIG. 16: Rate coefficient for electron-impact excitation.

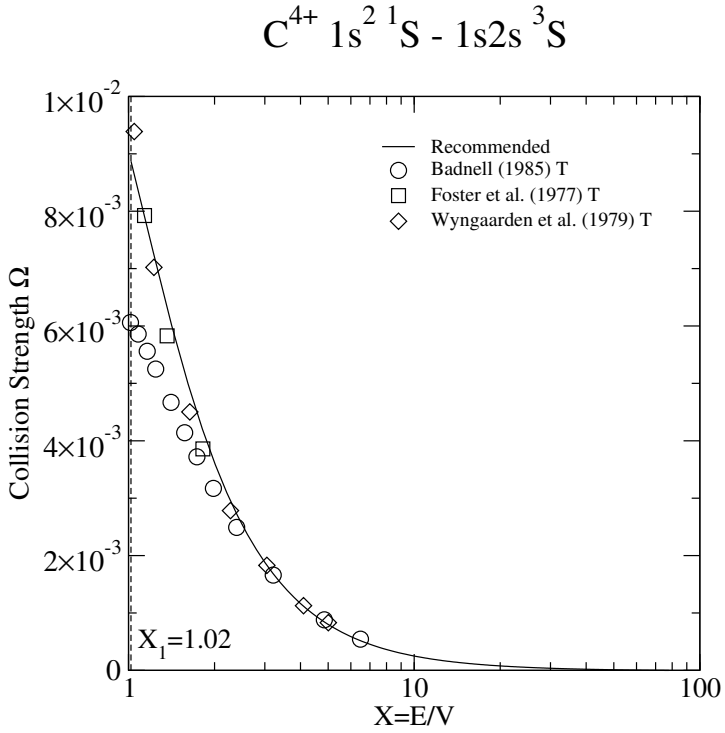

FIG. 17: Collision strength for electron-impact excitation.

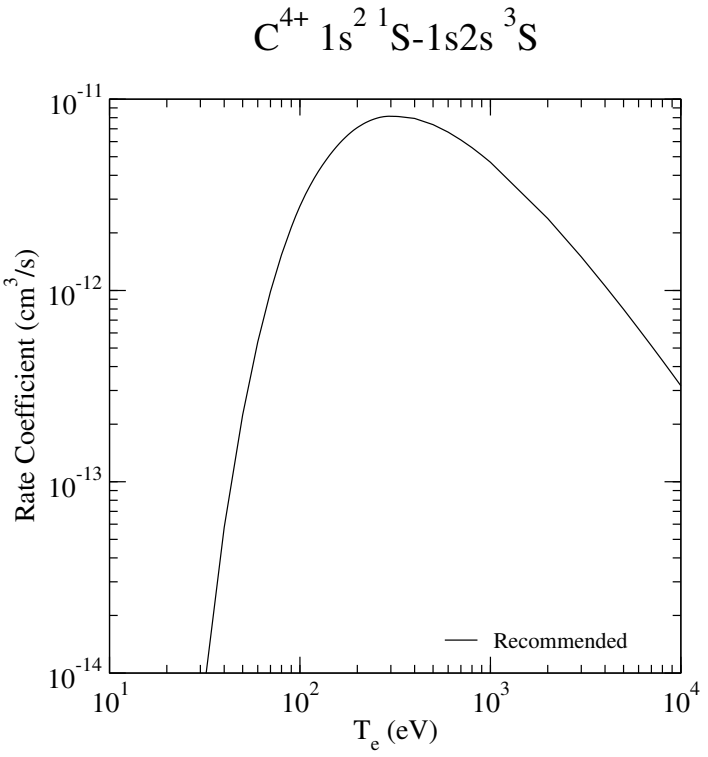

FIG. 18: Rate coefficient for electron-impact excitation.

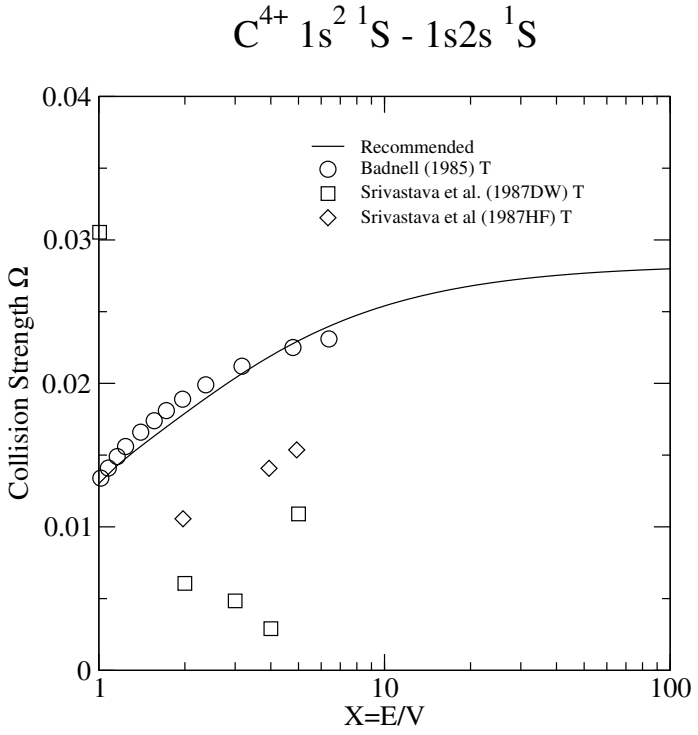

FIG. 19: Collision strength for electron-impact excitation.

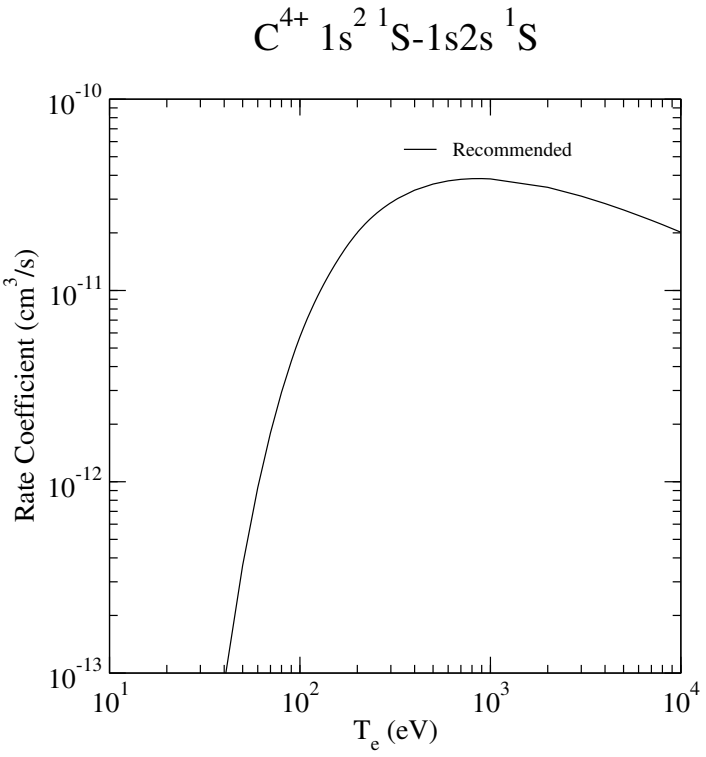

FIG. 20: Rate coefficient for electron-impact excitation.

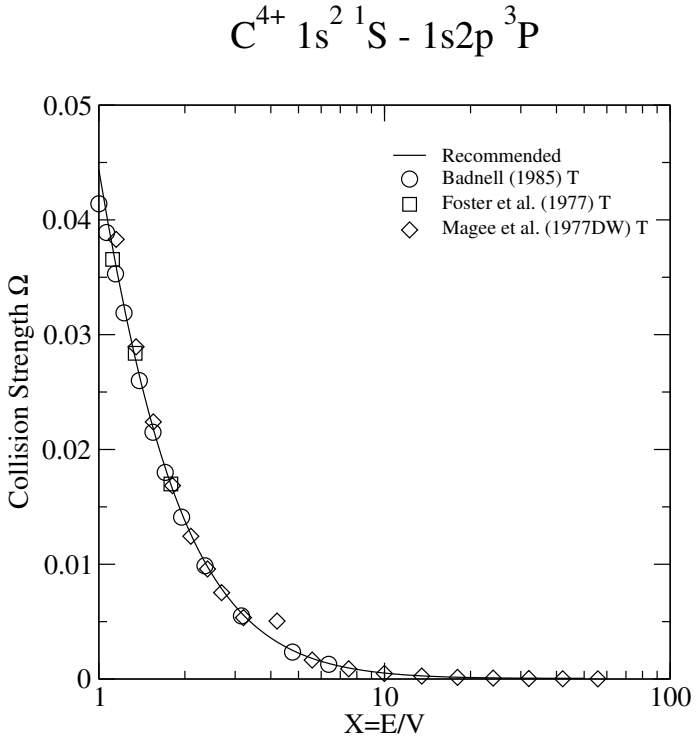

FIG. 21: Collision strength for electron-impact excitation.

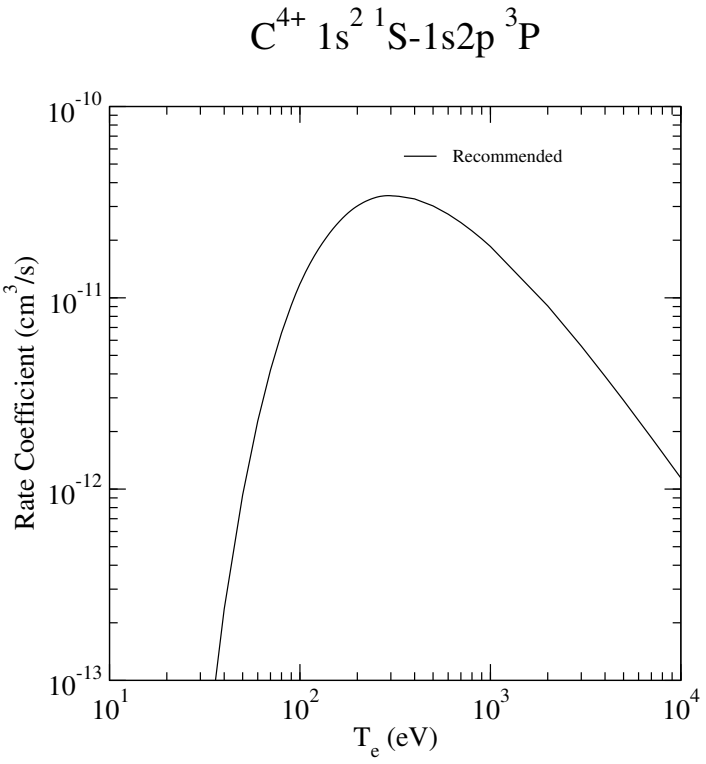

FIG. 22: Rate coefficient for electron-impact excitation.

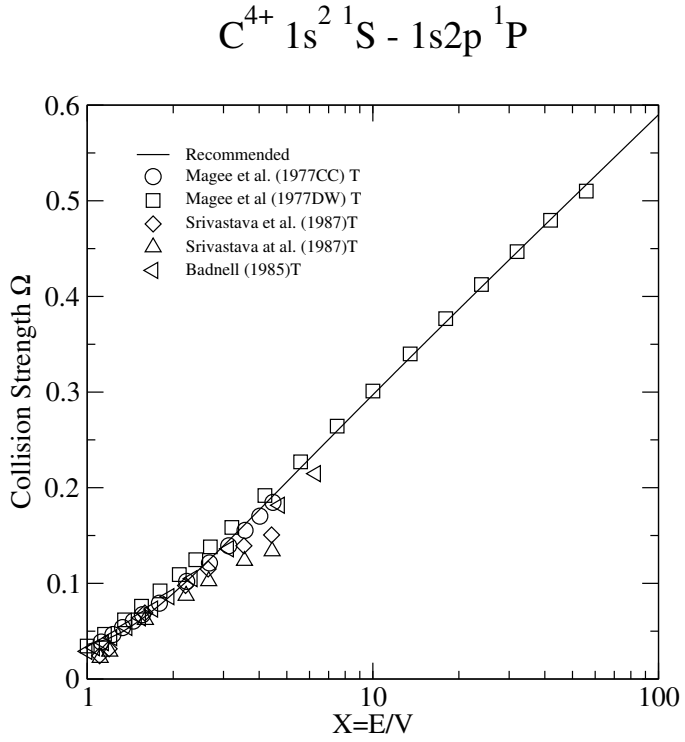

FIG. 23: Collision strength for electron-impact excitation.

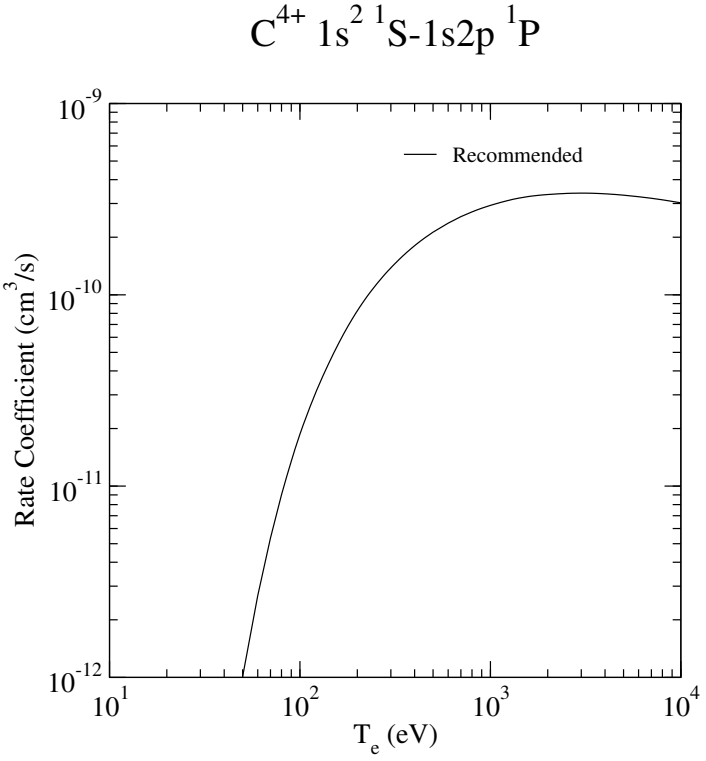

FIG. 24: Rate coefficient for electron-impact excitation.

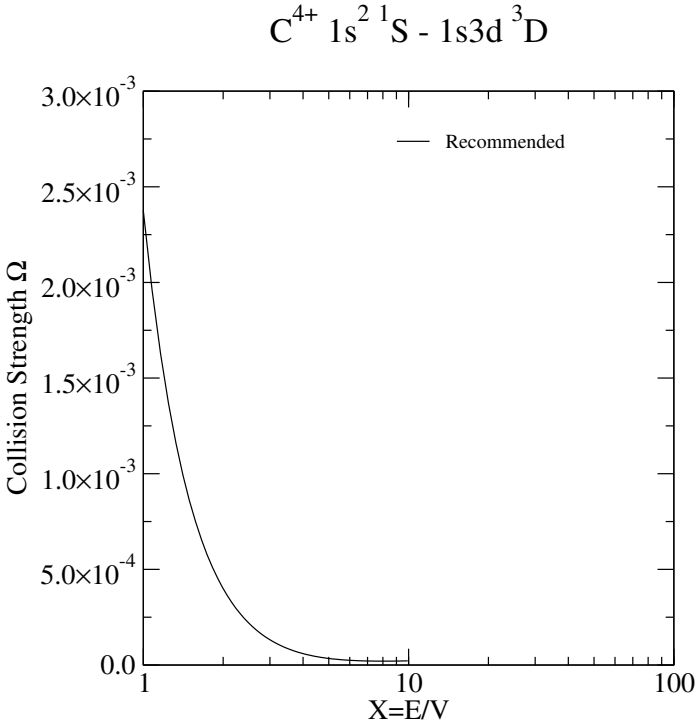

FIG. 25: Collision strength for electron-impact excitation.

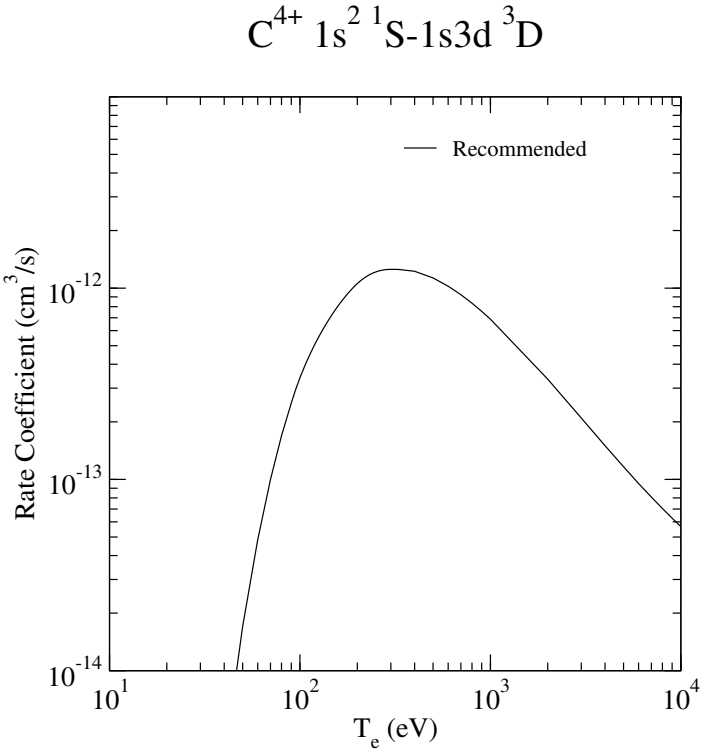

FIG. 26: Rate coefficient for electron-impact excitation.

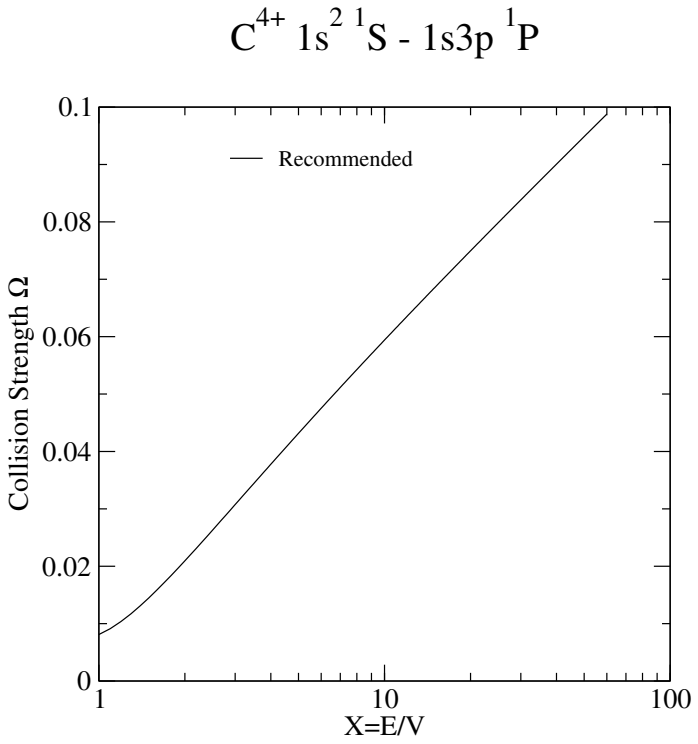

FIG. 27: Collision strength for electron-impact excitation.

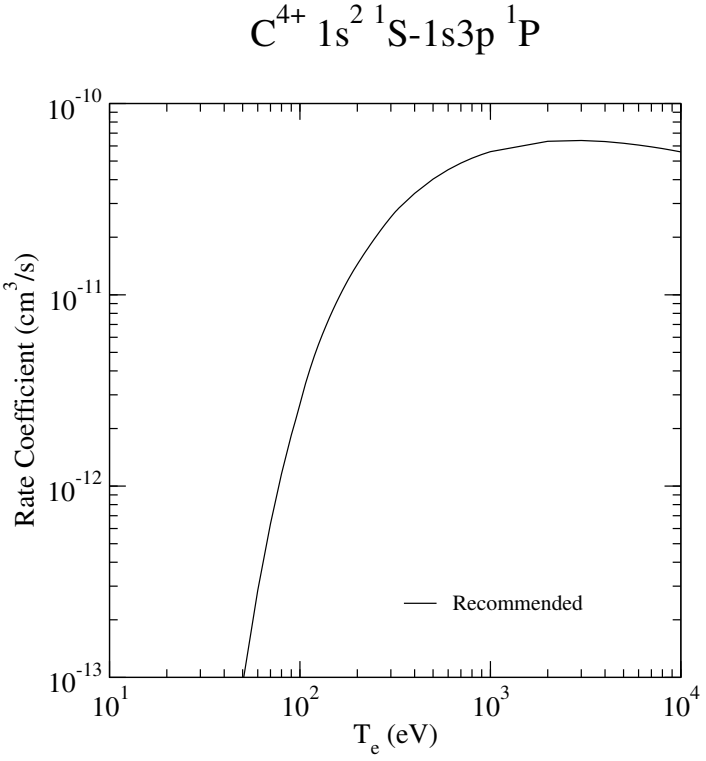

FIG. 28: Rate coefficient for electron-impact excitation.

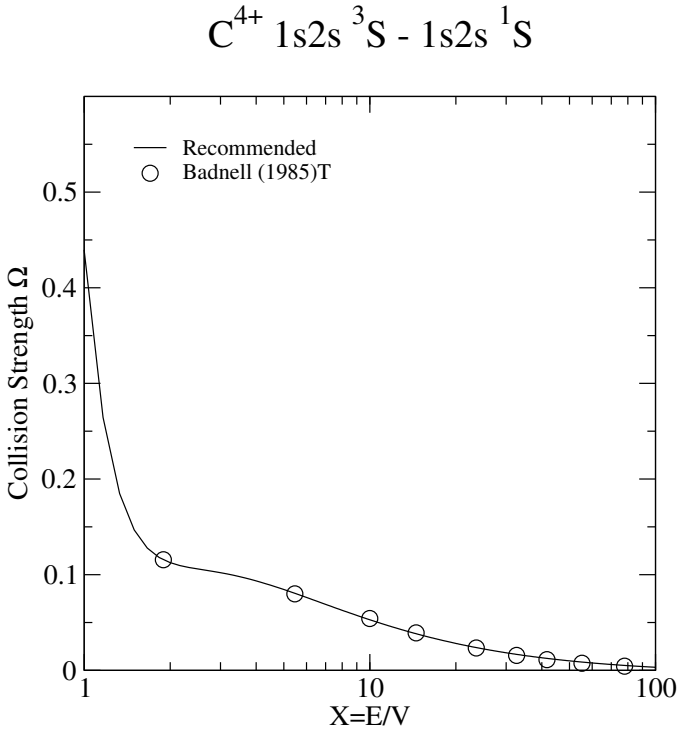

FIG. 29: Collision strength for electron-impact excitation.

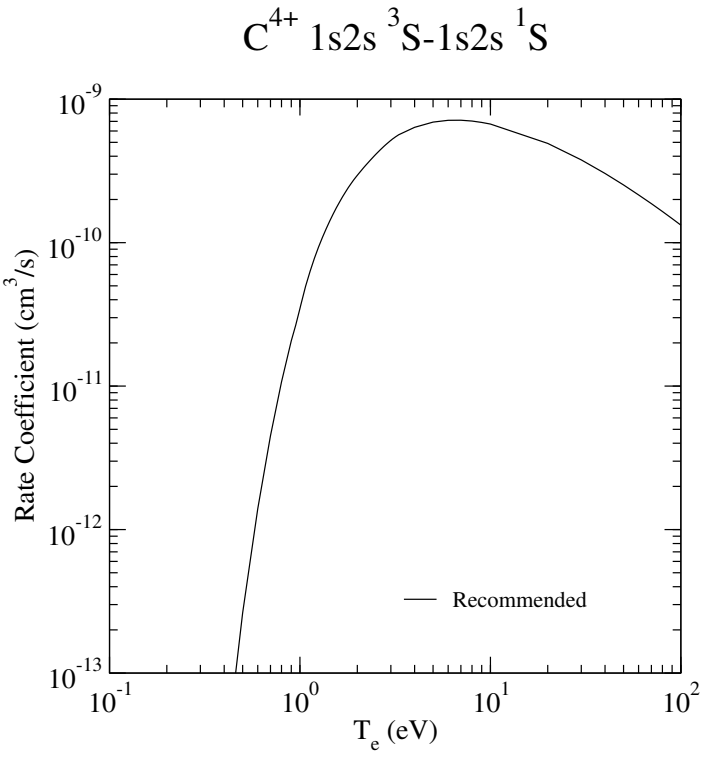

FIG. 30: Rate coefficient for electron-impact excitation.

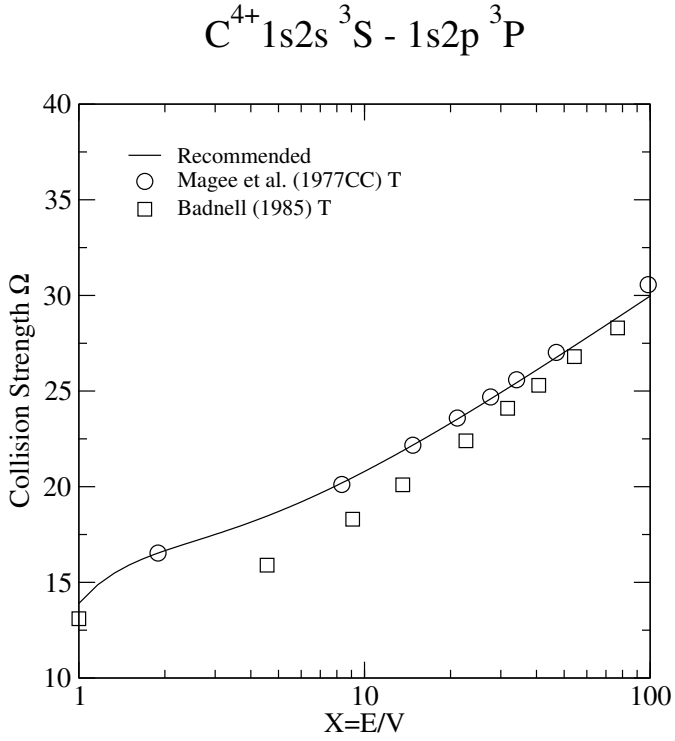

FIG. 31: Collision strength for electron-impact excitation.

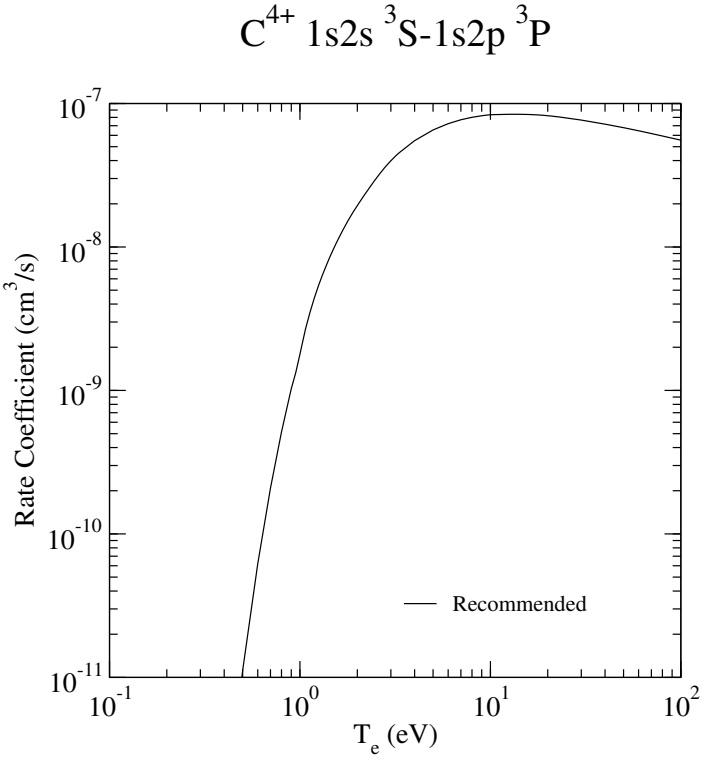

FIG. 32: Rate coefficient for electron-impact excitation.

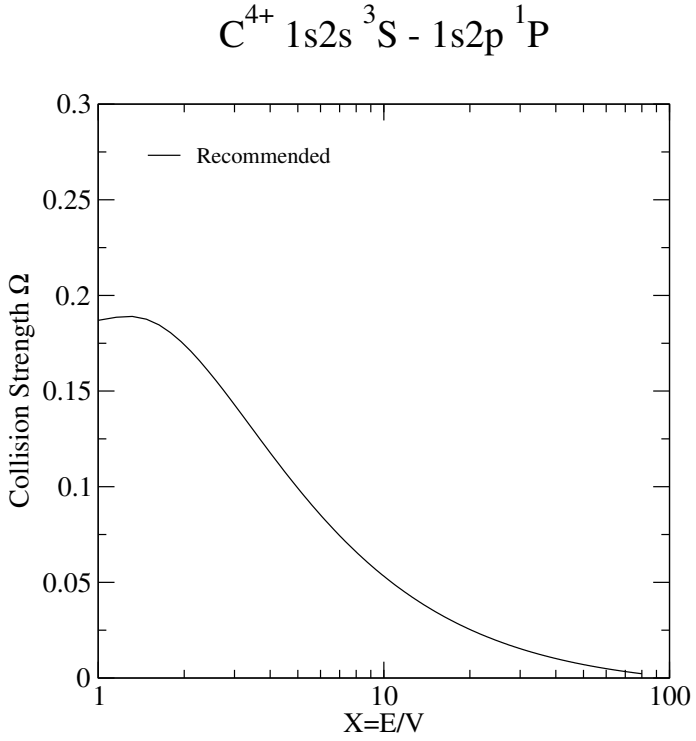

FIG. 33: Collision strength for electron-impact excitation.

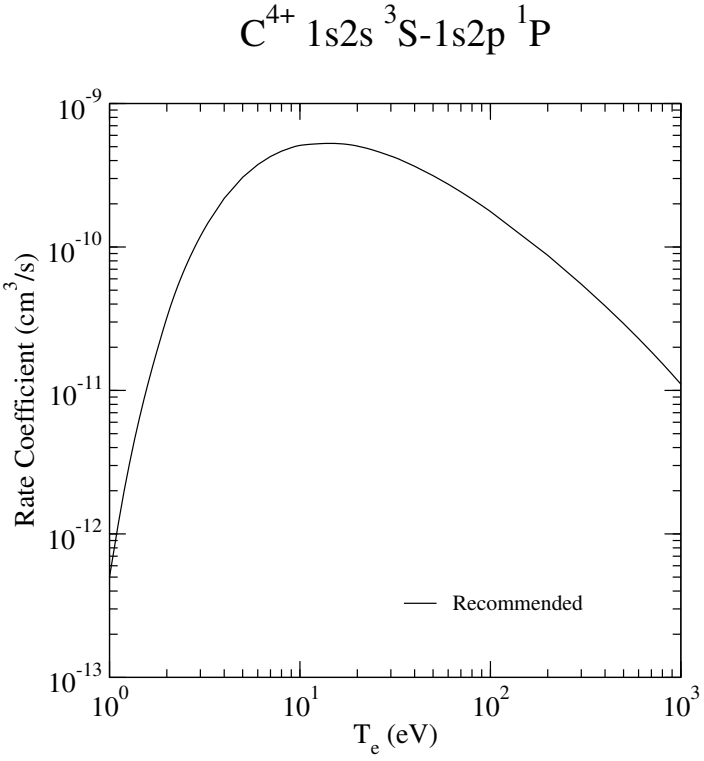

FIG. 34: Rate coefficient for electron-impact excitation.

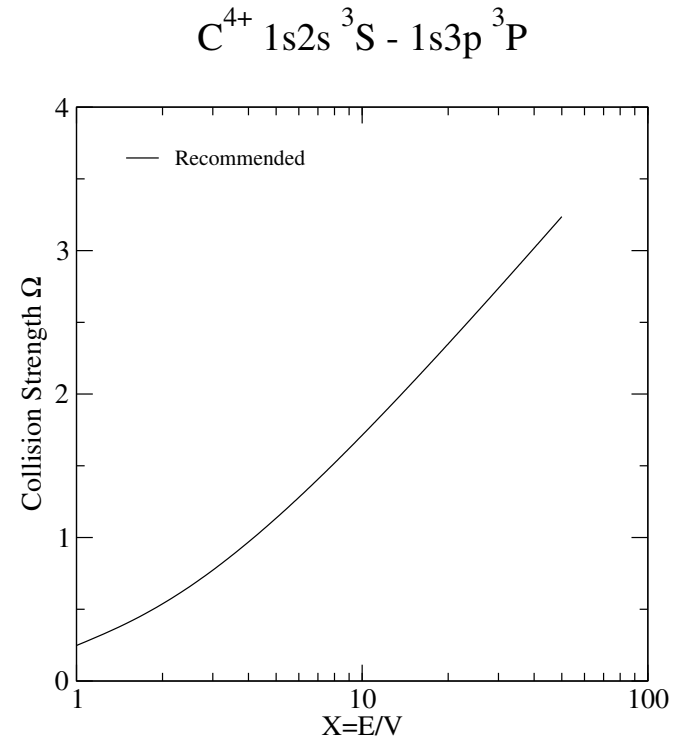

FIG. 35: Collision strength for electron-impact excitation.

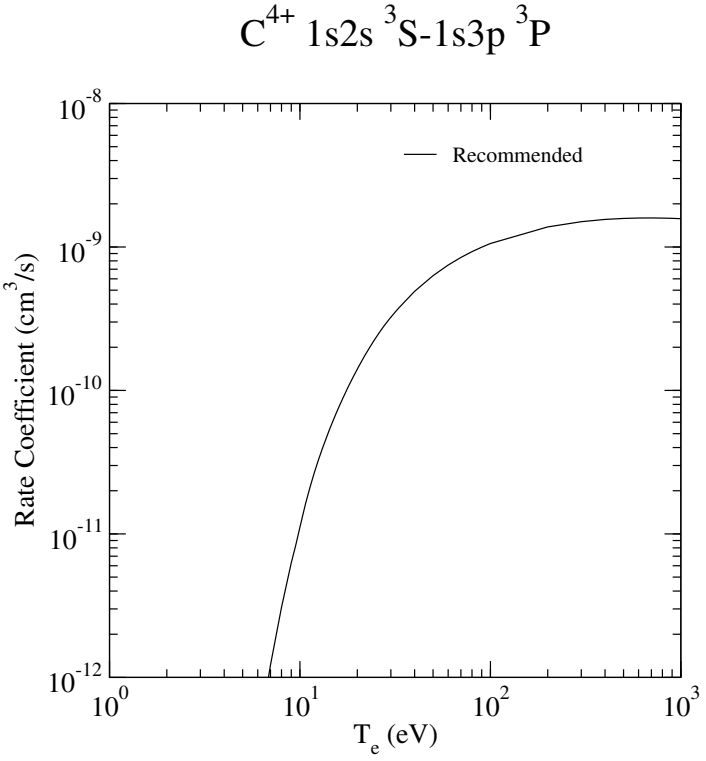

FIG. 36: Rate coefficient for electron-impact excitation.

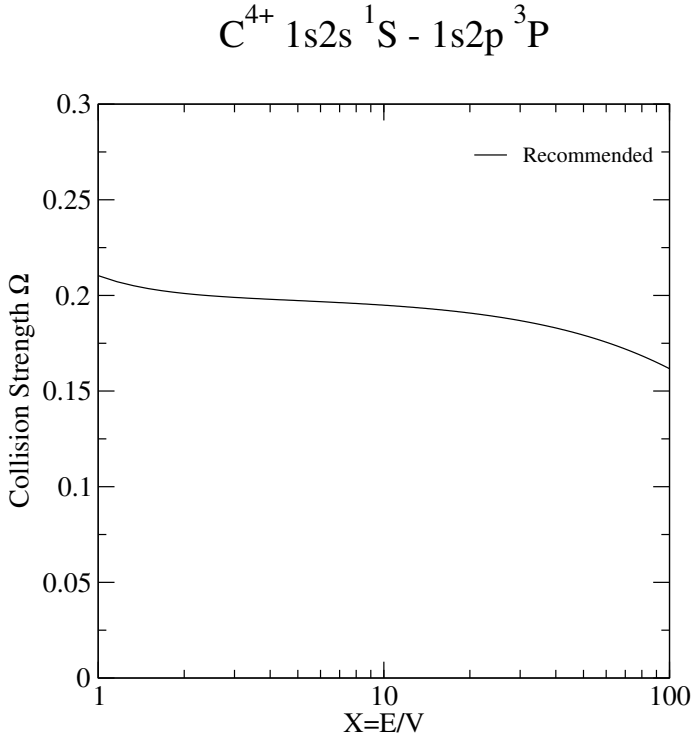

FIG. 37: Collision strength for electron-impact excitation.

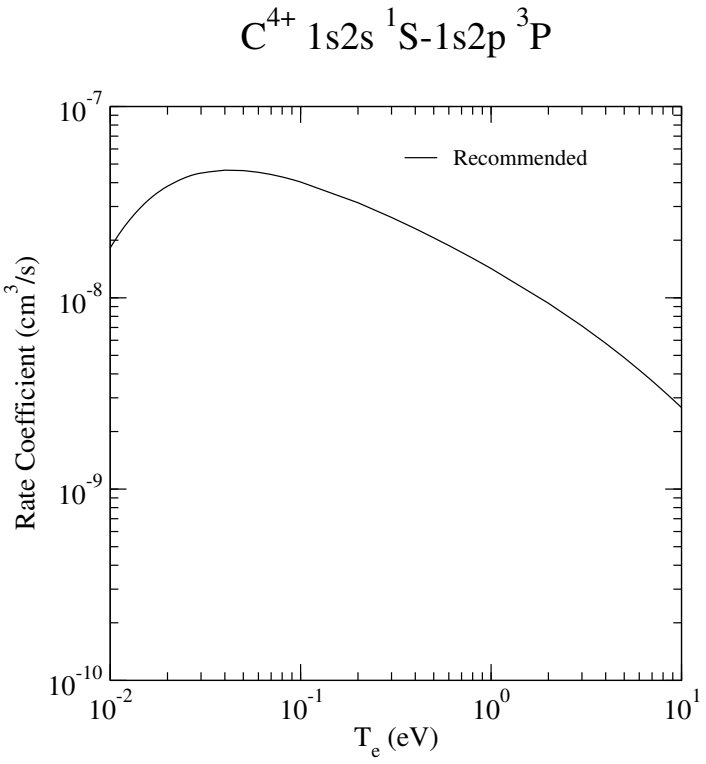

FIG. 38: Rate coefficient for electron-impact excitation.

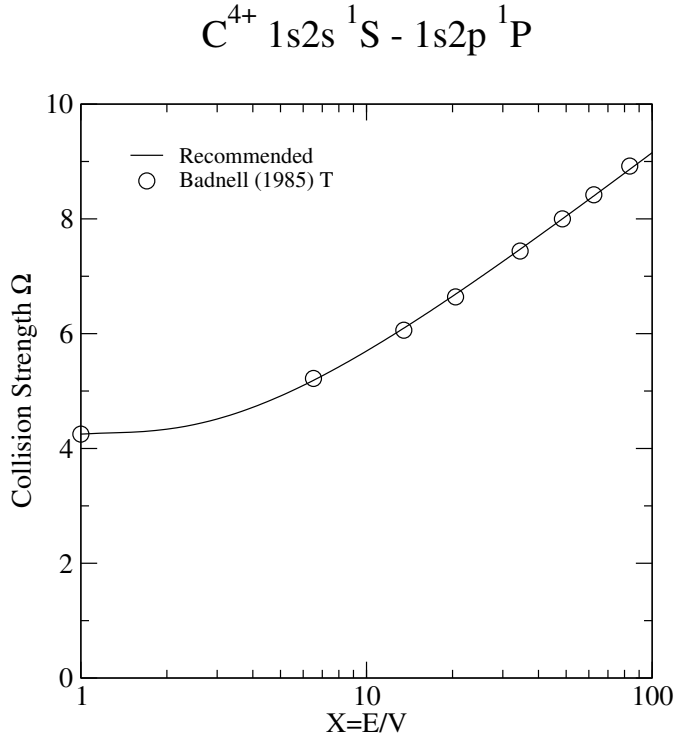

FIG. 39: Collision strength for electron-impact excitation.

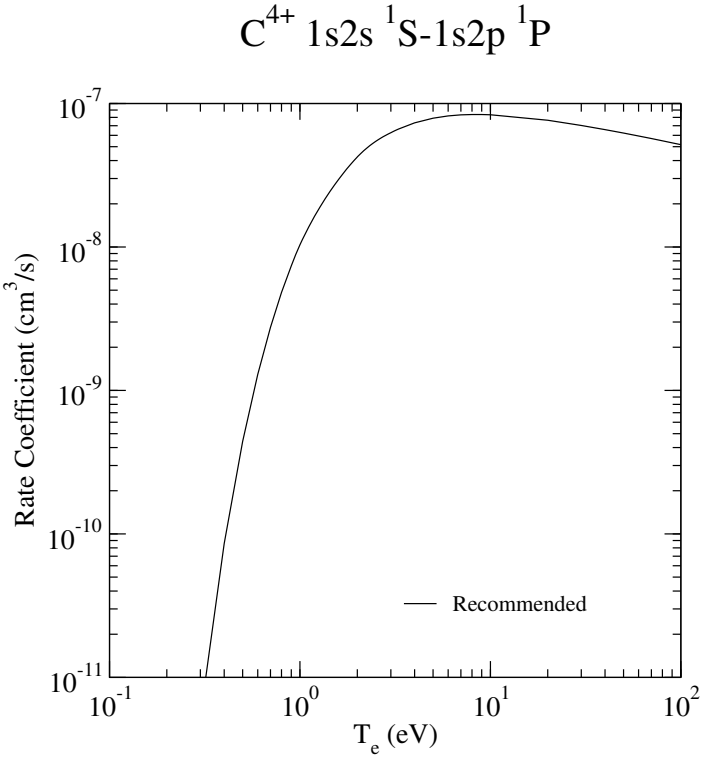

FIG. 40: Rate coefficient for electron-impact excitation.

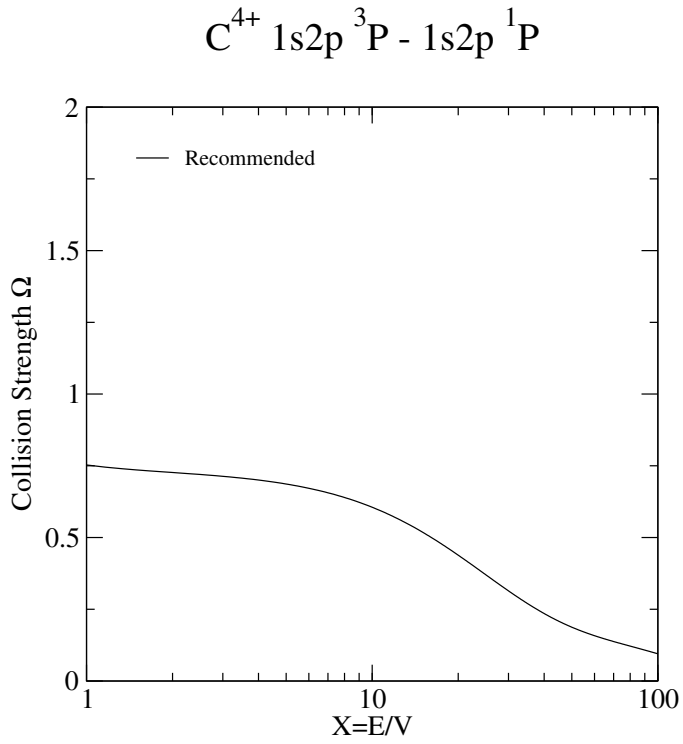

FIG. 41: Collision strength for electron-impact excitation.

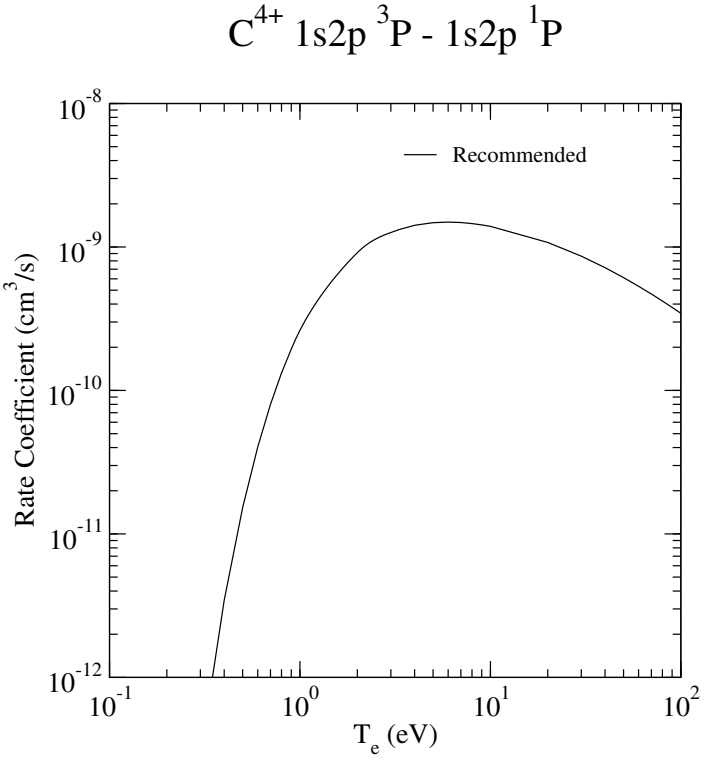

FIG. 42: Rate coefficient for electron-impact excitation.

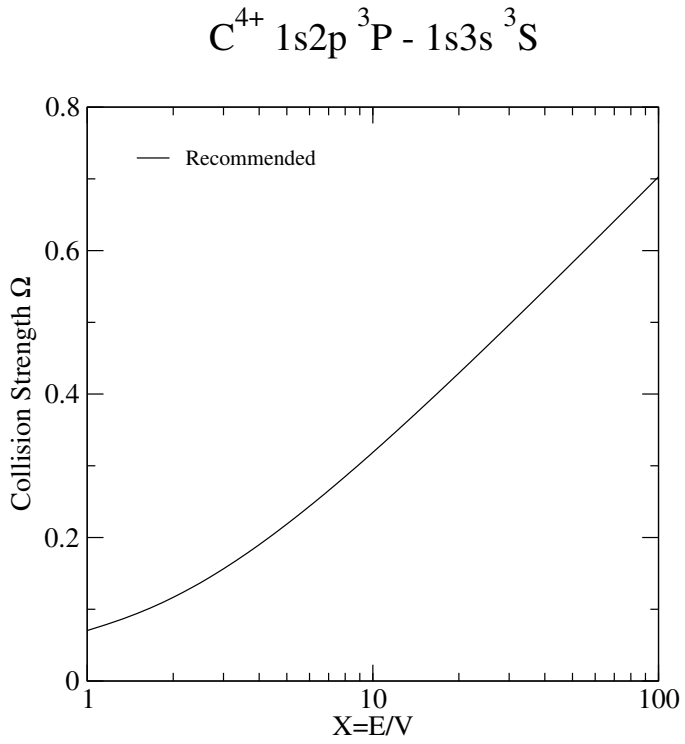

FIG. 43: Collision strength for electron-impact excitation.

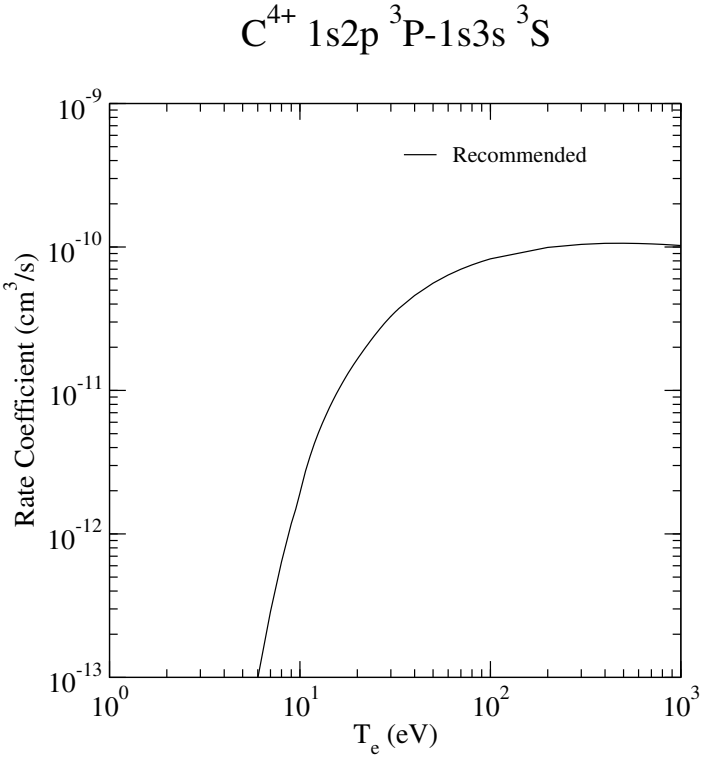

FIG. 44: Rate coefficient for electron-impact excitation.

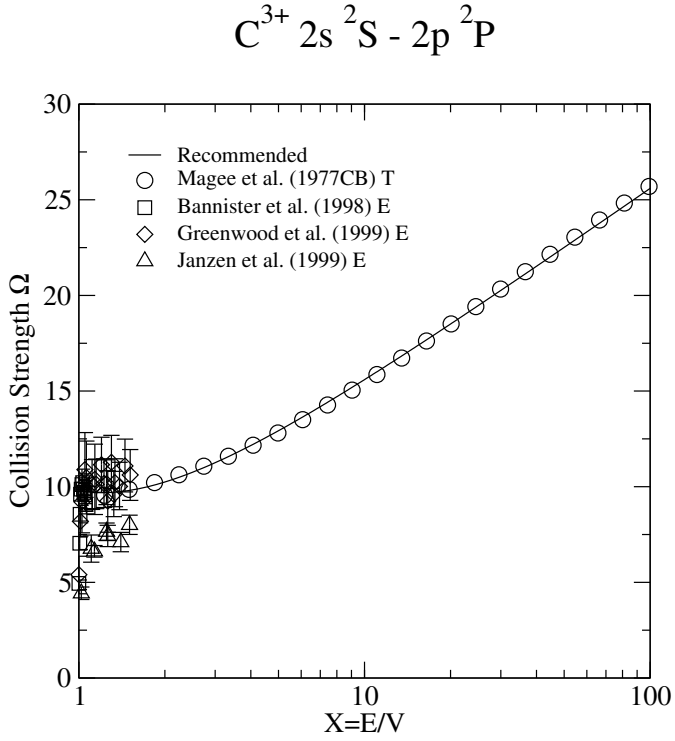

FIG. 45: Collision strength for electron-impact excitation.

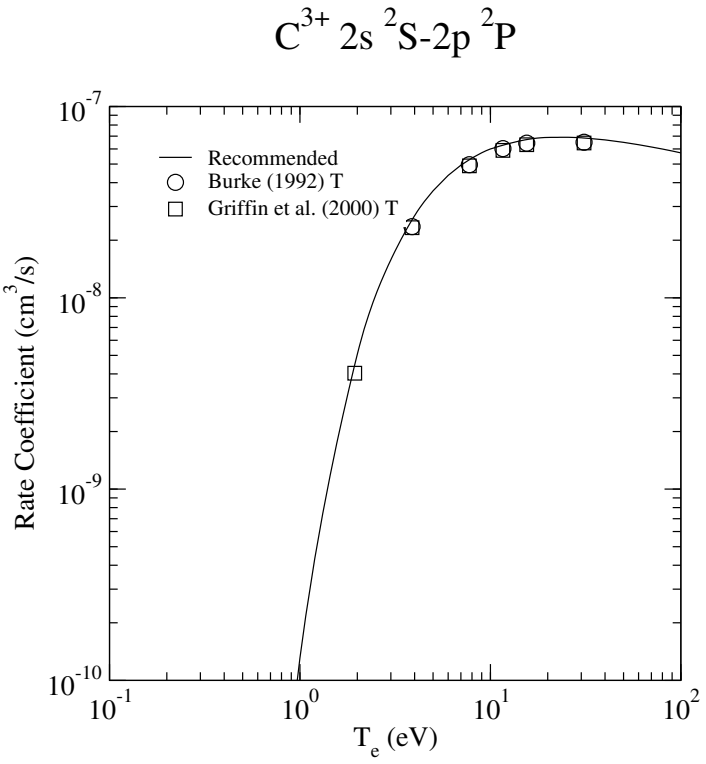

FIG. 46: Rate coefficient for electron-impact excitation.

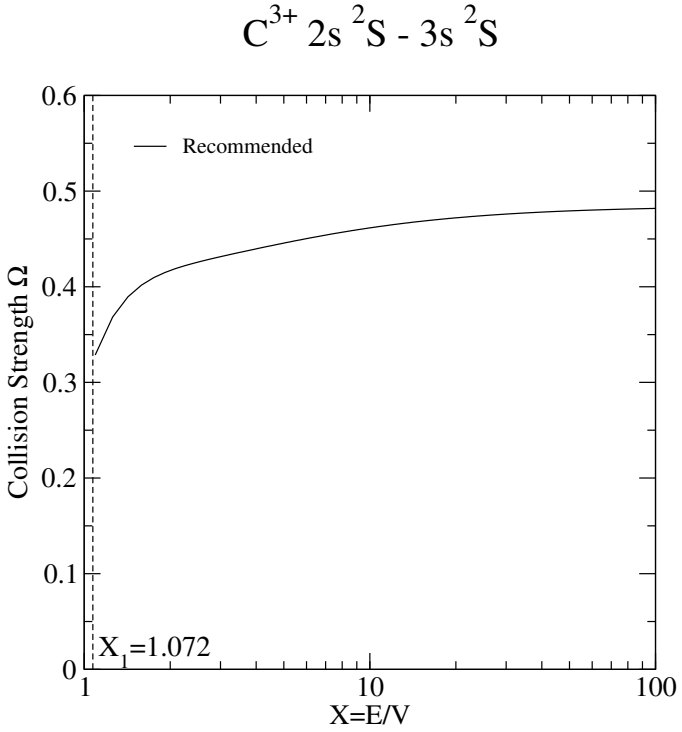

FIG. 47: Collision strength for electron-impact excitation.

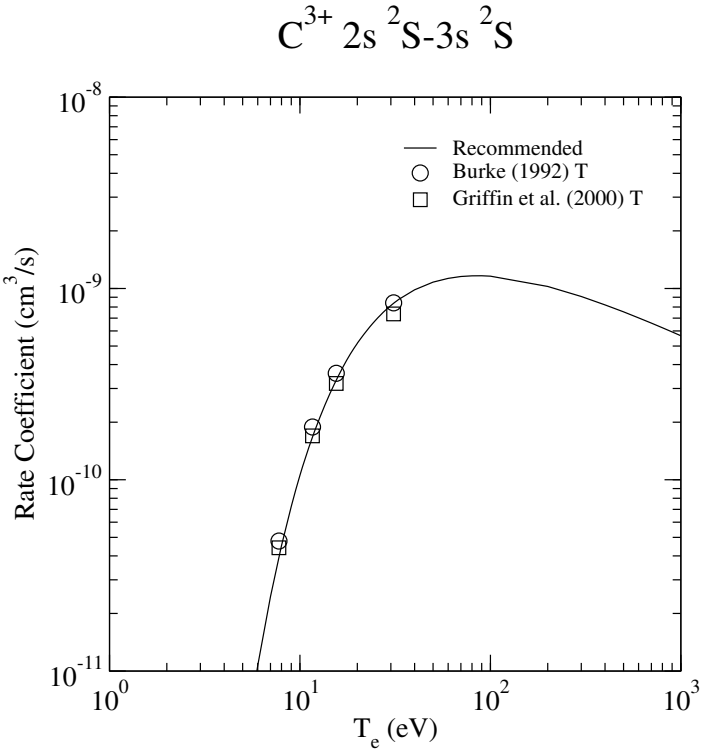

FIG. 48: Rate coefficient for electron-impact excitation.

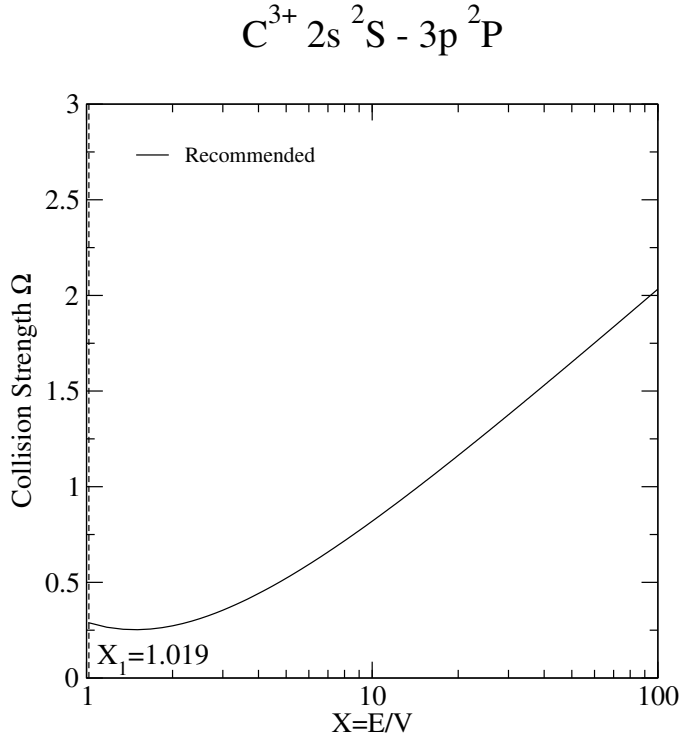

FIG. 49: Collision strength for electron-impact excitation.

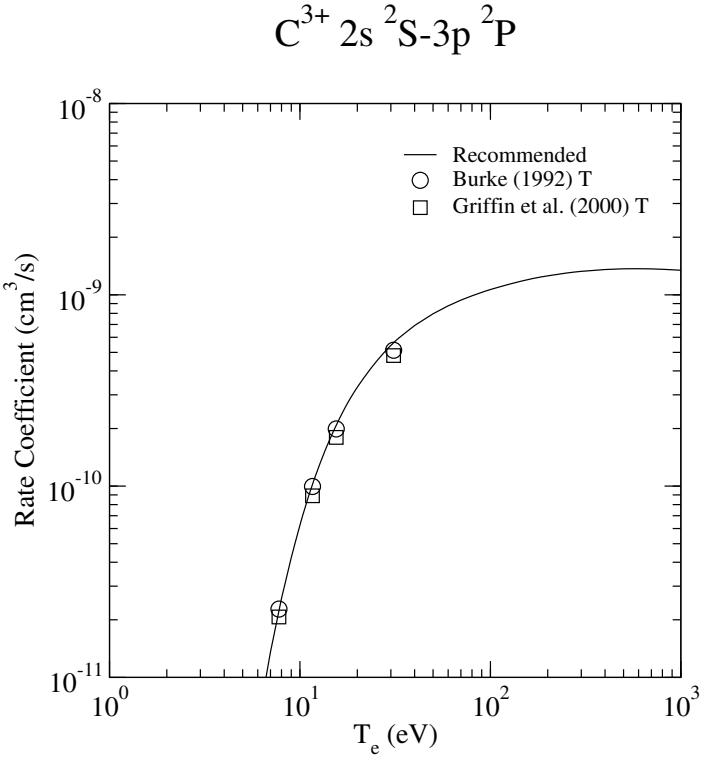

FIG. 50: Rate coefficient for electron-impact excitation.

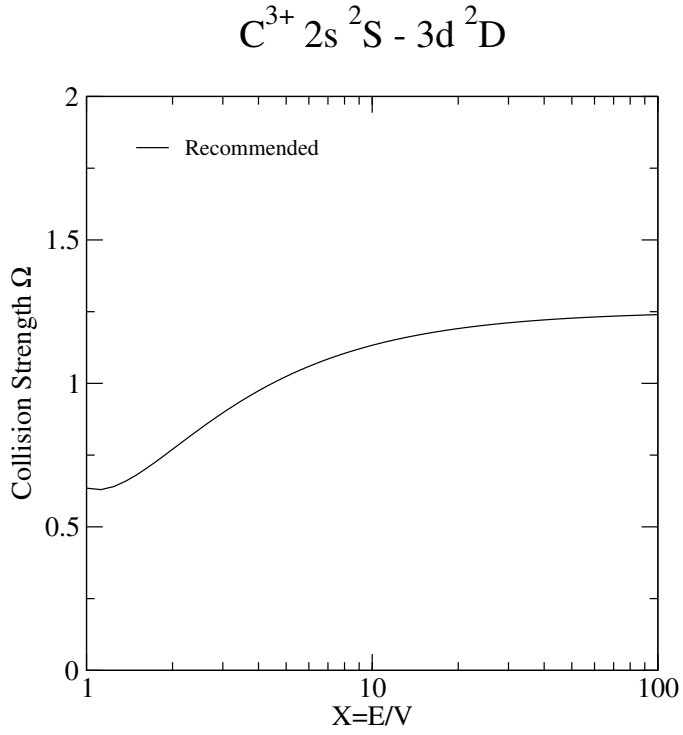

FIG. 51: Collision strength for electron-impact excitation.

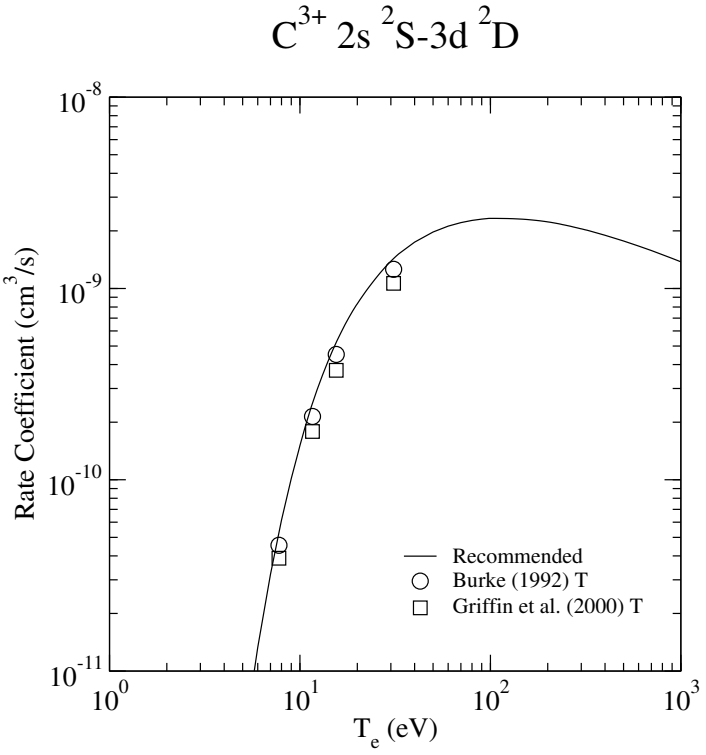

FIG. 52: Rate coefficient for electron-impact excitation.

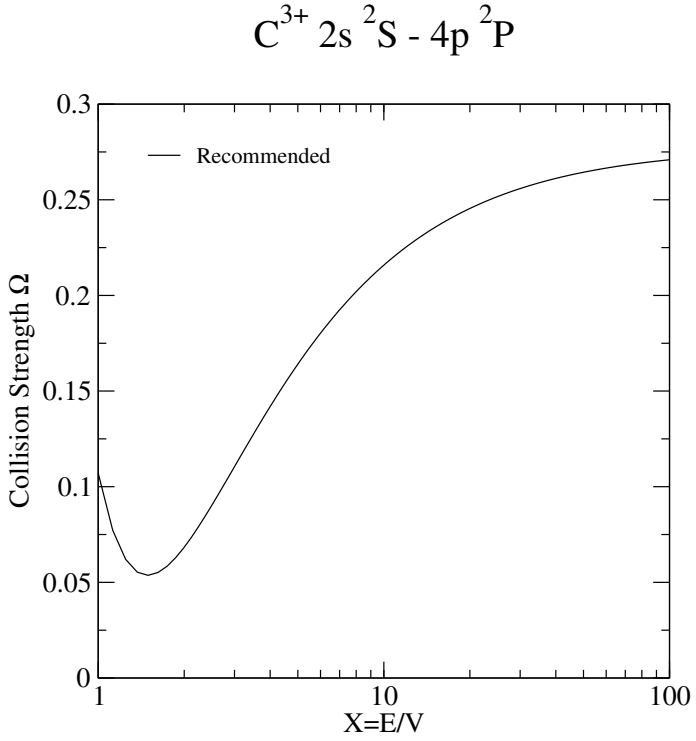

FIG. 53: Collision strength for electron-impact excitation.

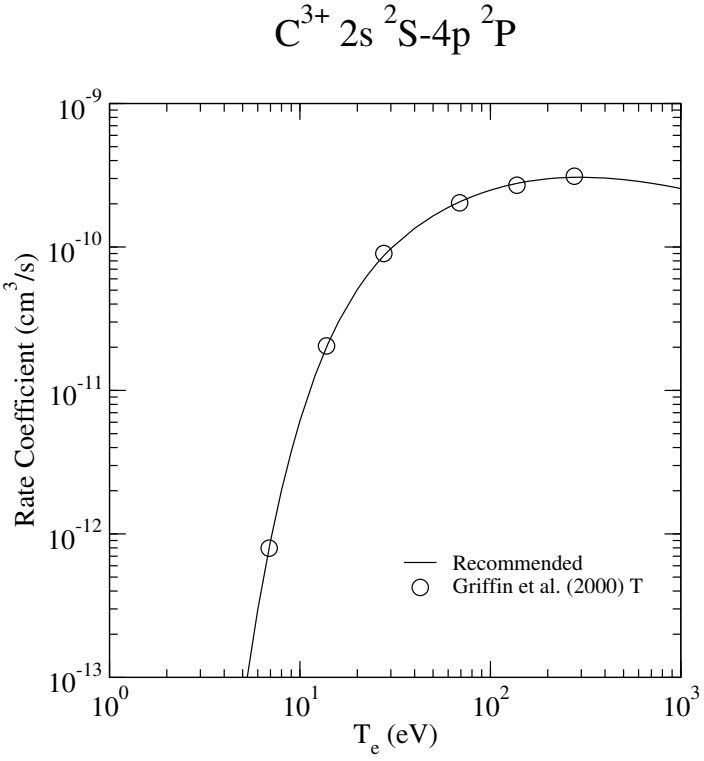

FIG. 54: Rate coefficient for electron-impact excitation.

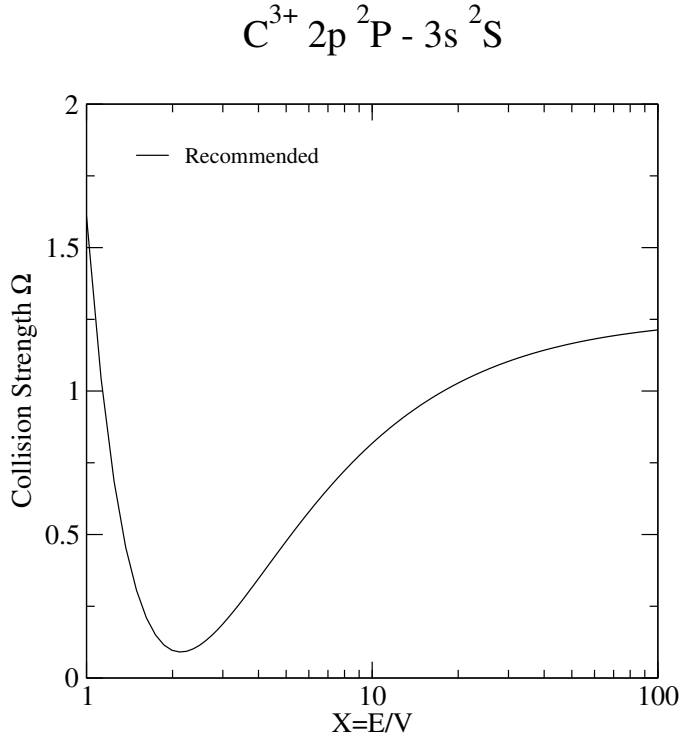

FIG. 55: Collision strength for electron-impact excitation.

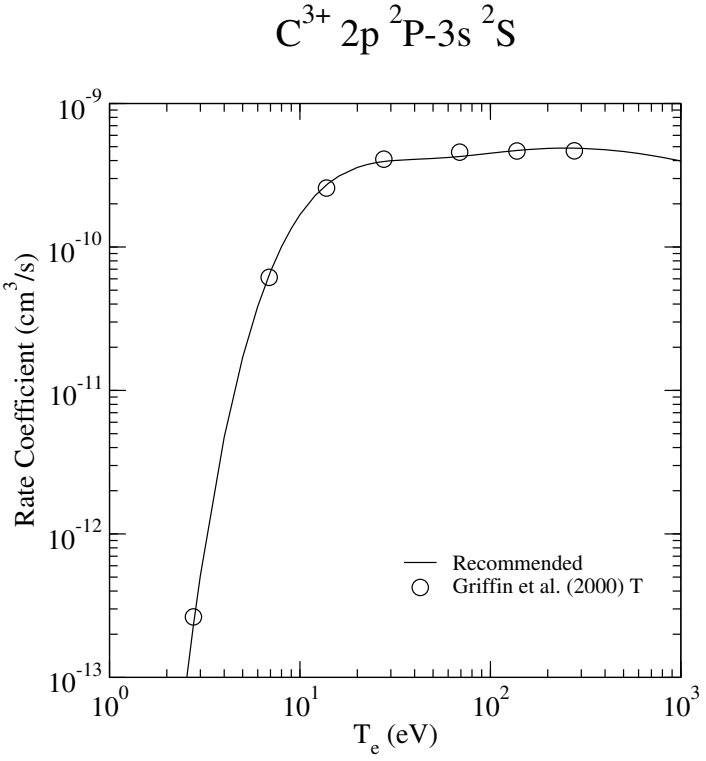

FIG. 56: Rate coefficient for electron-impact excitation.

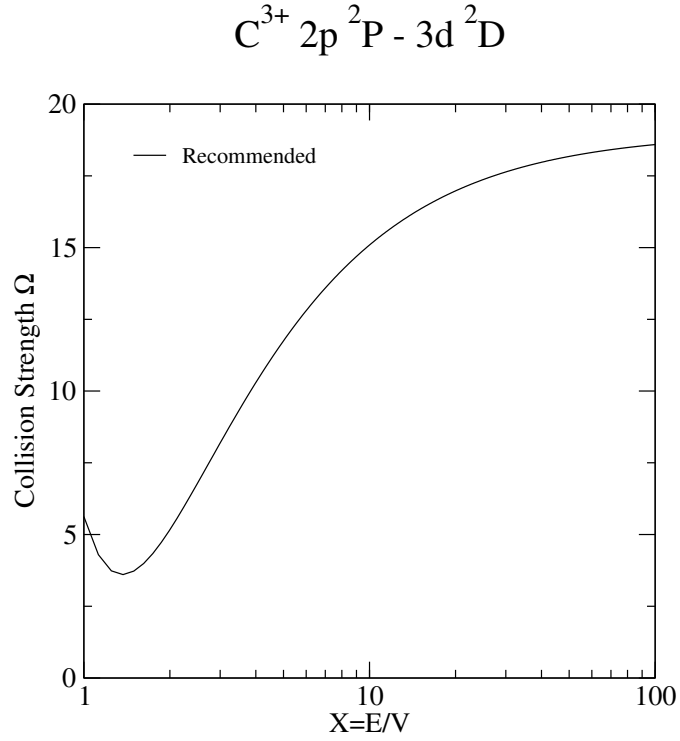

FIG. 57: Collision strength for electron-impact excitation.

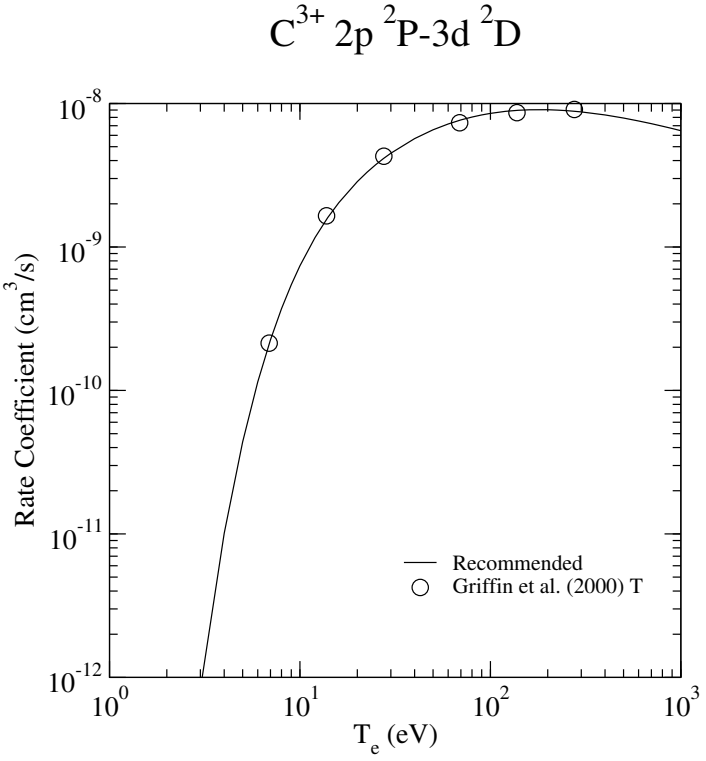

FIG. 58: Rate coefficient for electron-impact excitation.

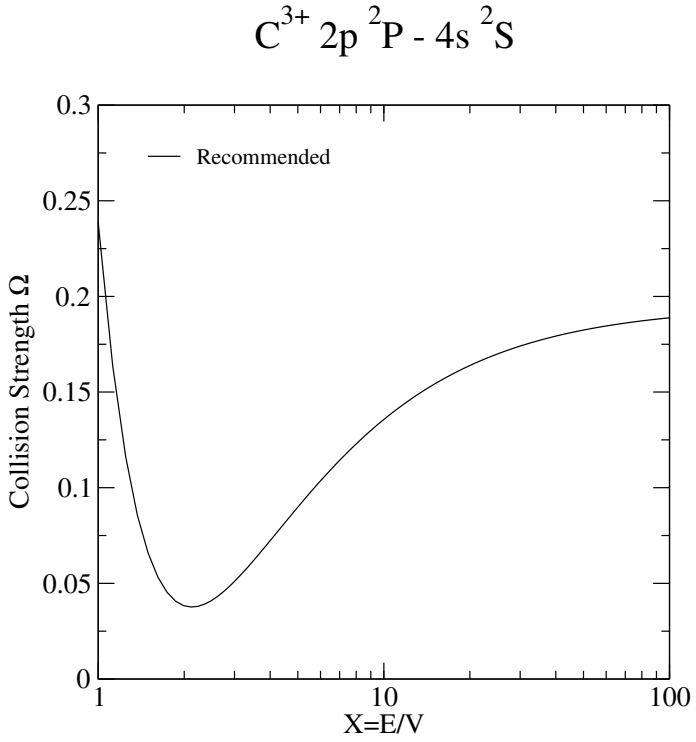

FIG. 59: Collision strength for electron-impact excitation.

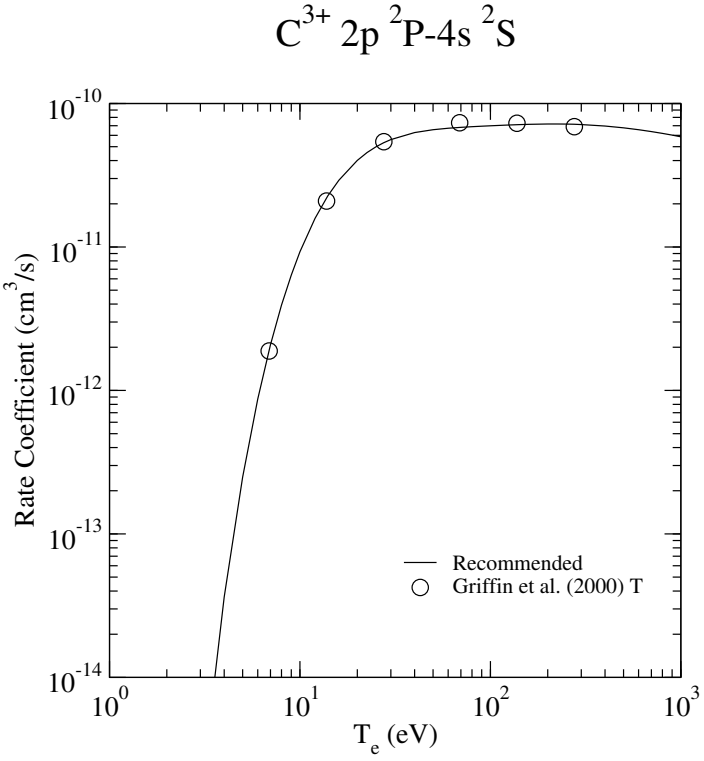

FIG. 60: Rate coefficient for electron-impact excitation.

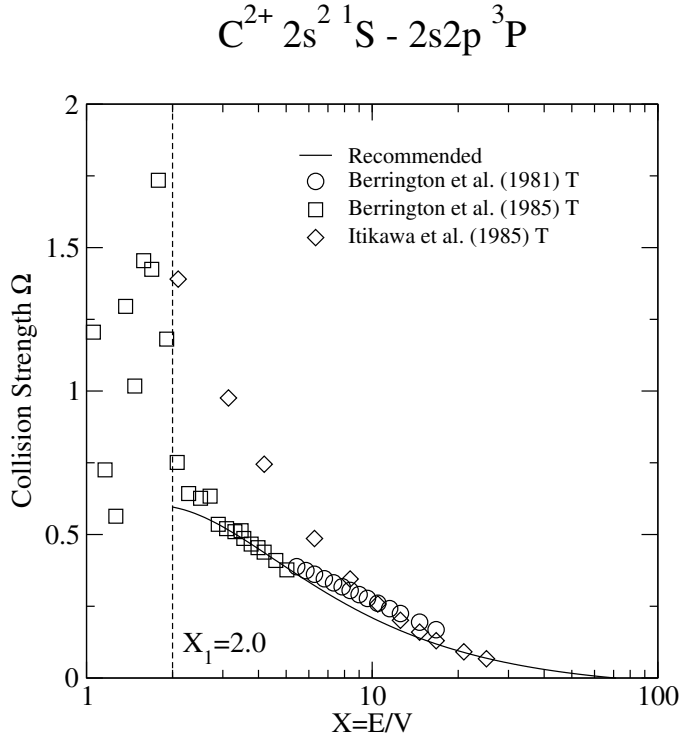

FIG. 61: Collision strength for electron-impact excitation.

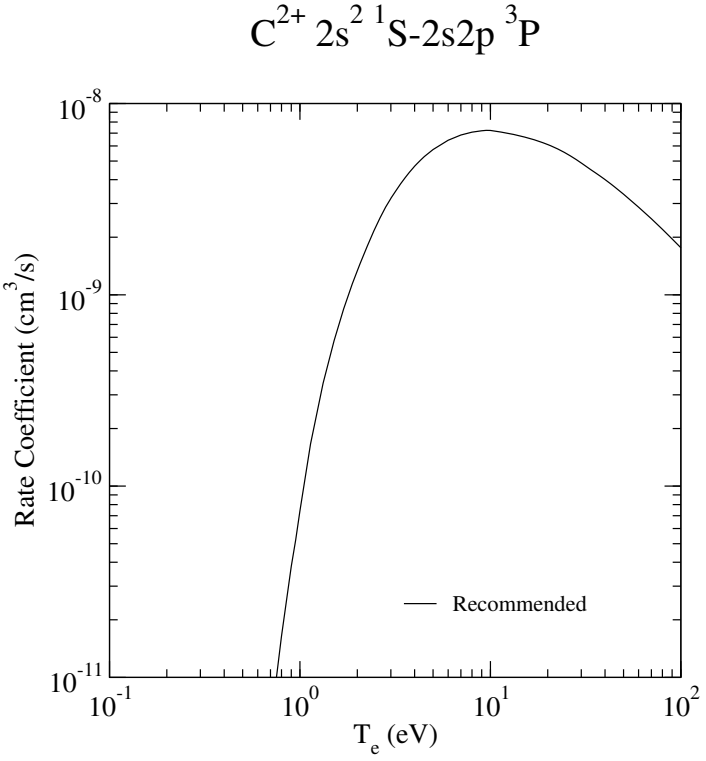

FIG. 62: Rate coefficient for electron-impact excitation.

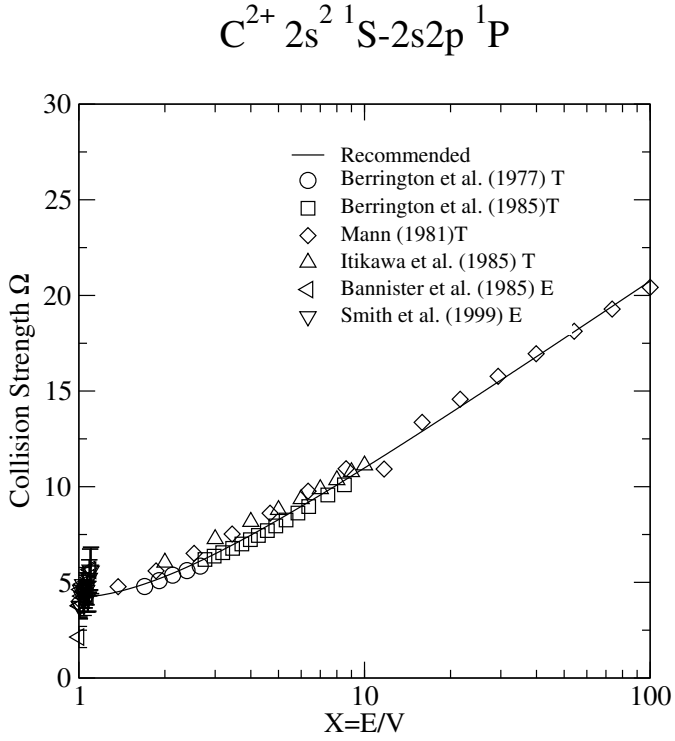

FIG. 63: Collision strength for electron-impact excitation.

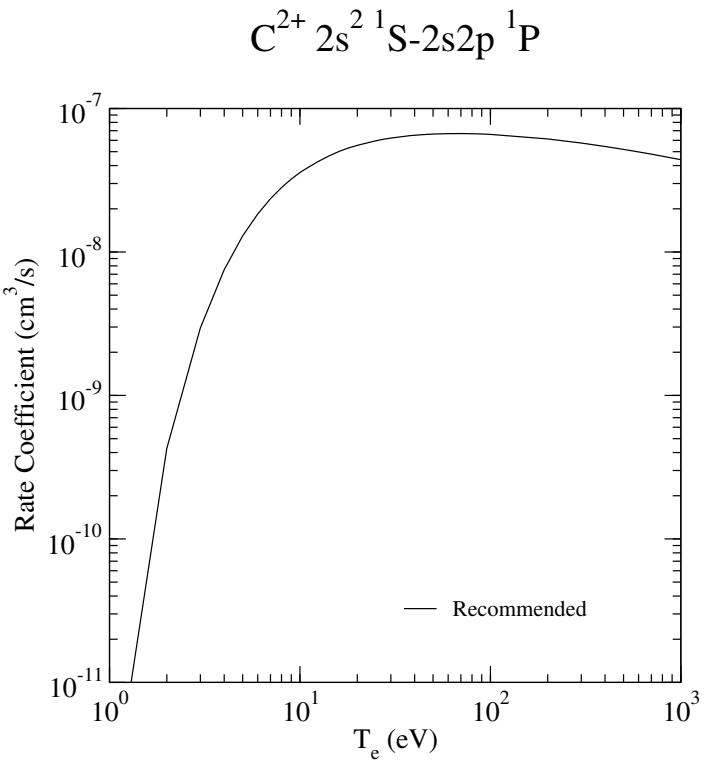

FIG. 64: Rate coefficient for electron-impact excitation.

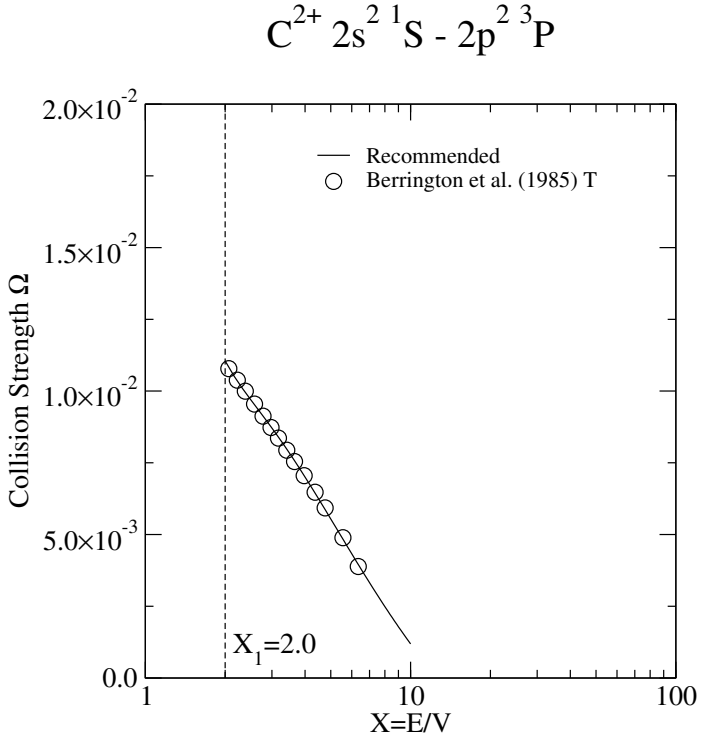

FIG. 65: Collision strength for electron-impact excitation.

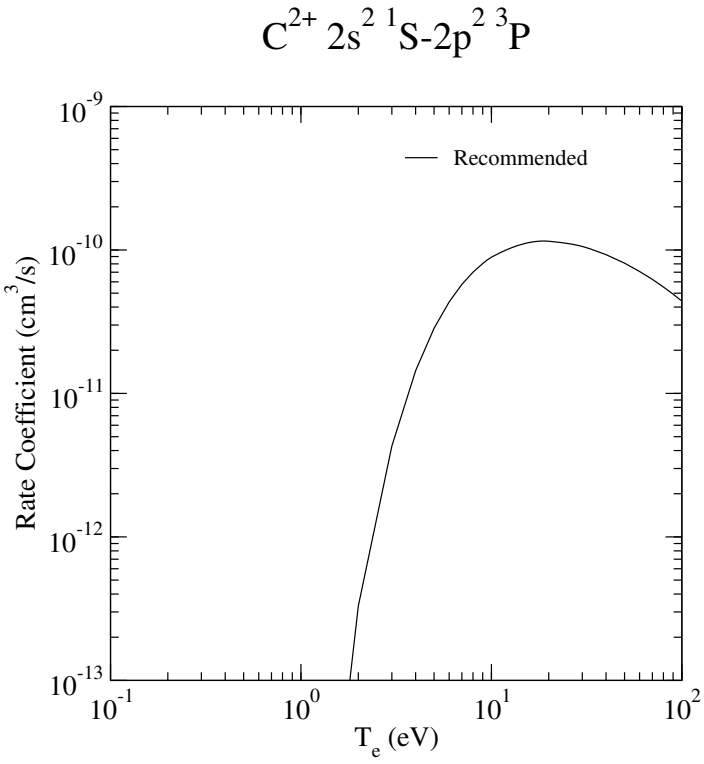

FIG. 66: Rate coefficient for electron-impact excitation.

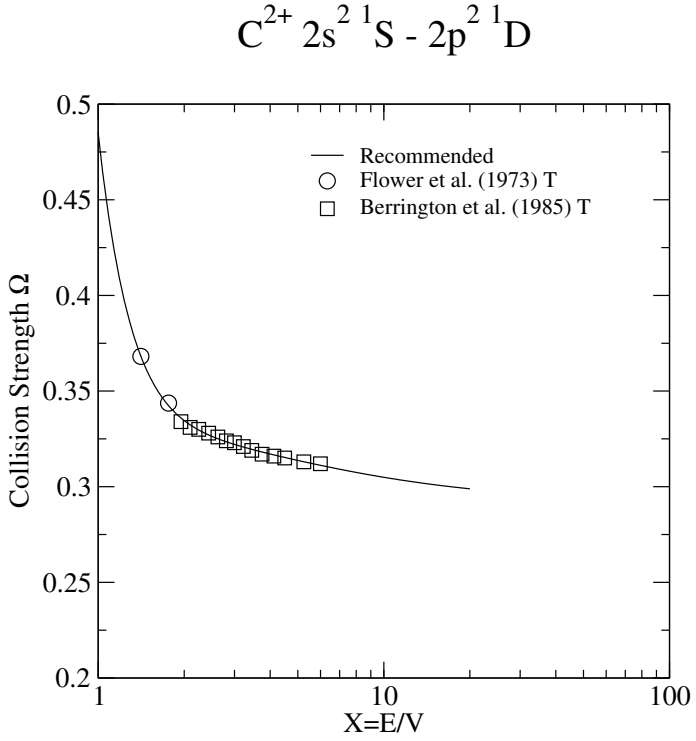

FIG. 67: Collision strength for electron-impact excitation.

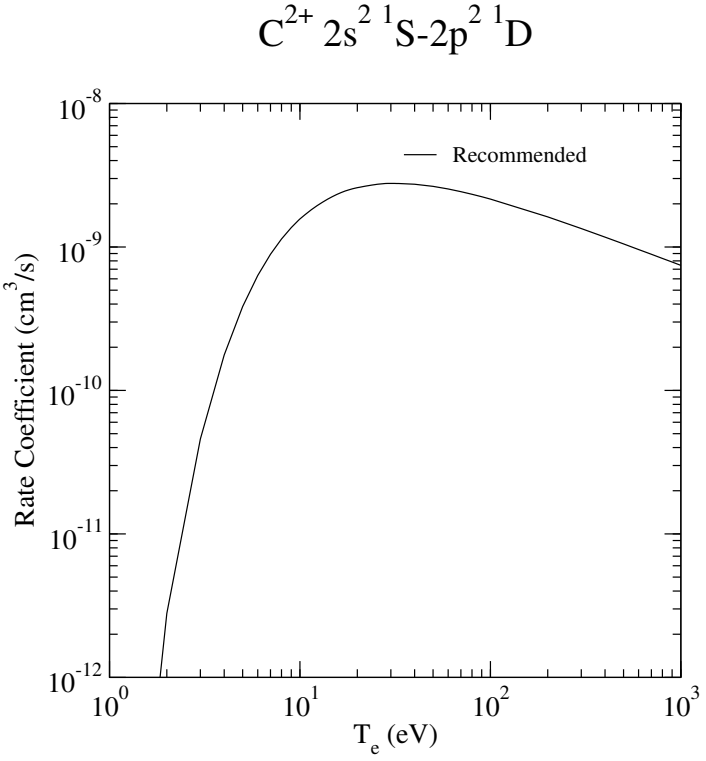

FIG. 68: Rate coefficient for electron-impact excitation.

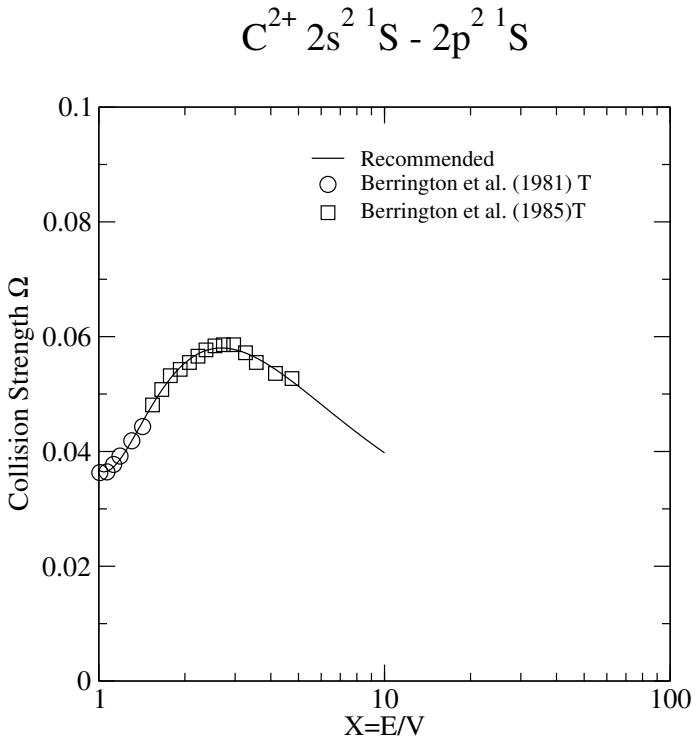

FIG. 69: Collision strength for electron-impact excitation.

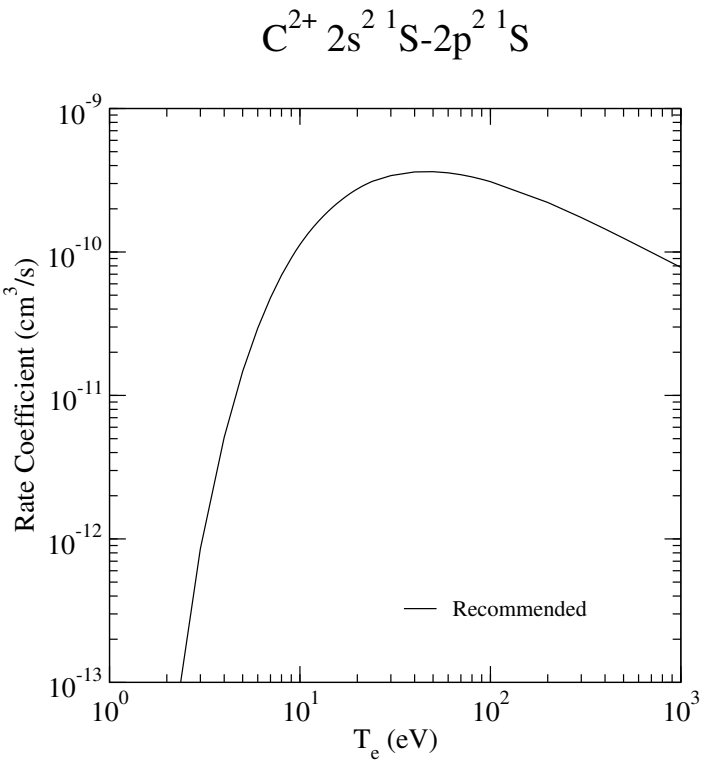

FIG. 70: Rate coefficient for electron-impact excitation.

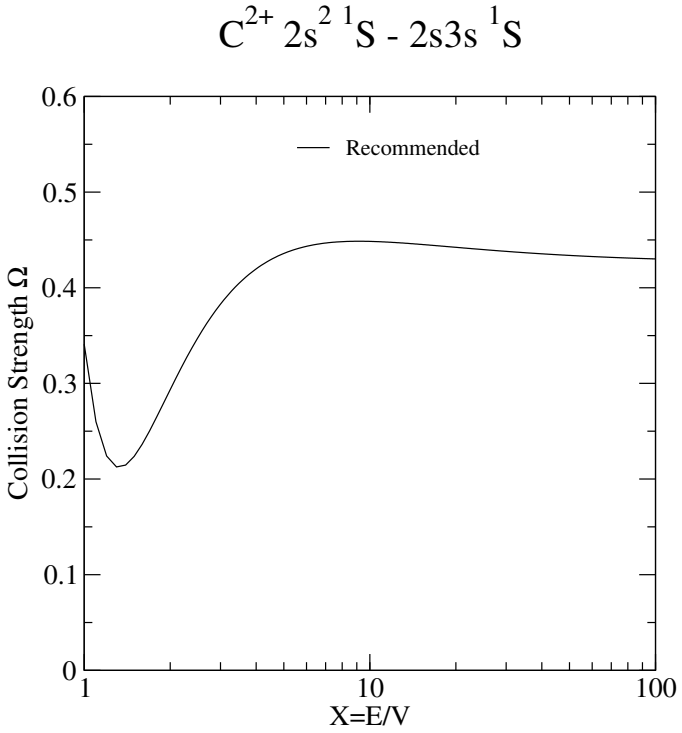

FIG. 71: Collision strength for electron-impact excitation.

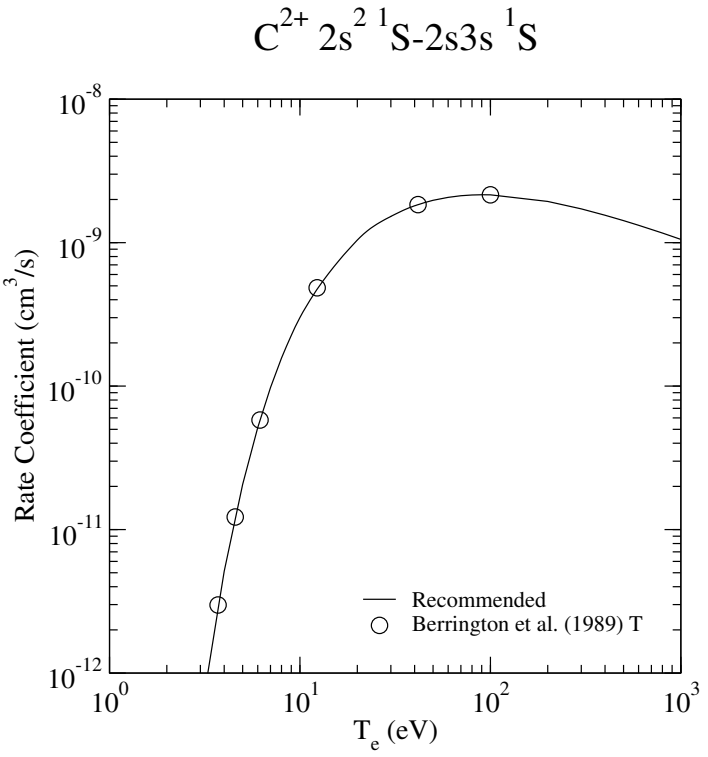

FIG. 72: Rate coefficient for electron-impact excitation.

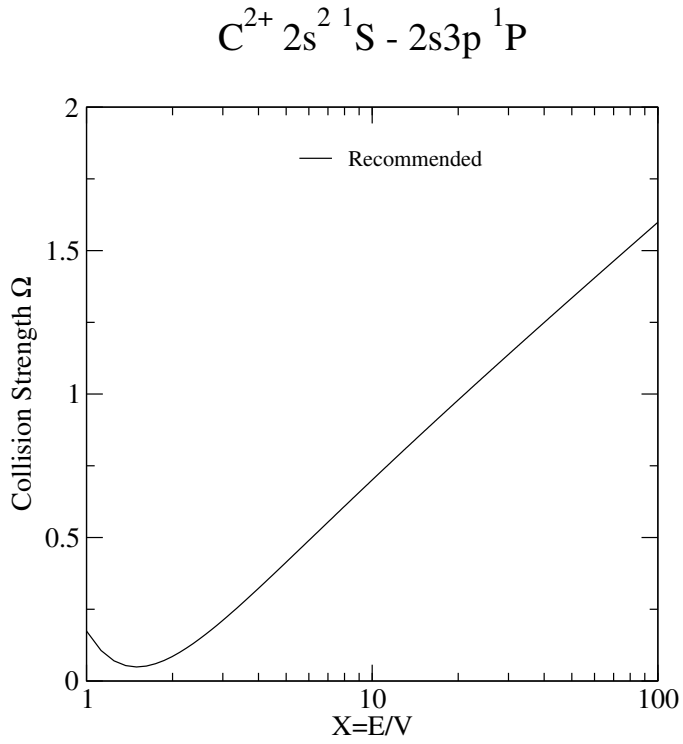

FIG. 73: Collision strength for electron-impact excitation.

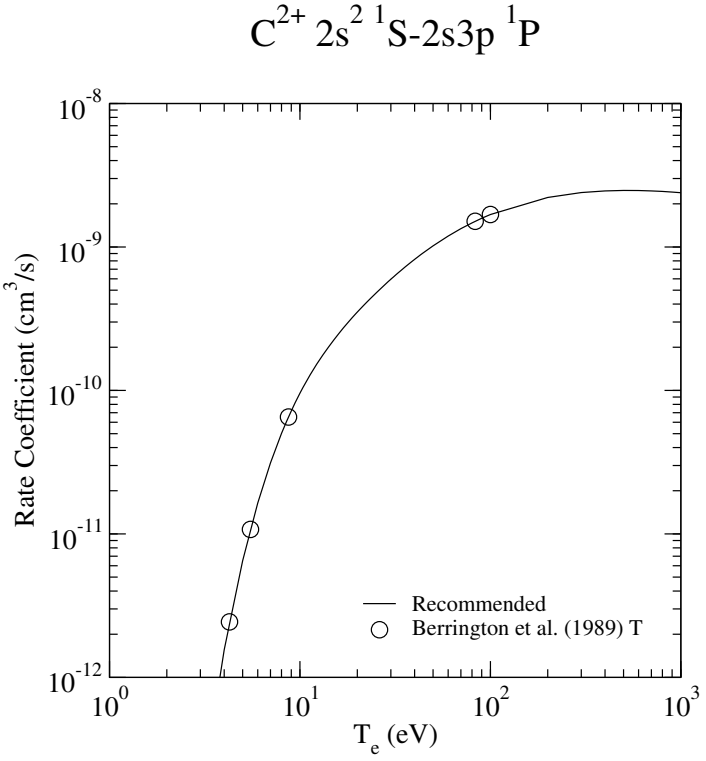

FIG. 74: Rate coefficient for electron-impact excitation.

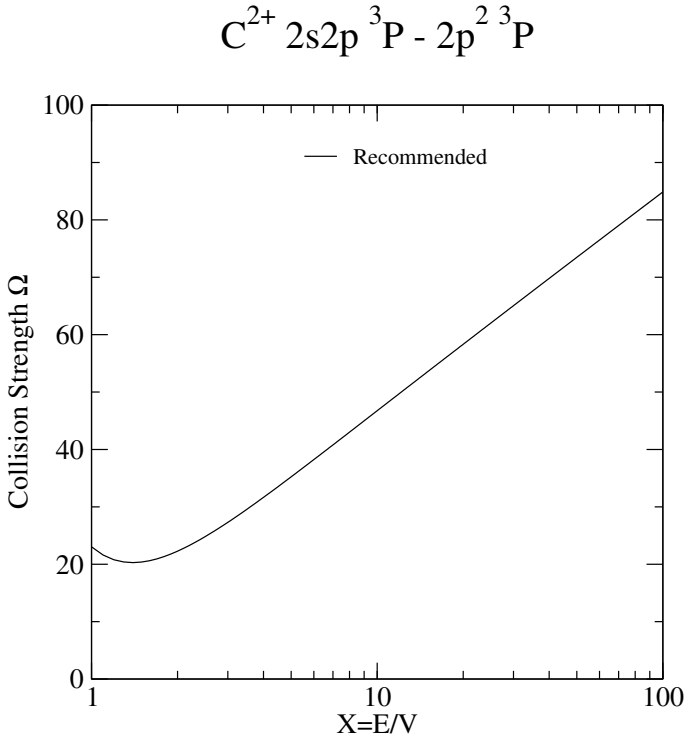

FIG. 75: Collision strength for electron-impact excitation.

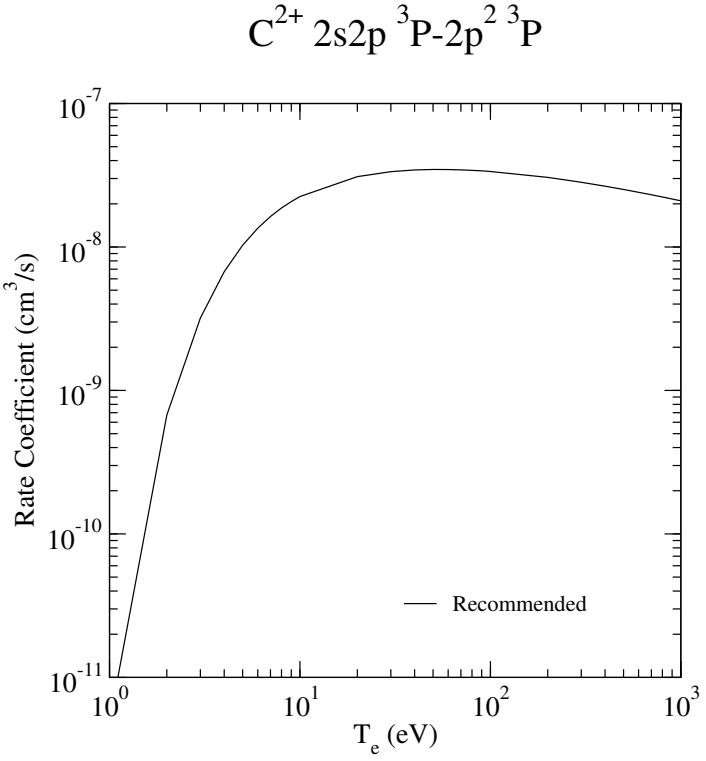

FIG. 76: Rate coefficient for electron-impact excitation.

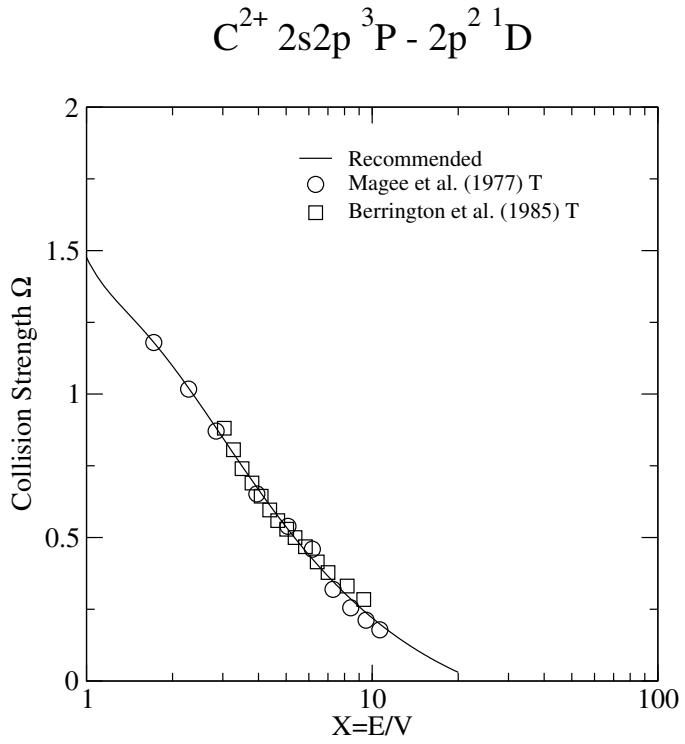

FIG. 77: Collision strength for electron-impact excitation.

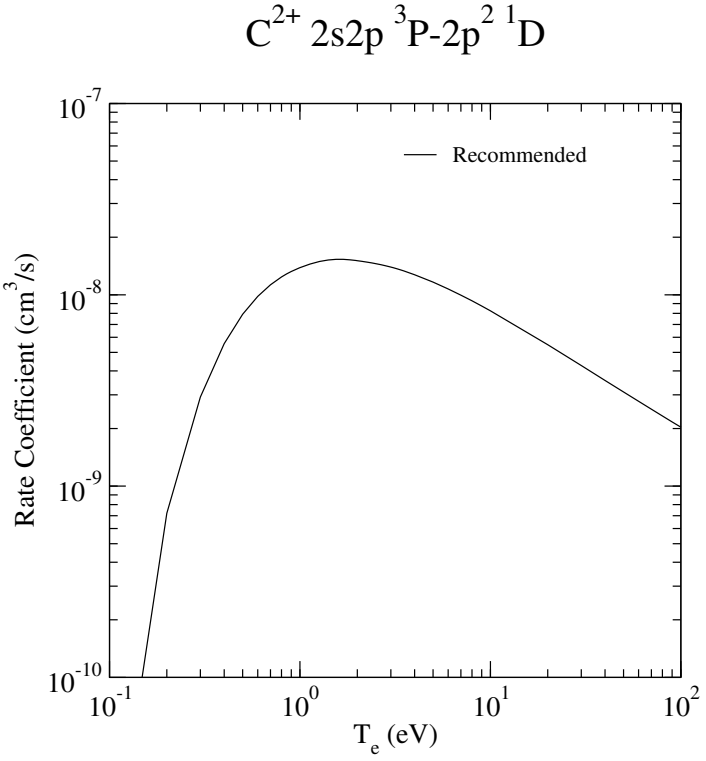

FIG. 78: Rate coefficient for electron-impact excitation.

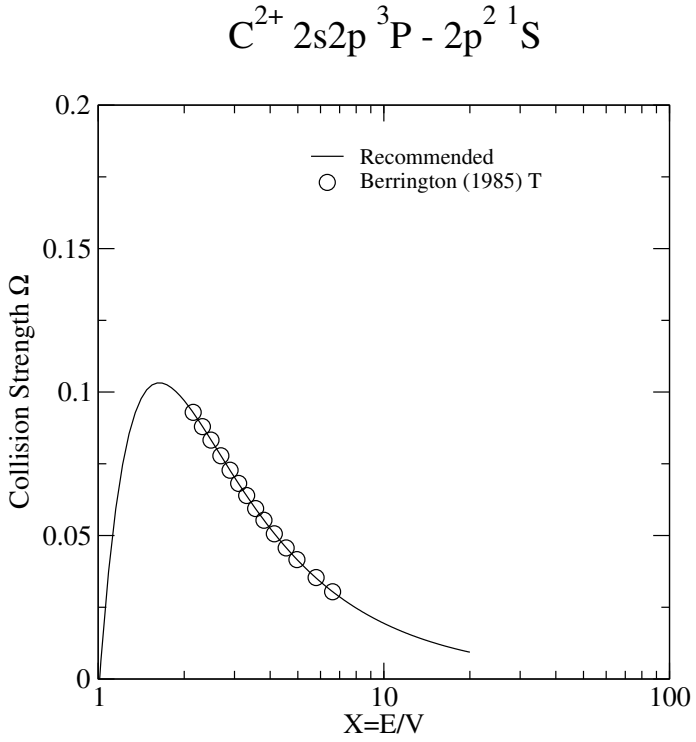

FIG. 79: Collision strength for electron-impact excitation.

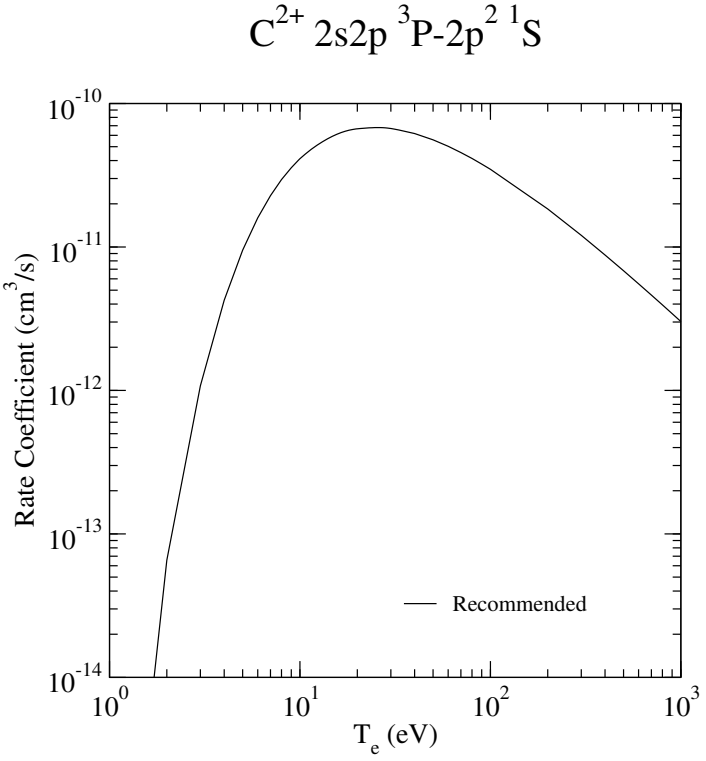

FIG. 80: Rate coefficient for electron-impact excitation.

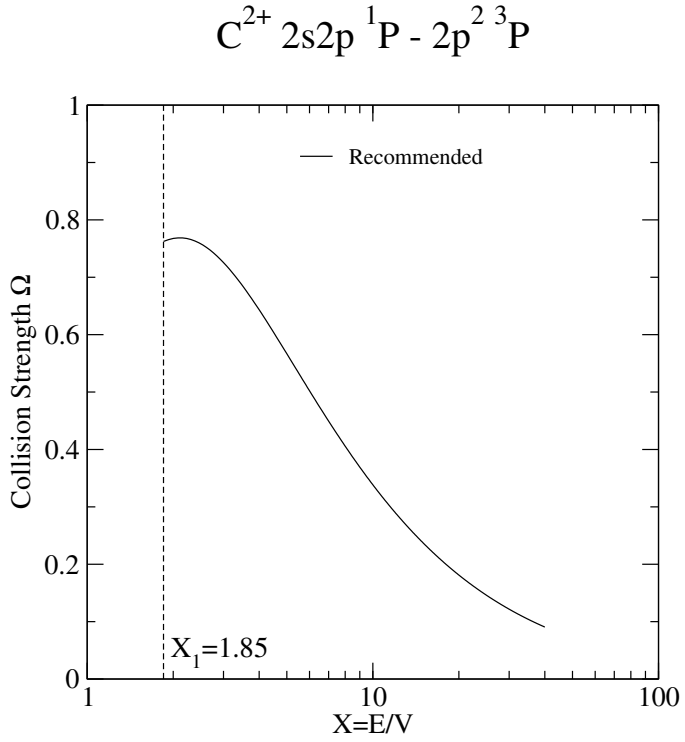

FIG. 81: Collision strength for electron-impact excitation.

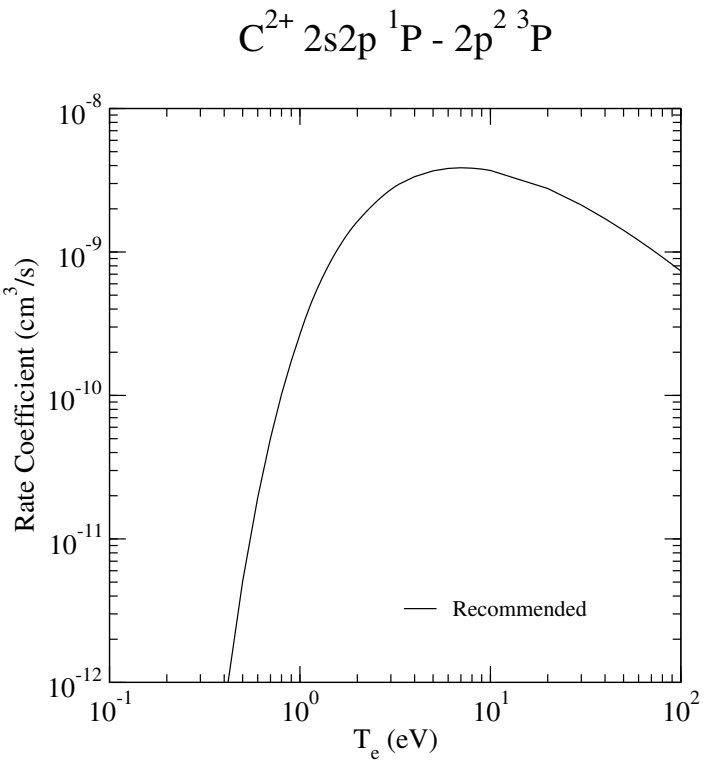

FIG. 82: Rate coefficient for electron-impact excitation.

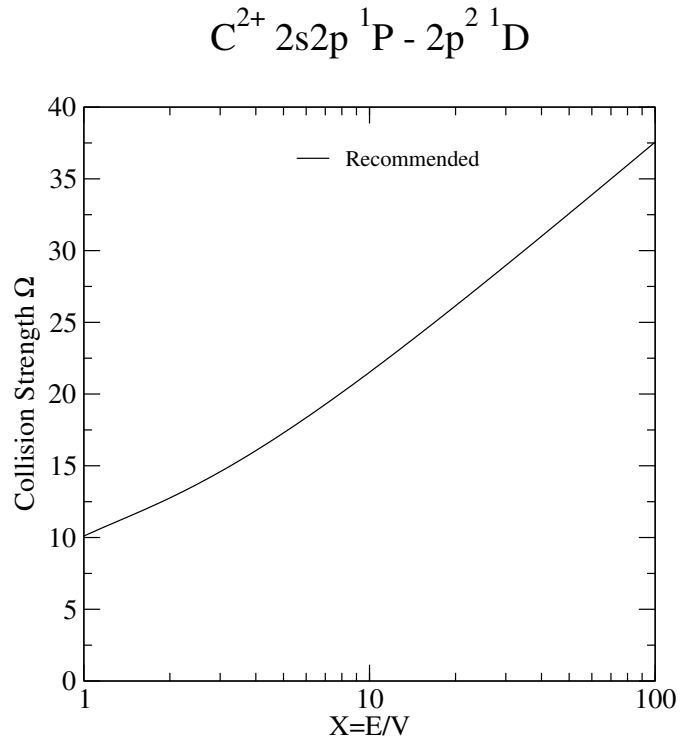

FIG. 83: Collision strength for electron-impact excitation.

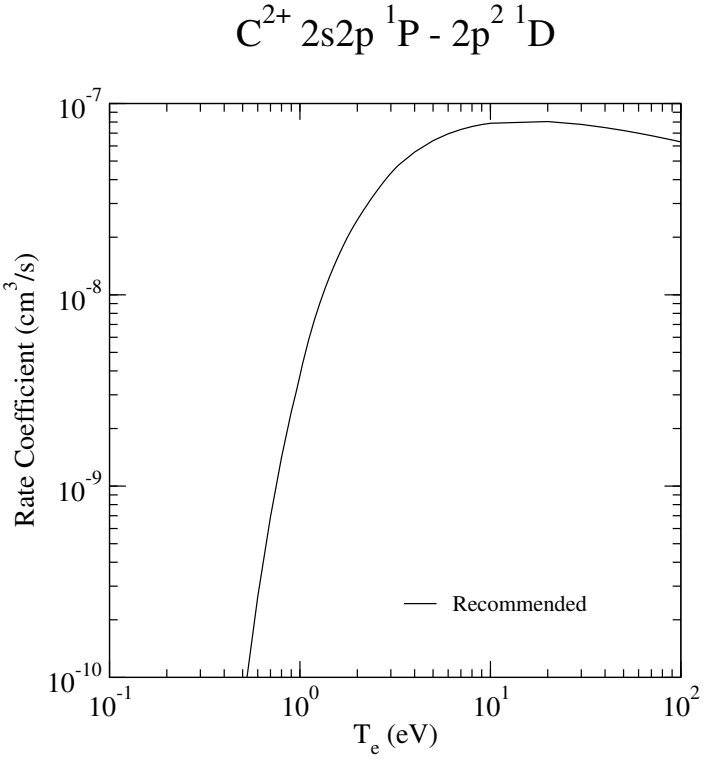

FIG. 84: Rate coefficient for electron-impact excitation.

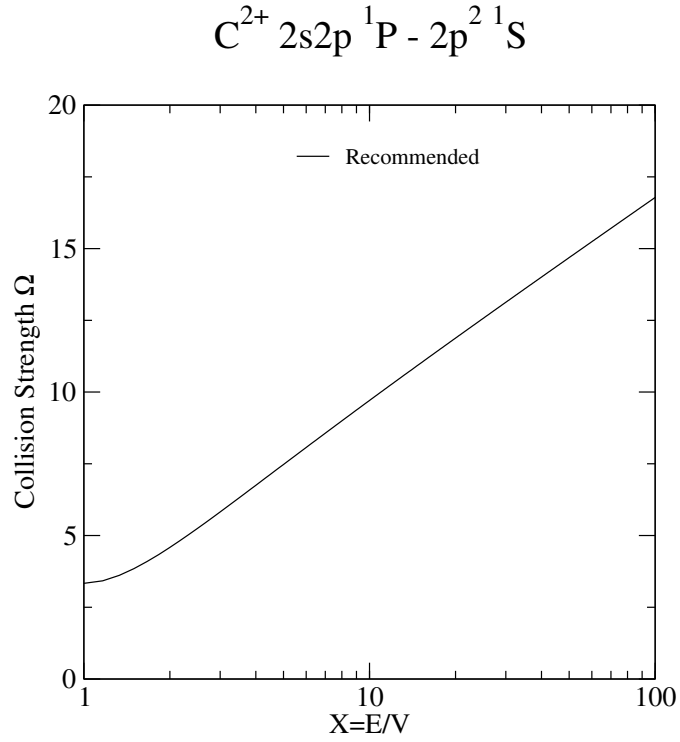

FIG. 85: Collision strength for electron-impact excitation.

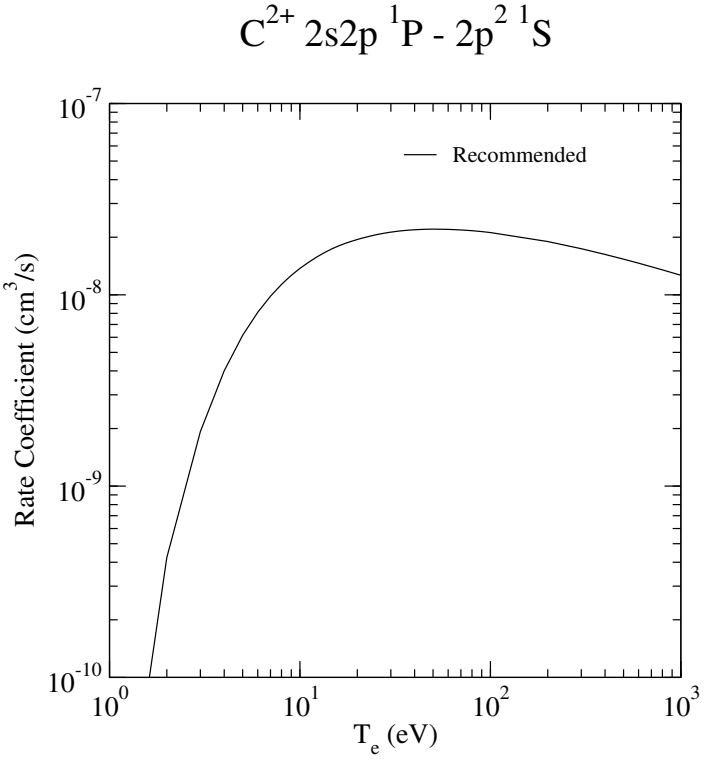

FIG. 86: Rate coefficient for electron-impact excitation.

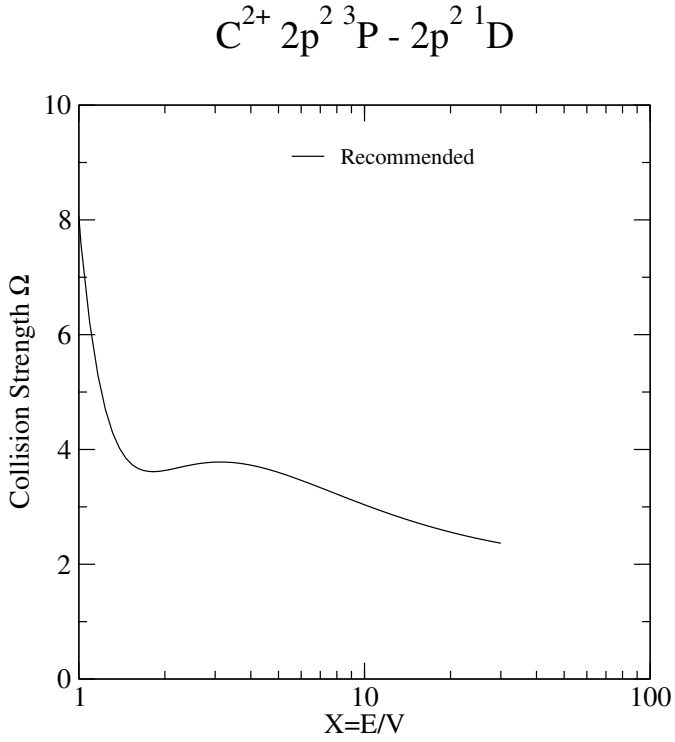

FIG. 87: Collision strength for electron-impact excitation.

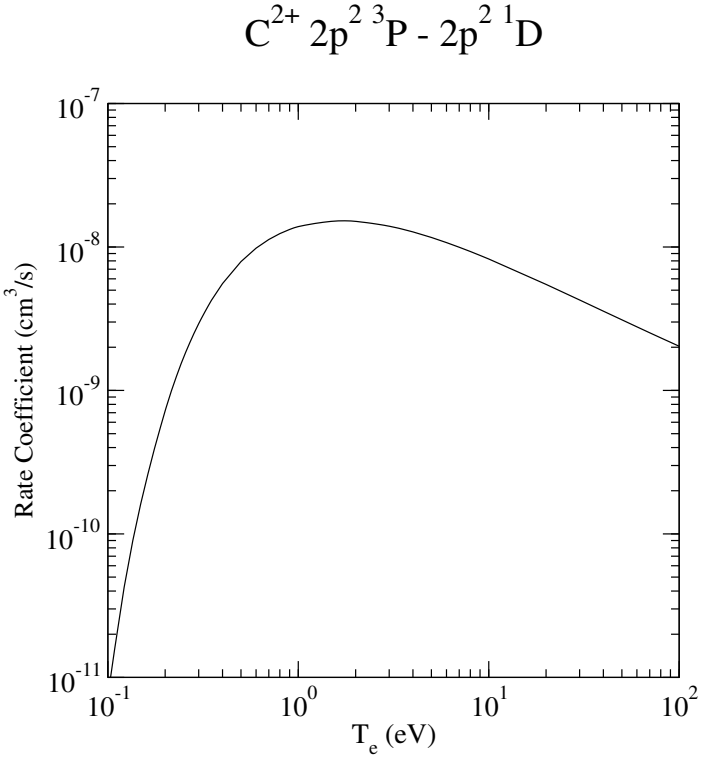

FIG. 88: Rate coefficient for electron-impact excitation.

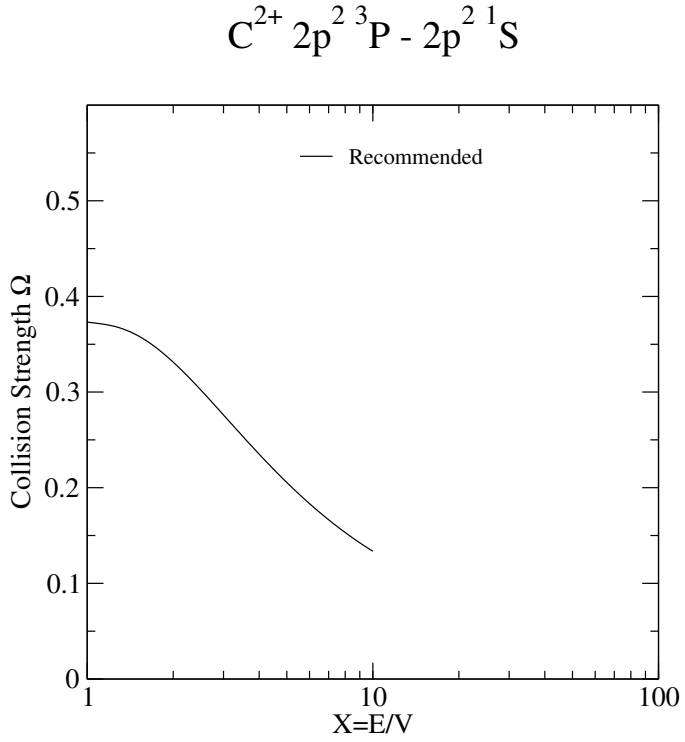

FIG. 89: Collision strength for electron-impact excitation.

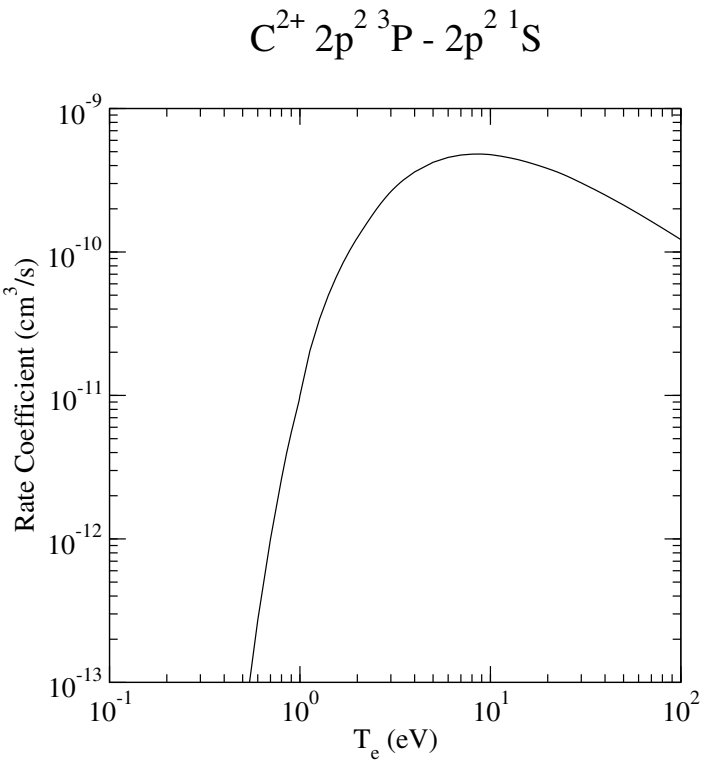

FIG. 90: Rate coefficient for electron-impact excitation.

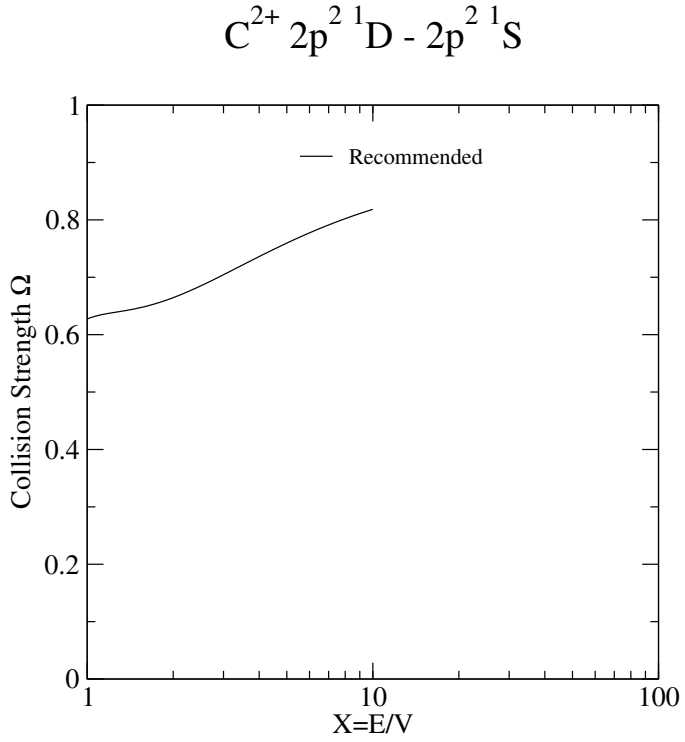

FIG. 91: Collision strength for electron-impact excitation.

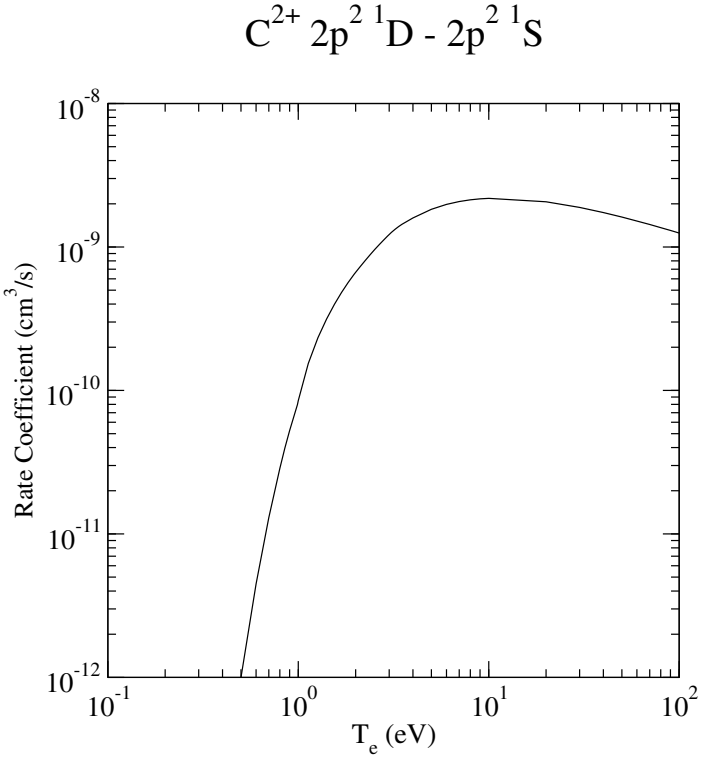

FIG. 92: Rate coefficient for electron-impact excitation.

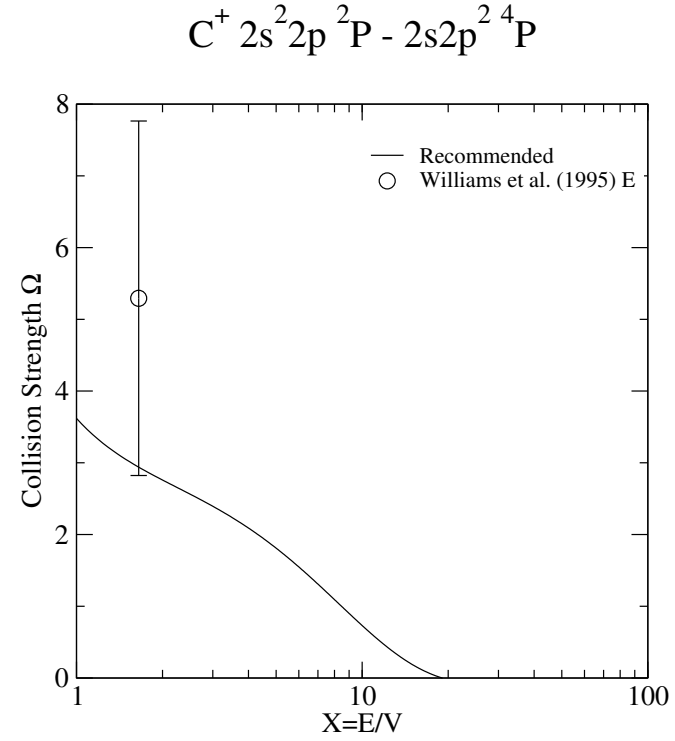

FIG. 93: Collision strength for electron-impact excitation.

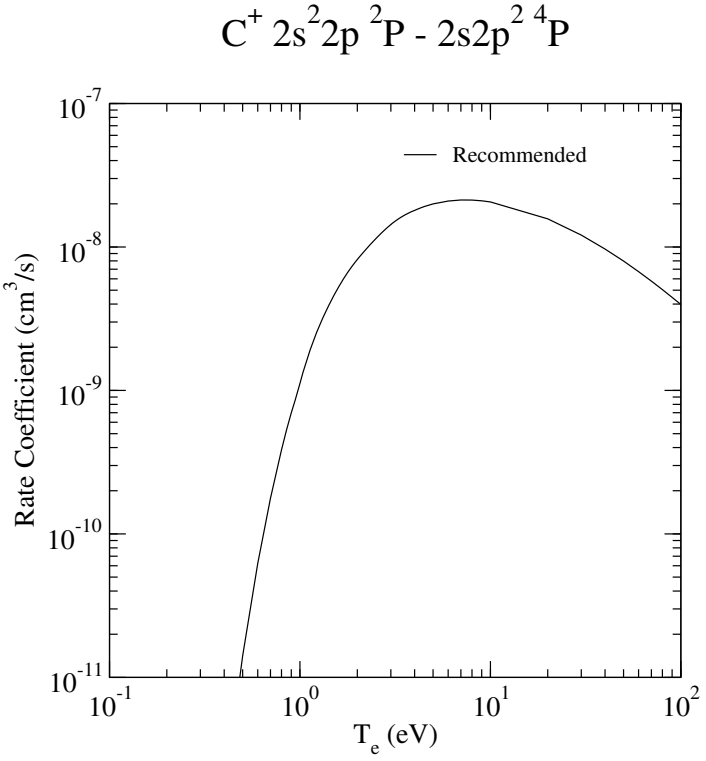

FIG. 94: Rate coefficient for electron-impact excitation.

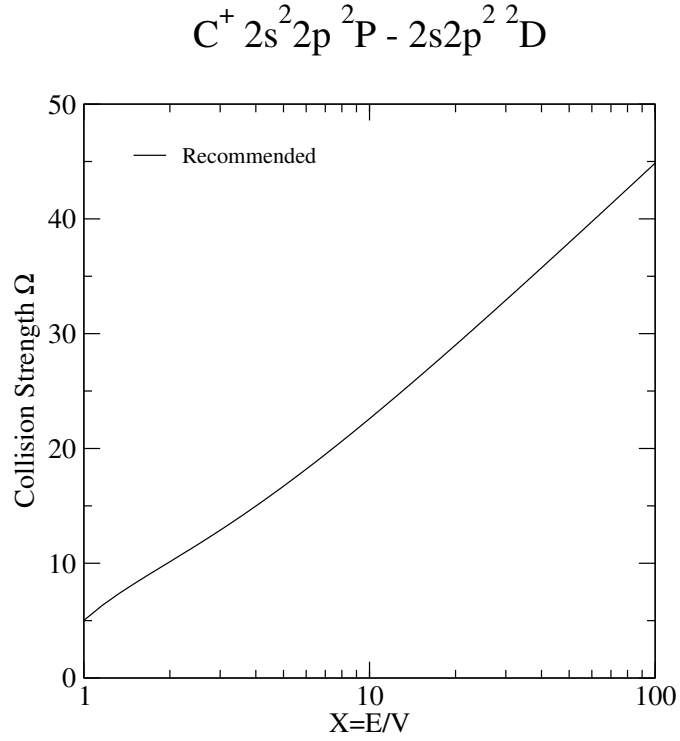

FIG. 95: Collision strength for electron-impact excitation.

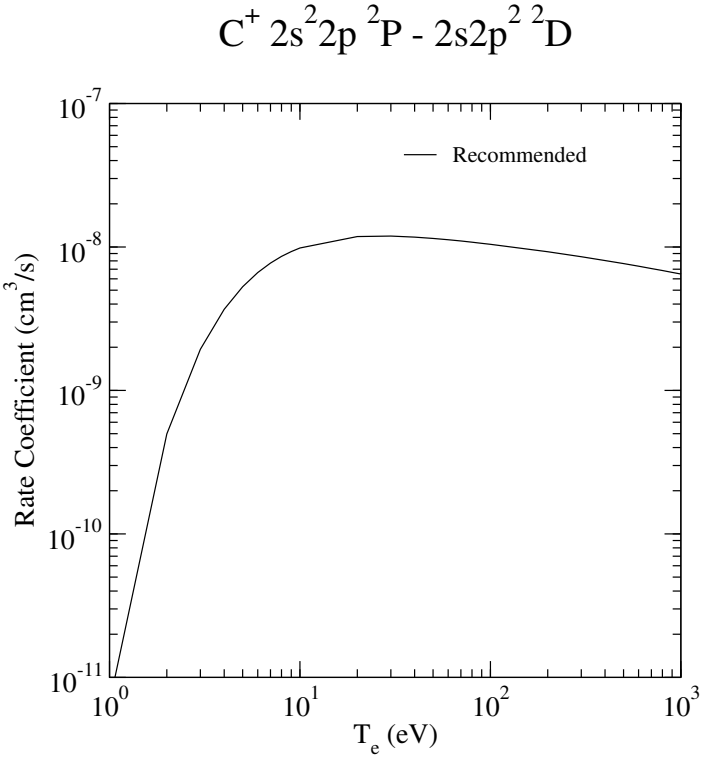

FIG. 96: Rate coefficient for electron-impact excitation.

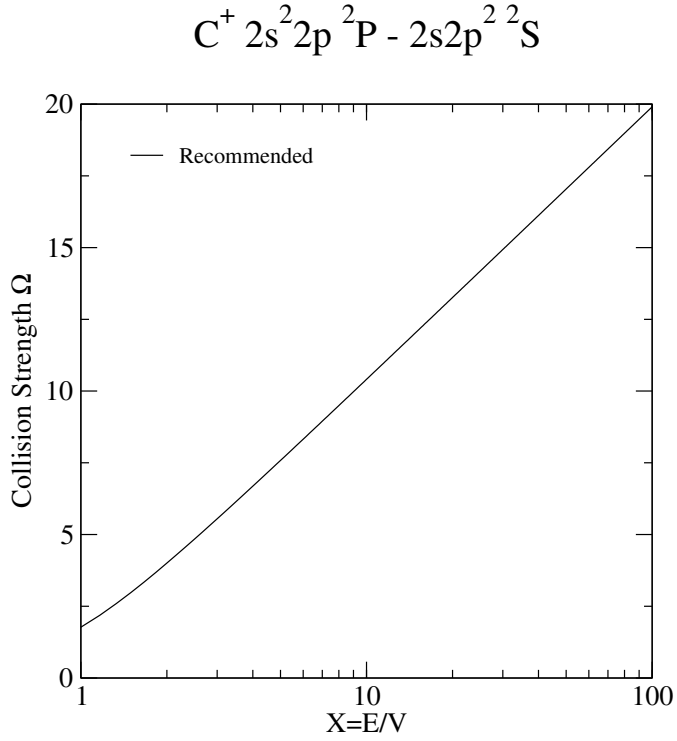

FIG. 97: Collision strength for electron-impact excitation.

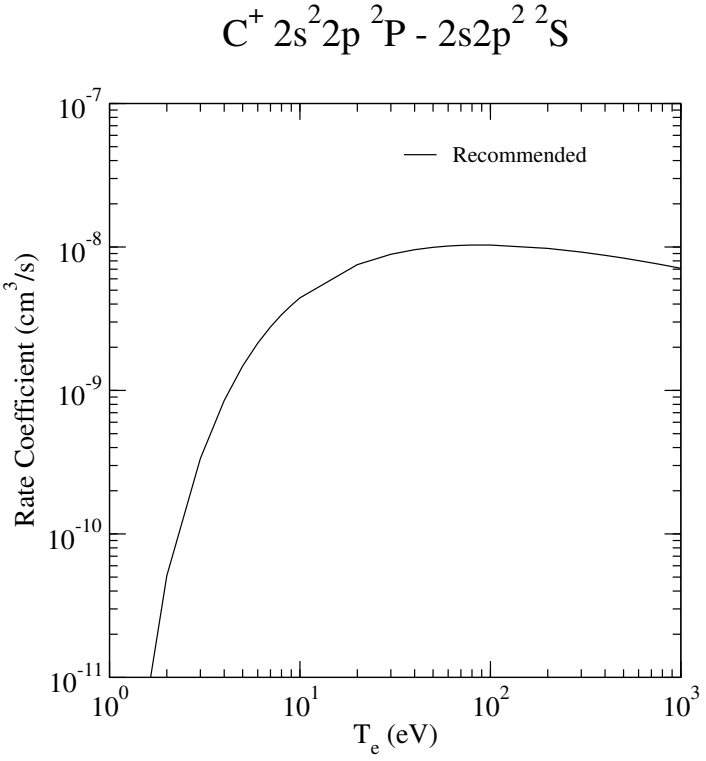

FIG. 98: Rate coefficient for electron-impact excitation.

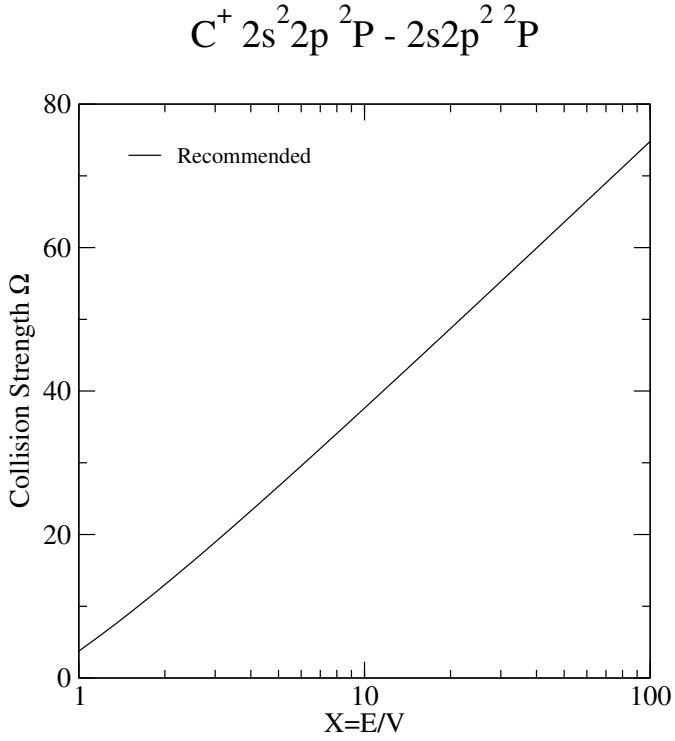

FIG. 99: Collision strength for electron-impact excitation.

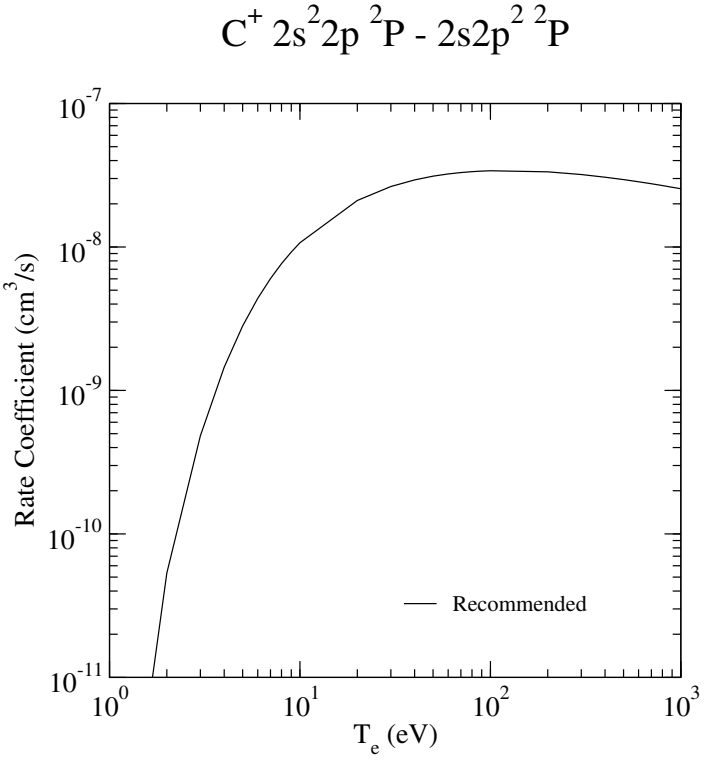

FIG. 100: Rate coefficient for electron-impact excitation.

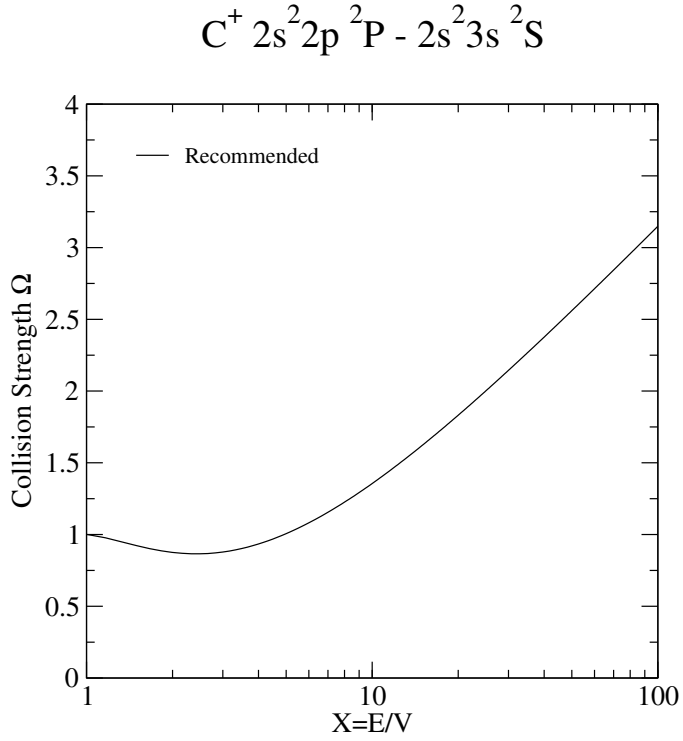

FIG. 101: Collision strength for electron-impact excitation.

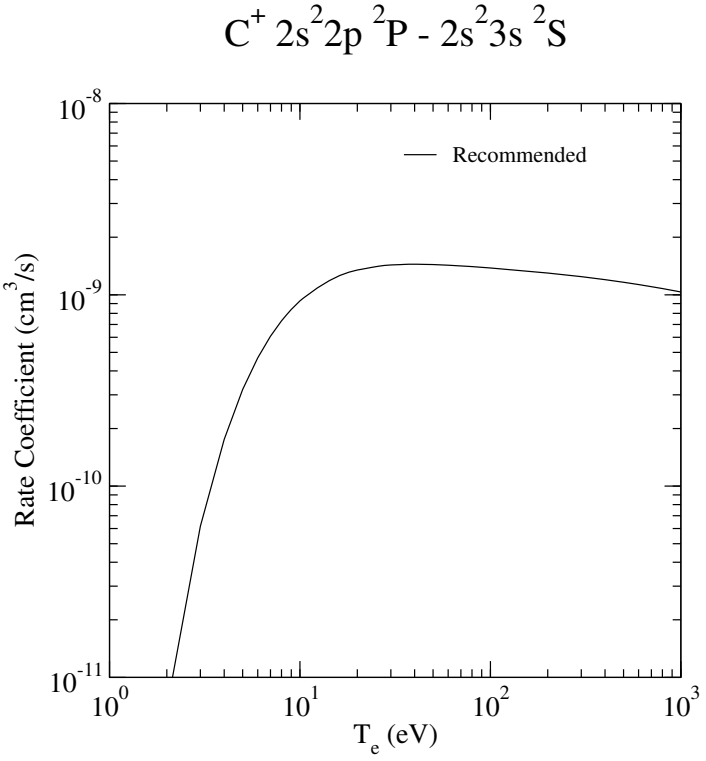

FIG. 102: Rate coefficient for electron-impact excitation.

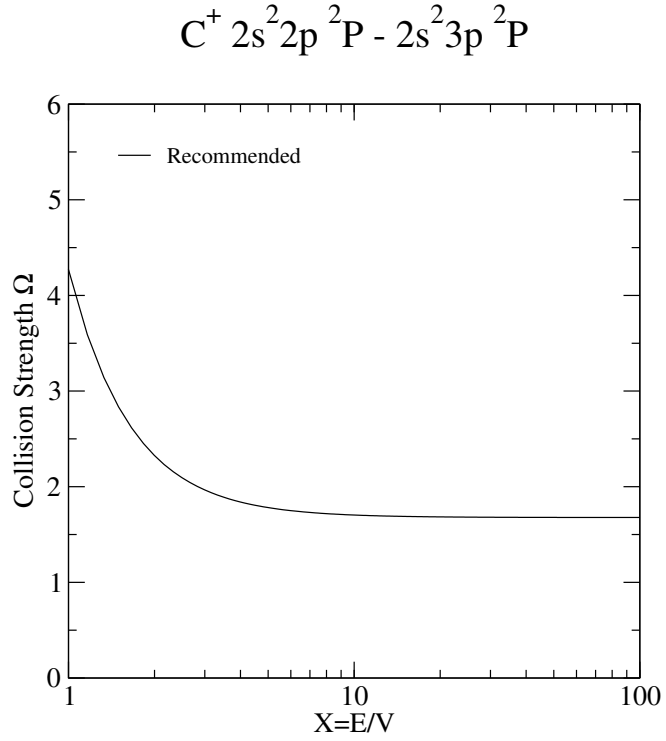

FIG. 103: Collision strength for electron-impact excitation.

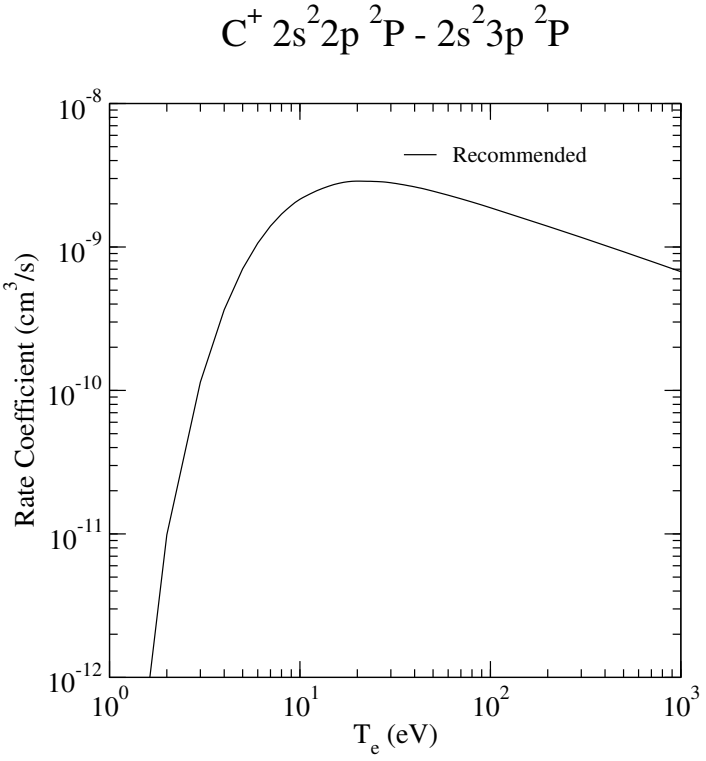

FIG. 104: Rate coefficient for electron-impact excitation.

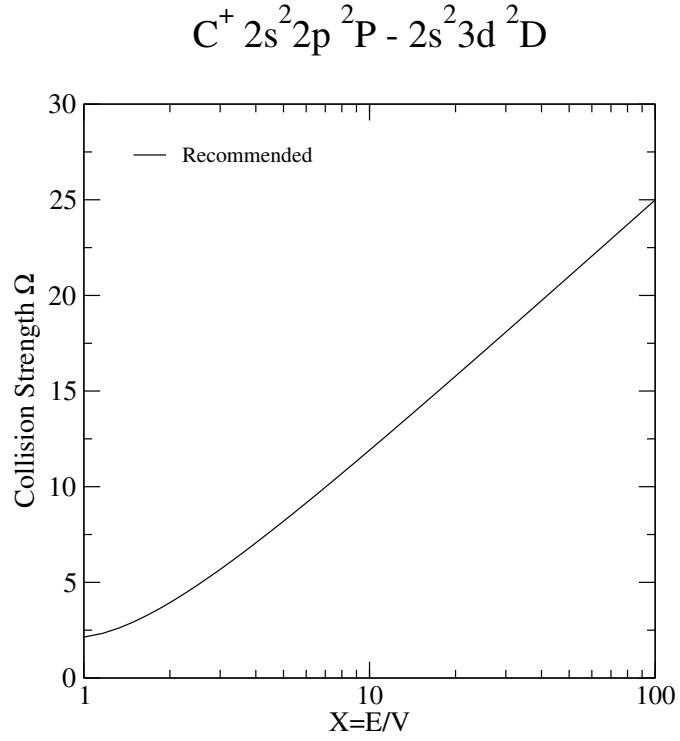

FIG. 105: Collision strength for electron-impact excitation.

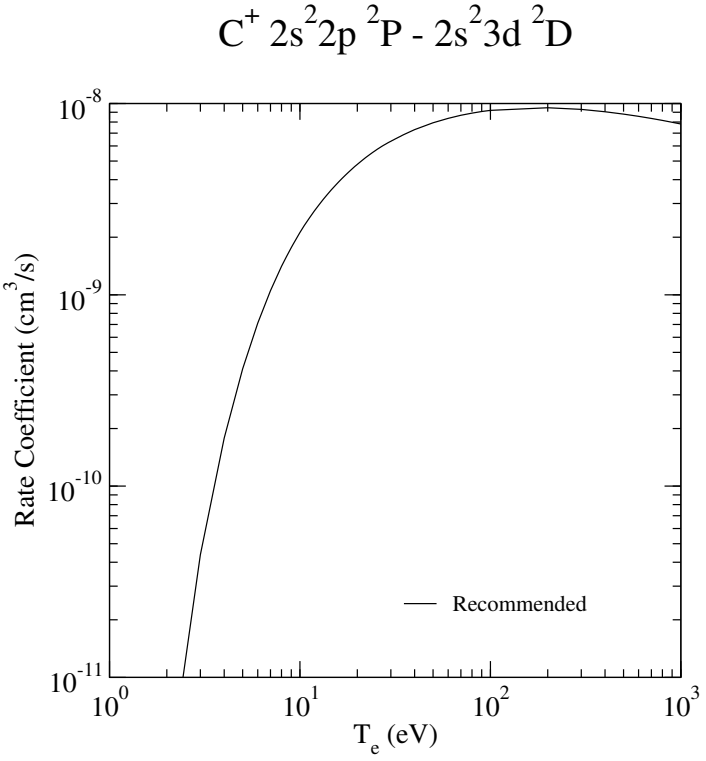

FIG. 106: Rate coefficient for electron-impact excitation.

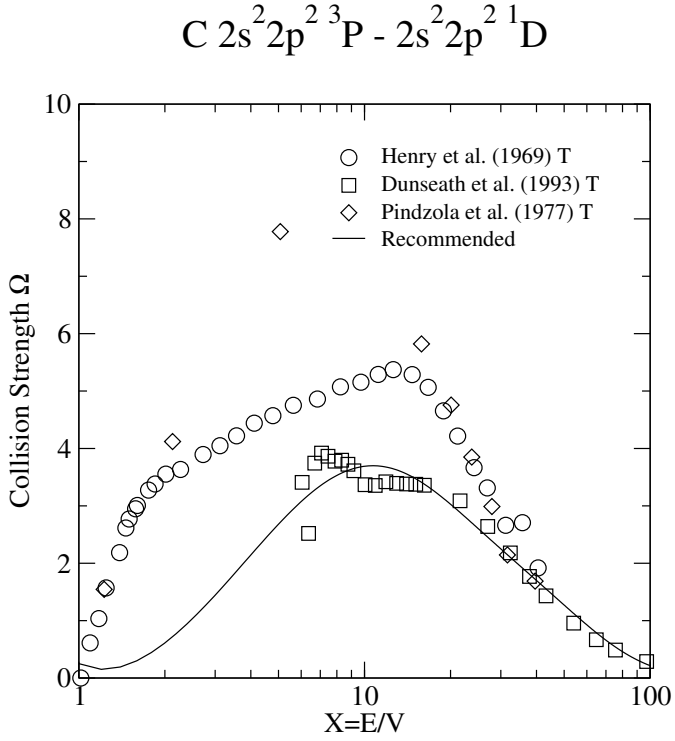

FIG. 107: Collision strength for electron-impact excitation.

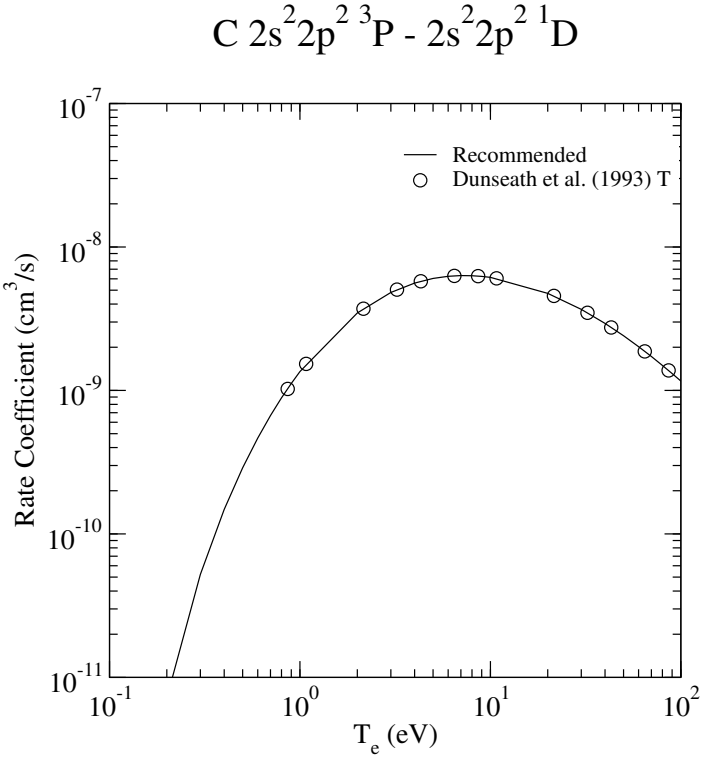

FIG. 108: Rate coefficient for electron-impact excitation.

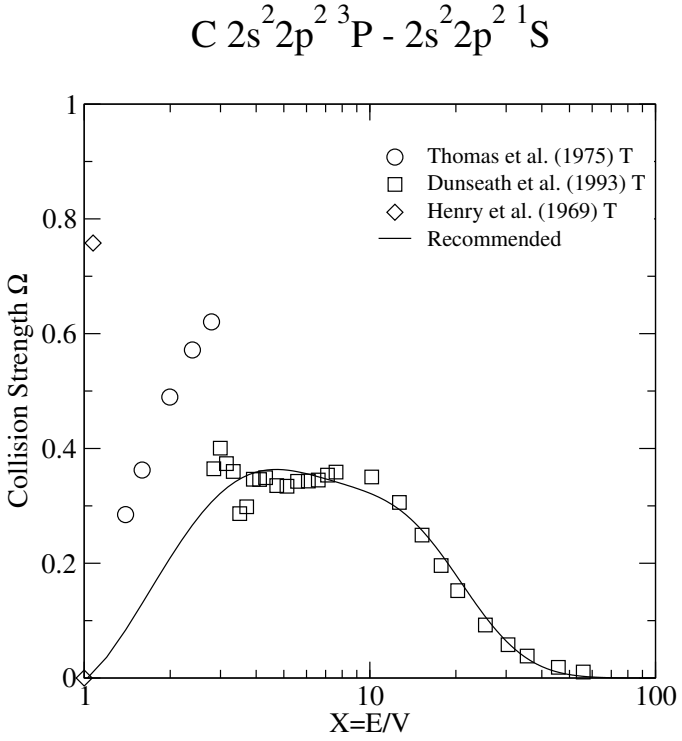

FIG. 109: Collision strength for electron-impact excitation.

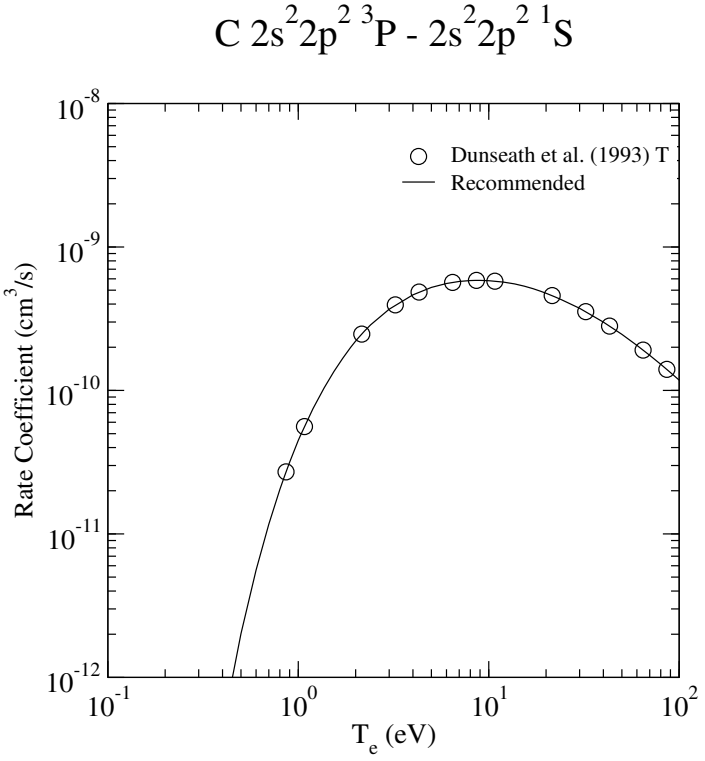

FIG. 110: Rate coefficient for electron-impact excitation.

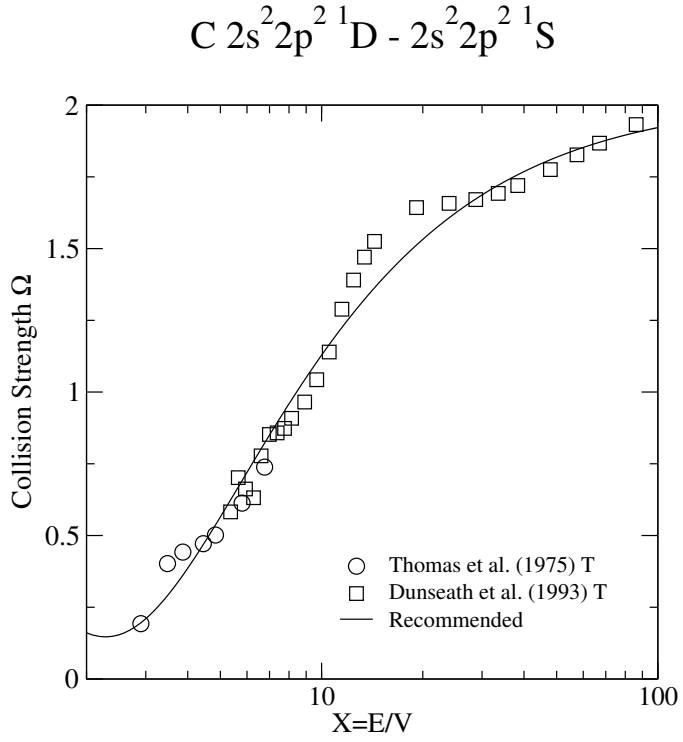

FIG. 111: Collision strength for electron-impact excitation.

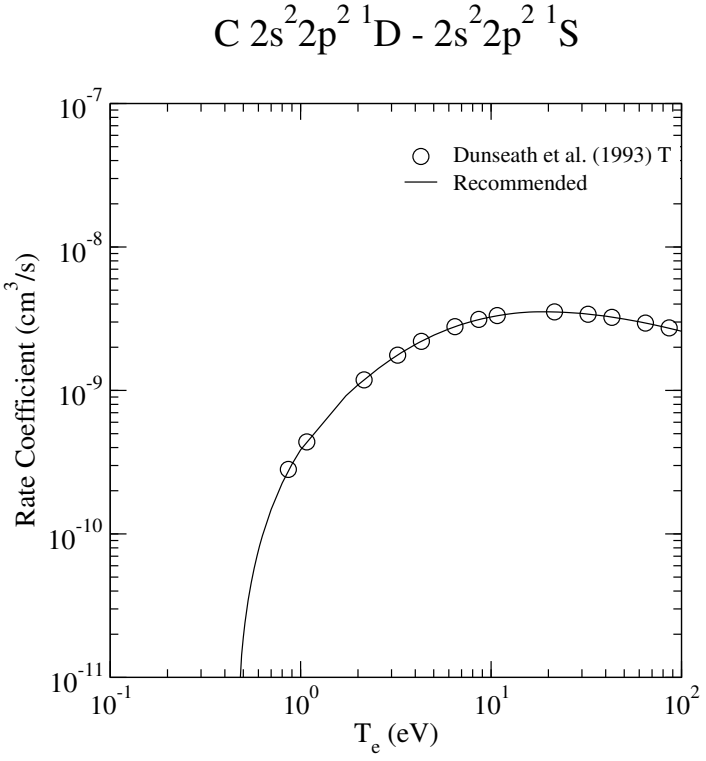

FIG. 112: Rate coefficient for electron-impact excitation.

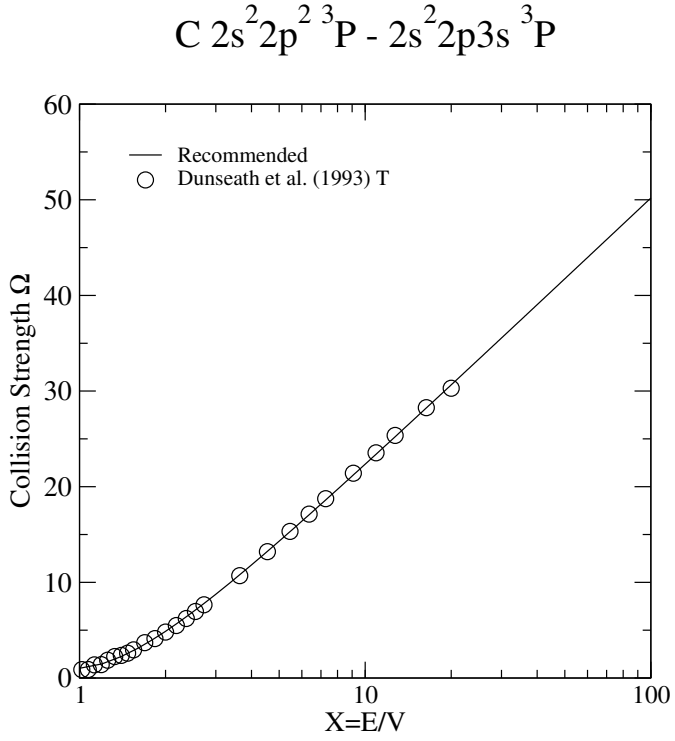

FIG. 113: Collision strength for electron-impact excitation.

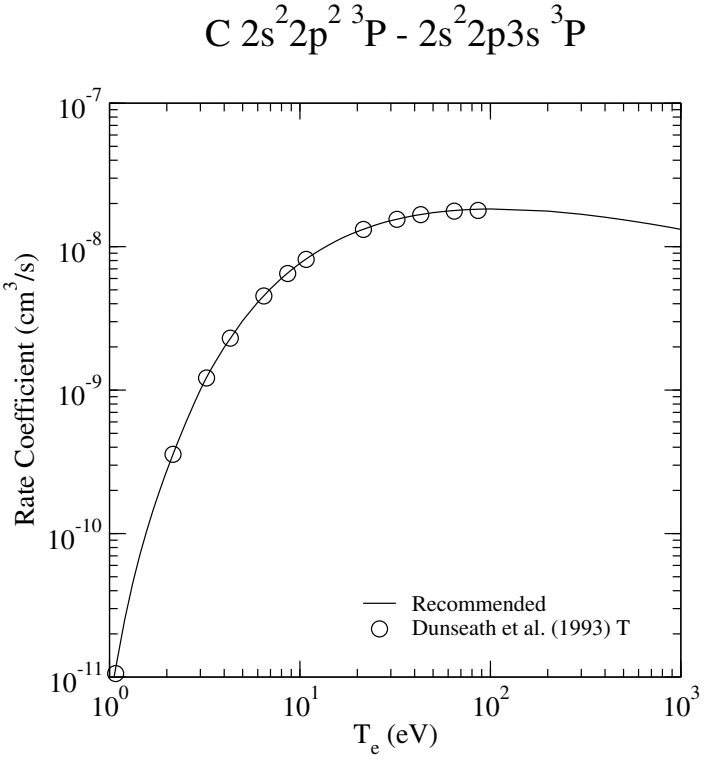

FIG. 114: Rate coefficient for electron-impact excitation.

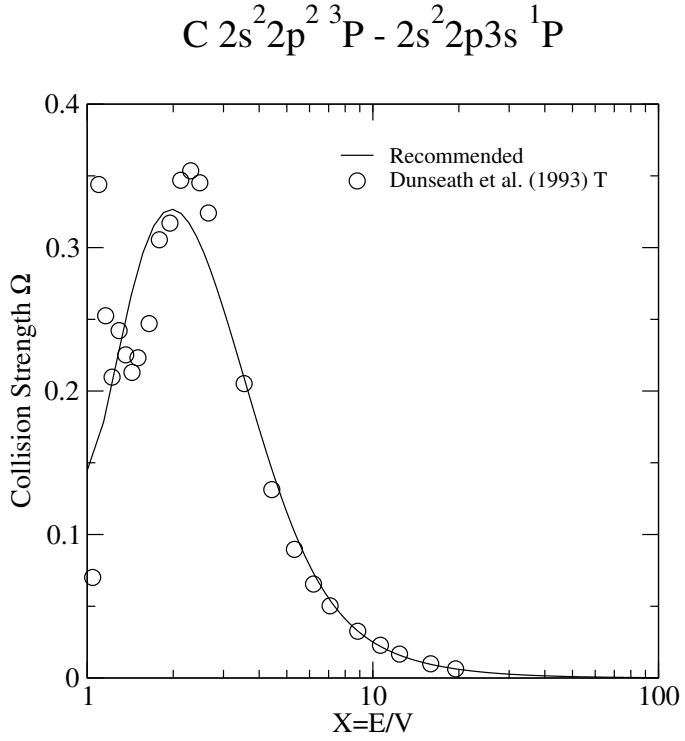

FIG. 115: Collision strength for electron-impact excitation.

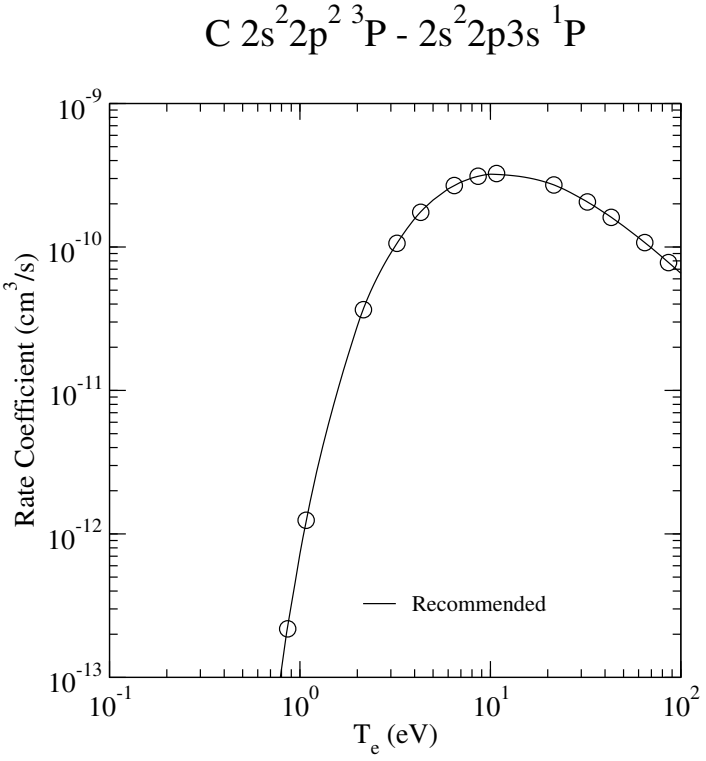

FIG. 116: Rate coefficient for electron-impact excitation.

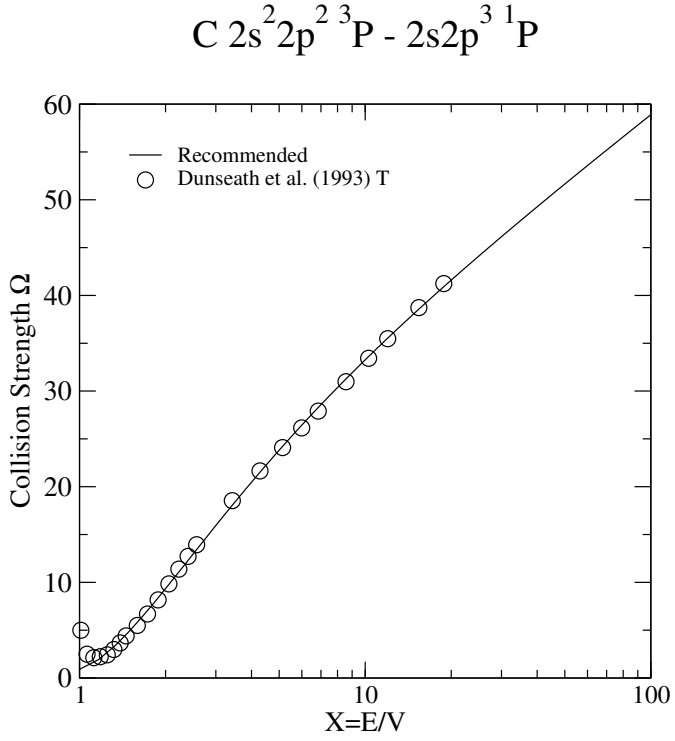

FIG. 117: Collision strength for electron-impact excitation.

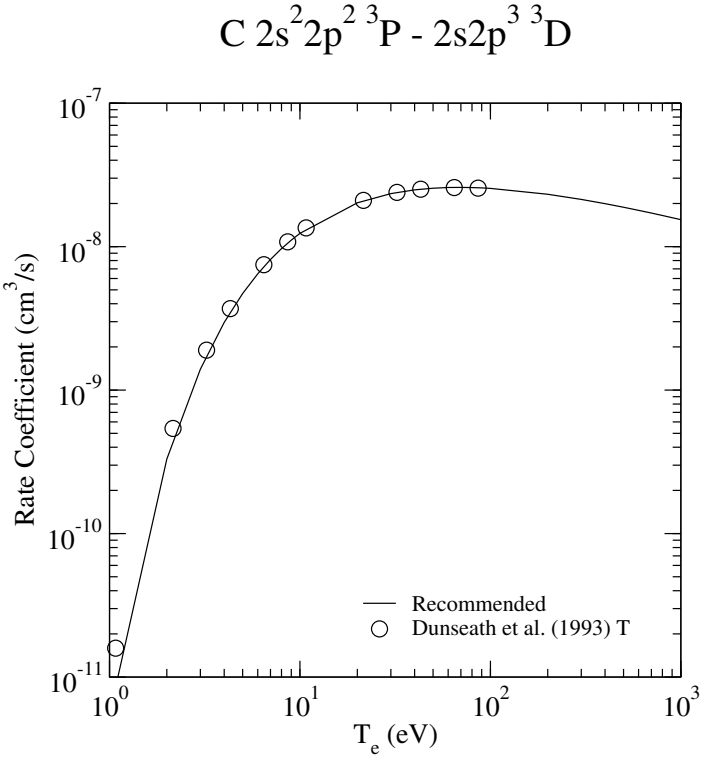

FIG. 118: Rate coefficient for electron-impact excitation.

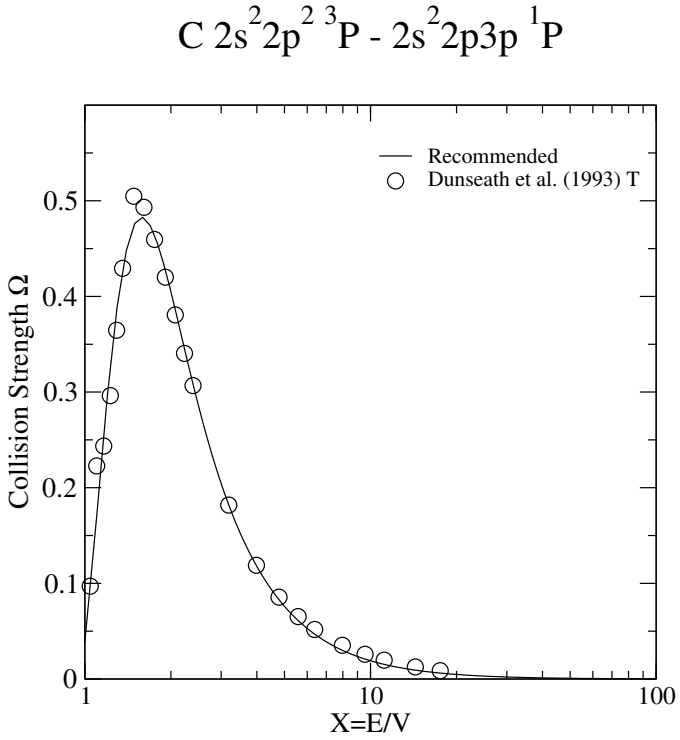

FIG. 119: Collision strength for electron-impact excitation.

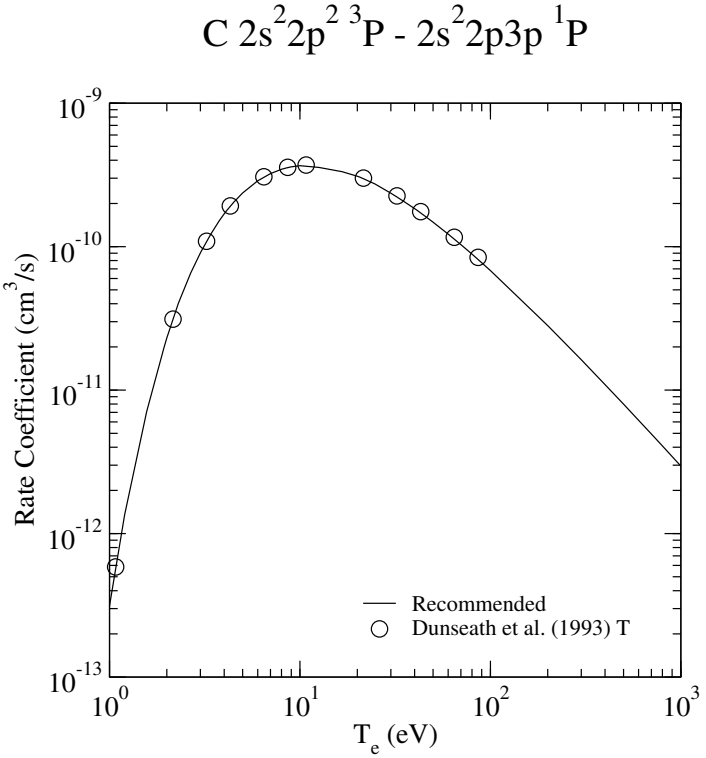

FIG. 120: Rate coefficient for electron-impact excitation.

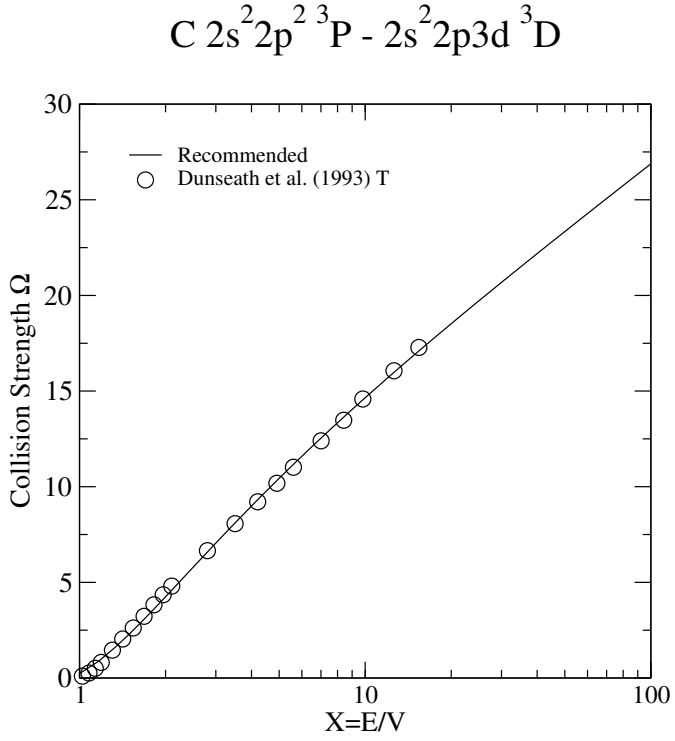

FIG. 121: Collision strength for electron-impact excitation.

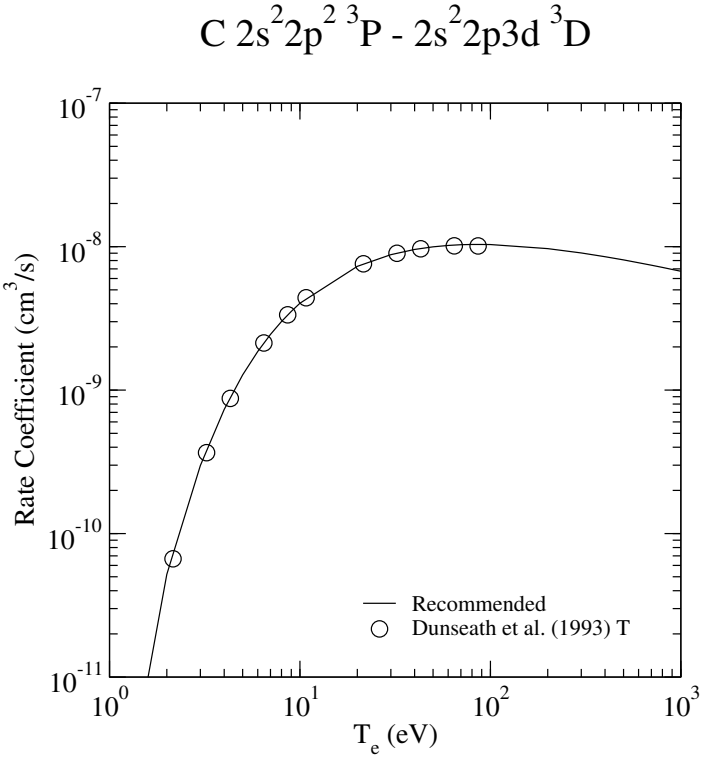

FIG. 122: Rate coefficient for electron-impact excitation.

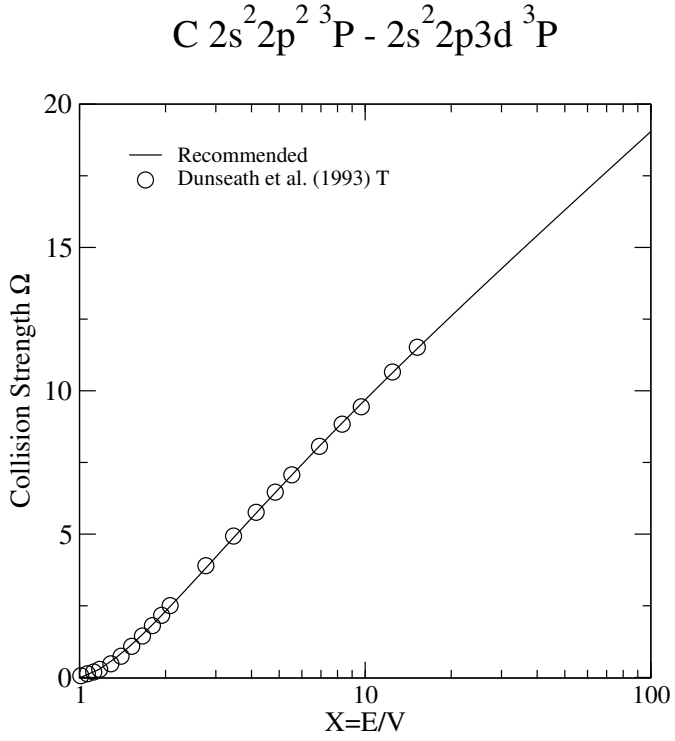

FIG. 123: Collision strength for electron-impact excitation.

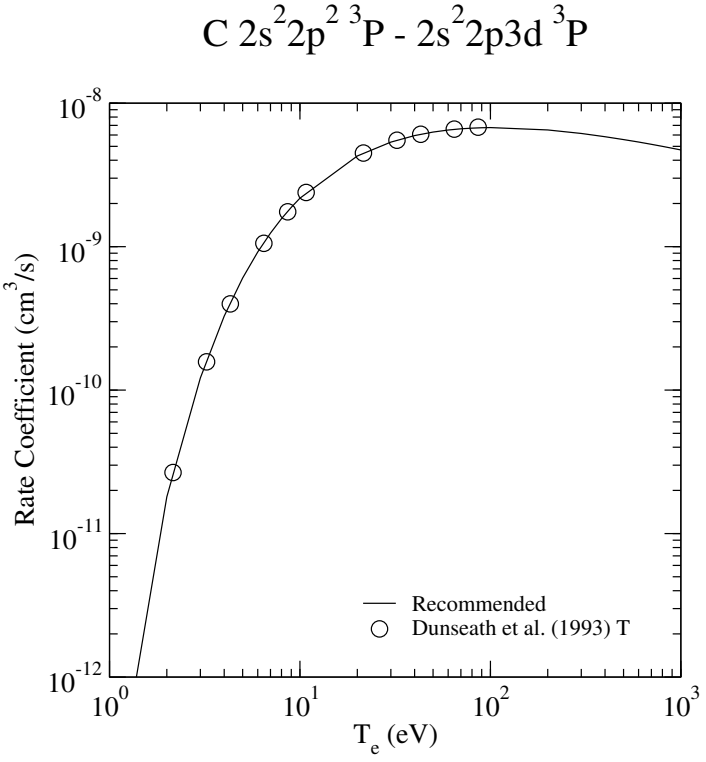

FIG. 124: Rate coefficient for electron-impact excitation.

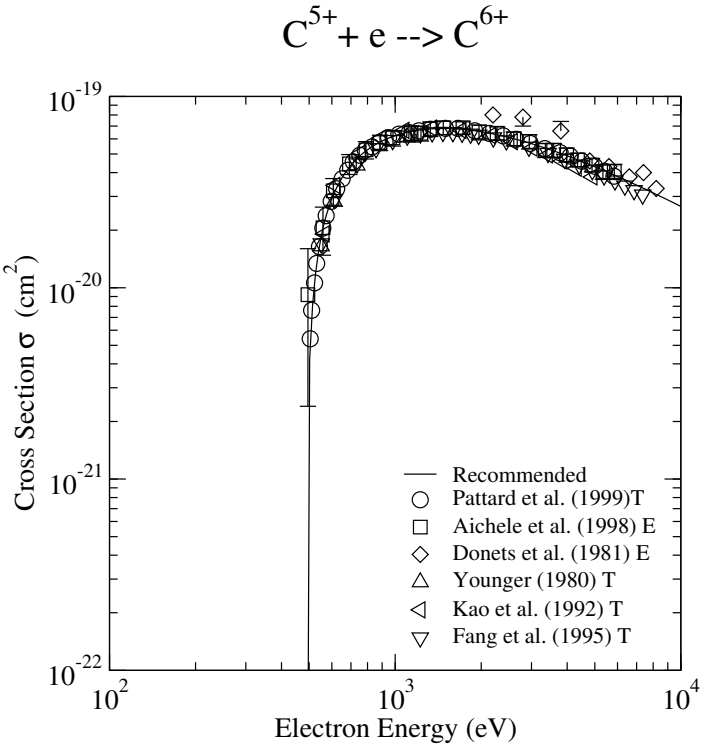

FIG. 125: Cross section for electron-impact ionization.

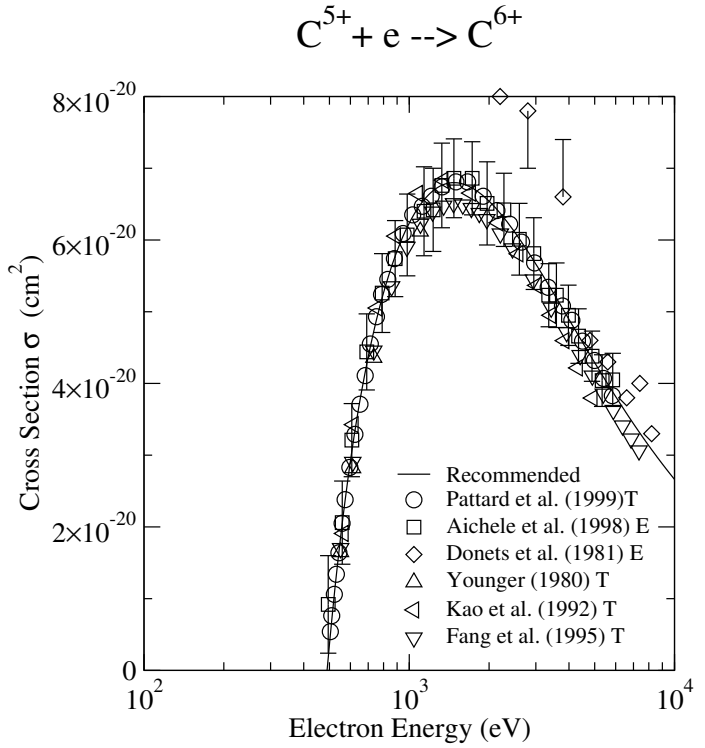

FIG. 126: Same as previous Fig., but with the linear scale for the vertical axe.

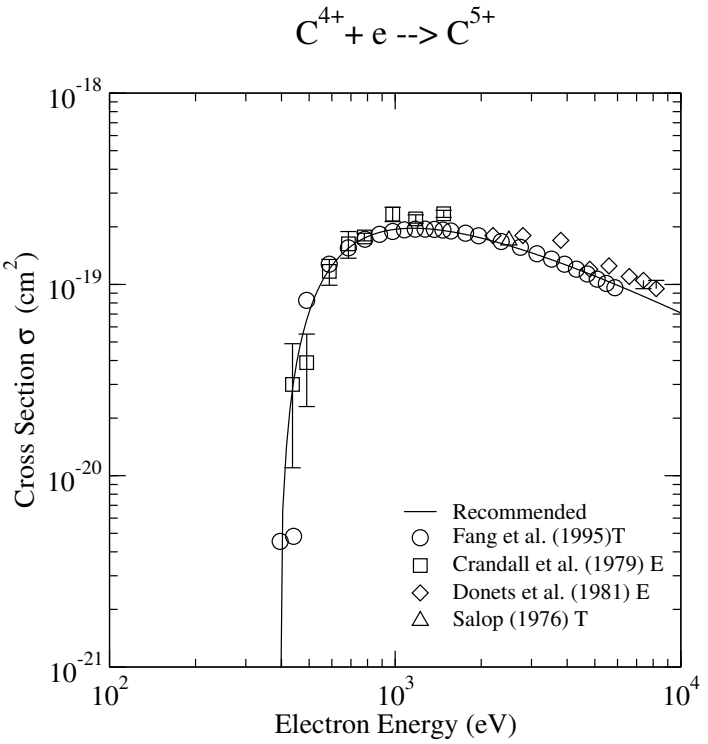

FIG. 127: Cross section for electron-impact ionization.

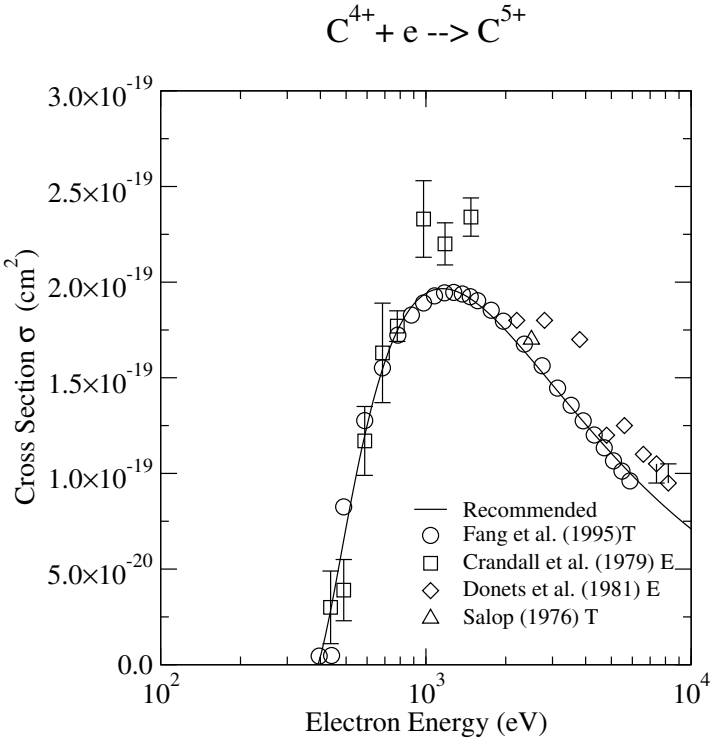

FIG. 128: Same as previous Fig., but with the linear scale for the vertical axe.

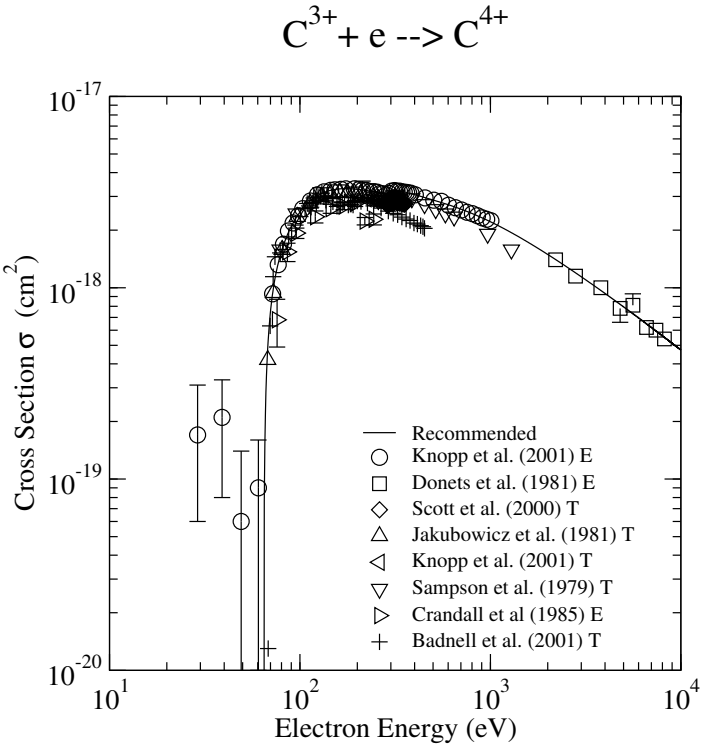

FIG. 129: Cross section for electron-impact ionization.

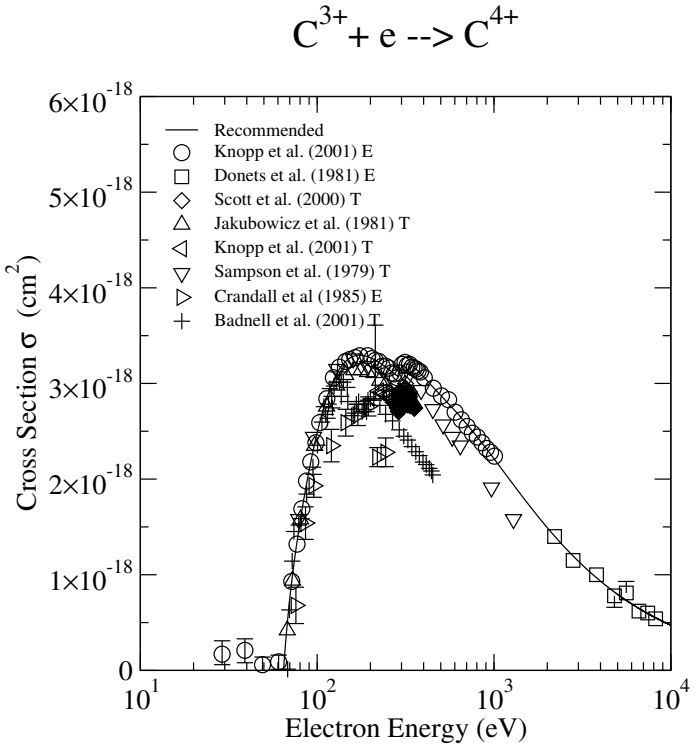

FIG. 130: Same as previous Fig., but with the linear scale for the vertical axe.

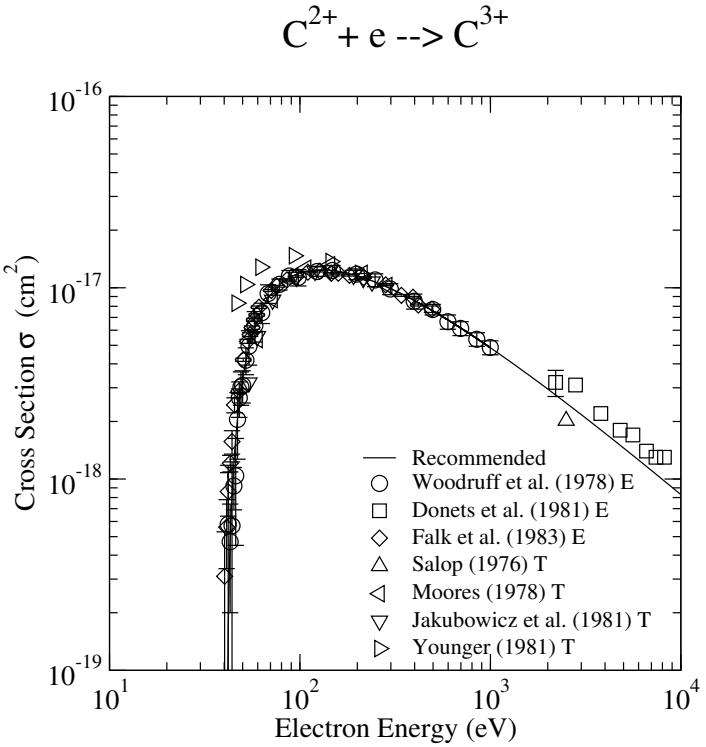

FIG. 131: Cross section for electron-impact ionization.

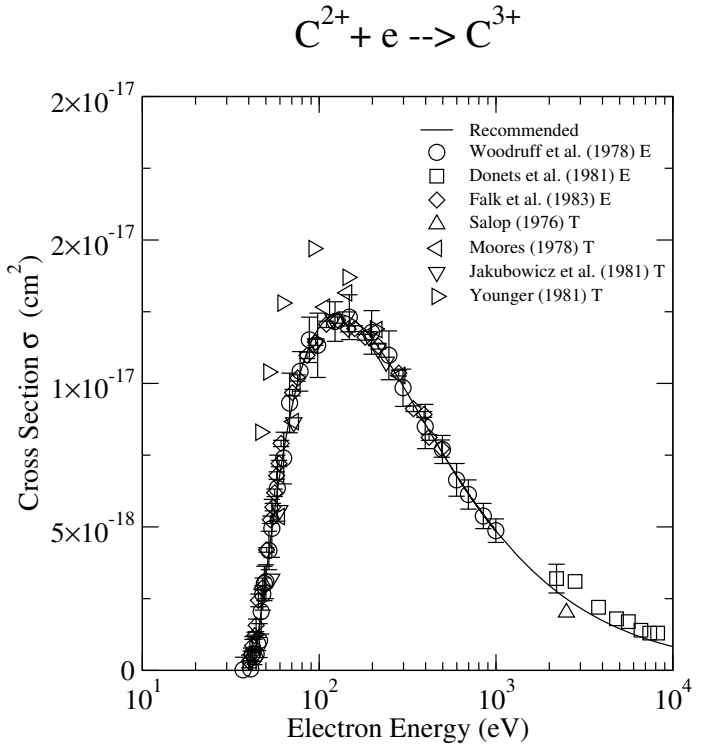

FIG. 132: Same as previous Fig., but with the linear scale for the vertical axe.

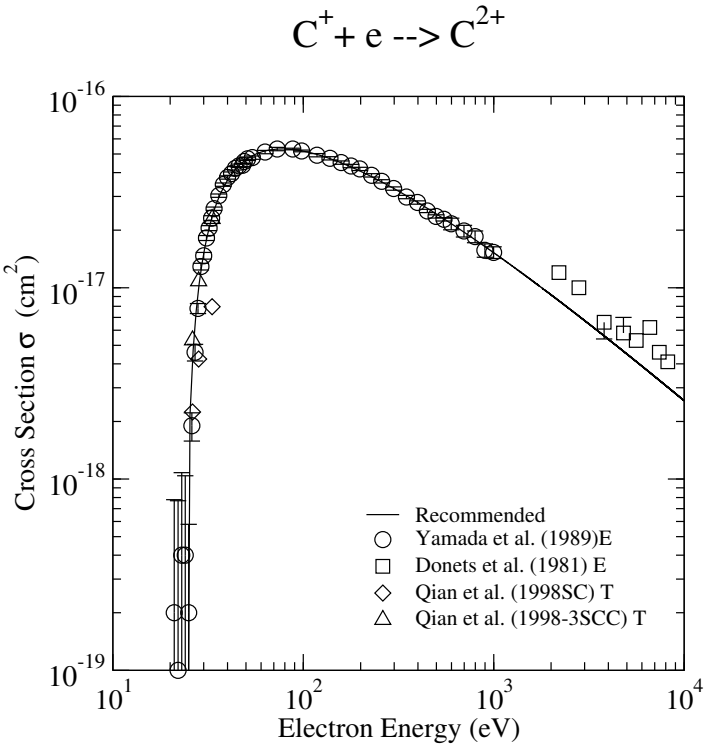

FIG. 133: Cross section for electron-impact ionization.

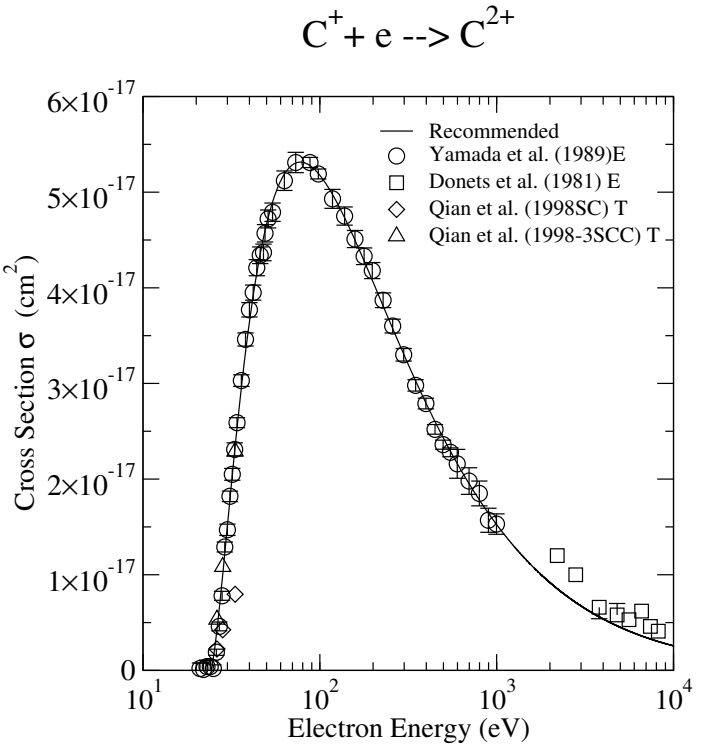

FIG. 134: Same as previous Fig., but with the linear scale for the vertical axe.

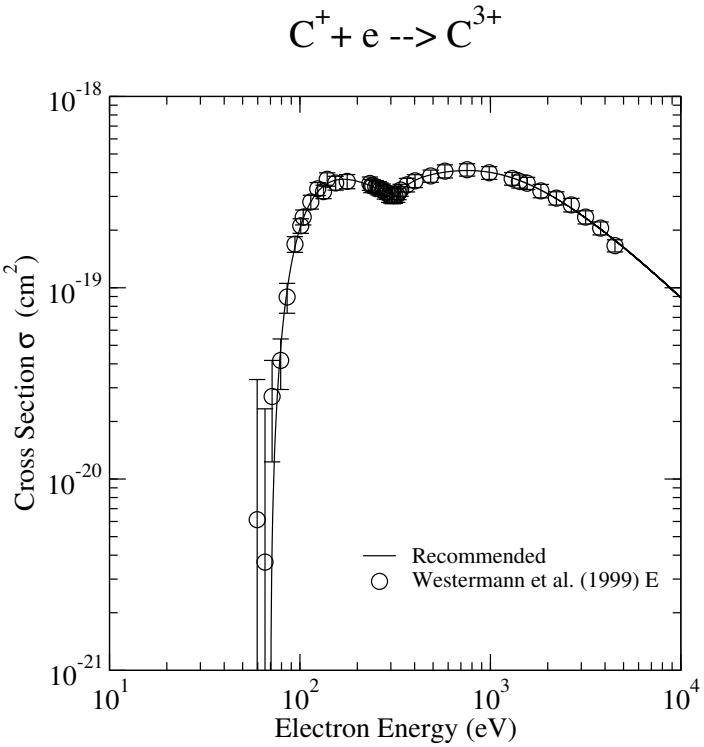

FIG. 135: Cross section for electron-impact ionization.

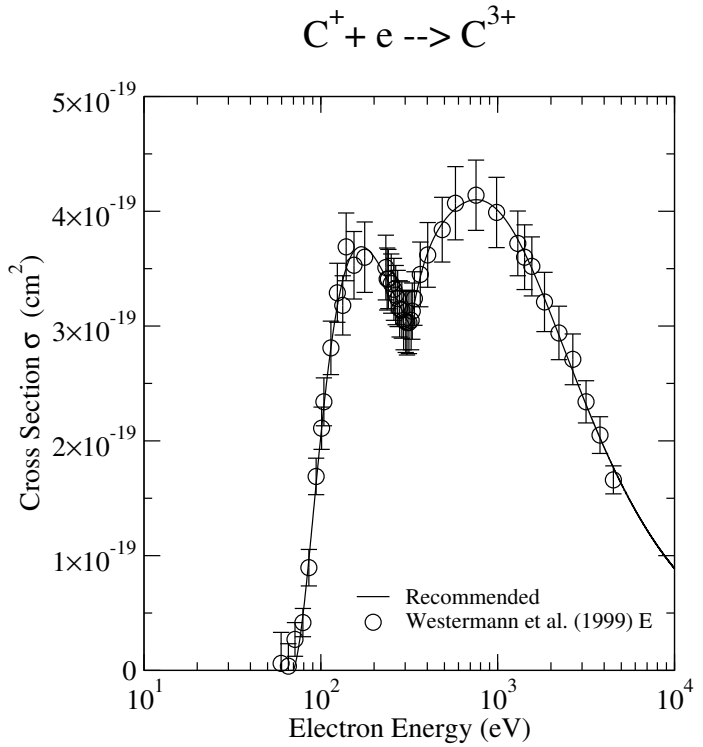

FIG. 136: Same as previous Fig., but with the linear scale for the vertical axe.

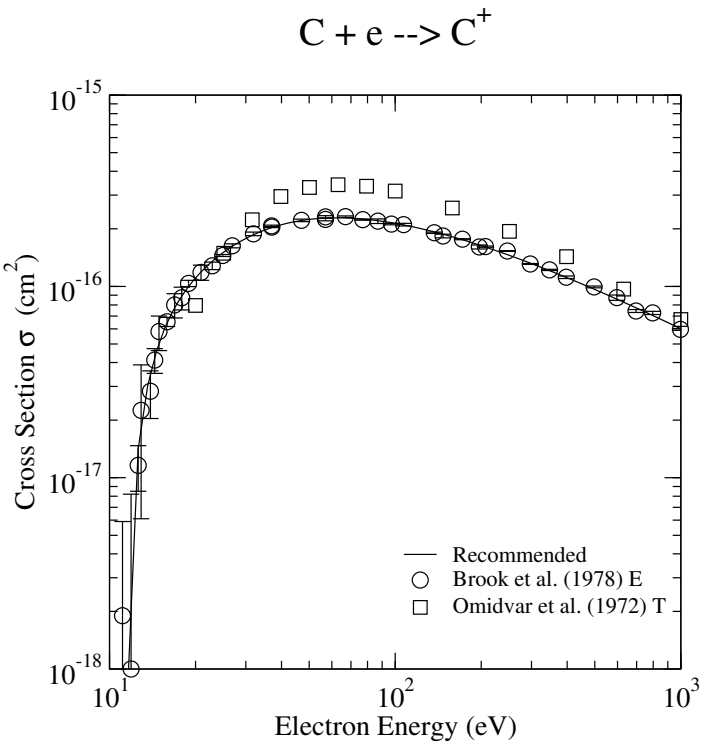

FIG. 137: Cross section for electron-impact ionization.

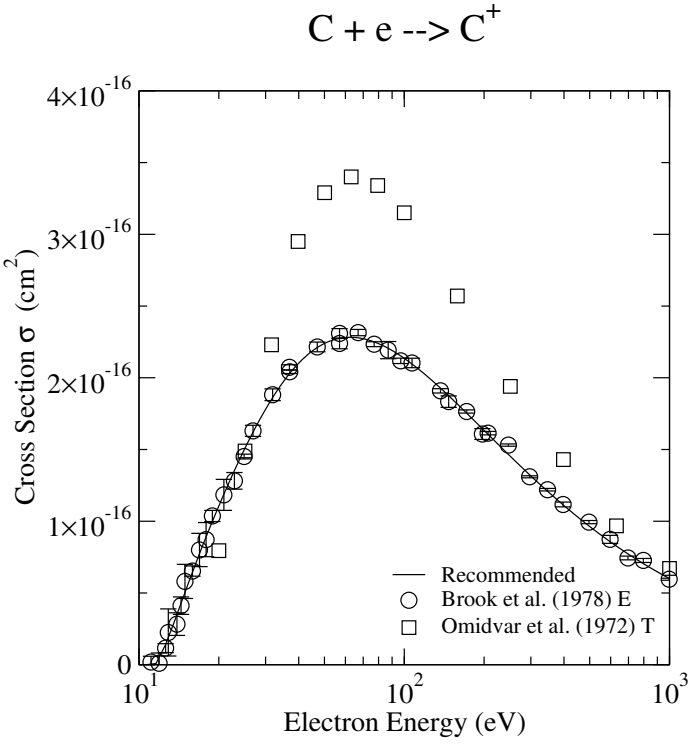

FIG. 138: Same as previous Fig., but with the linear scale for the vertical axe.

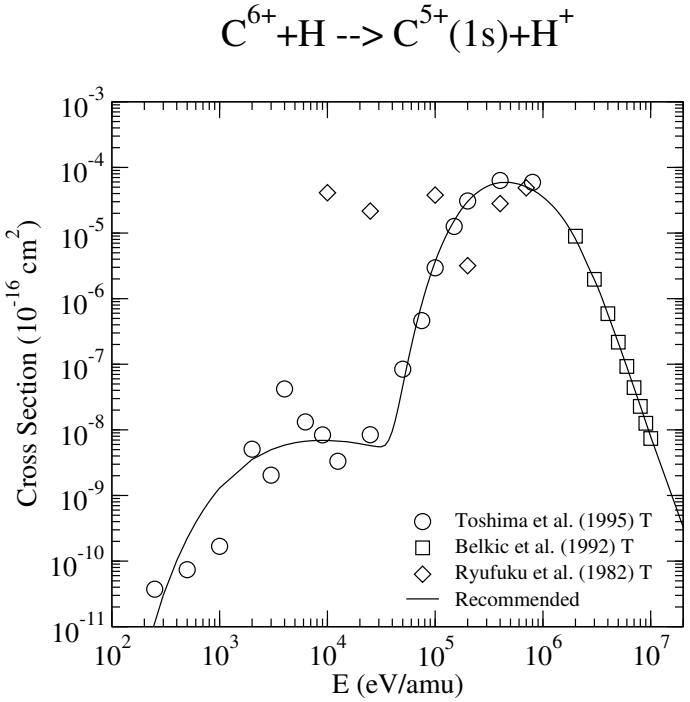

FIG. 139: Cross section for charge exchange.

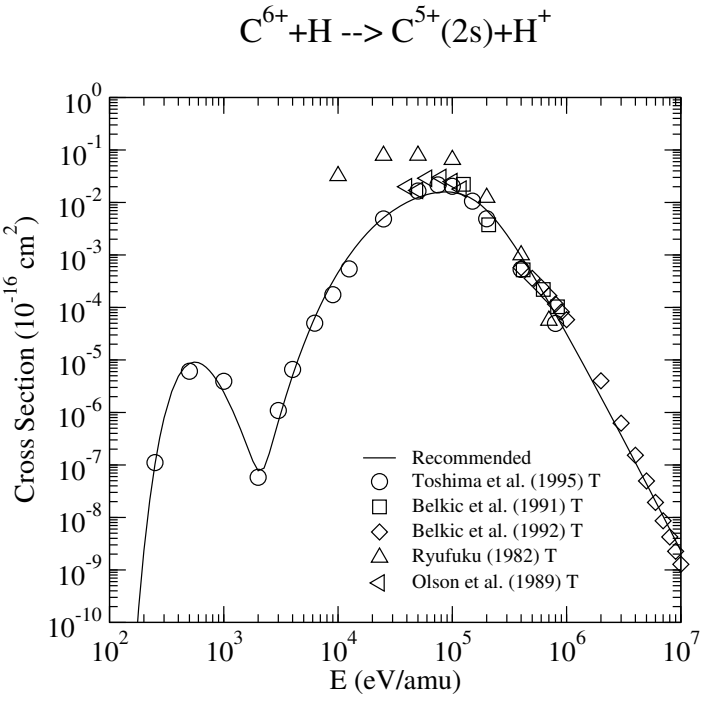

FIG. 140: Cross section for charge exchange.

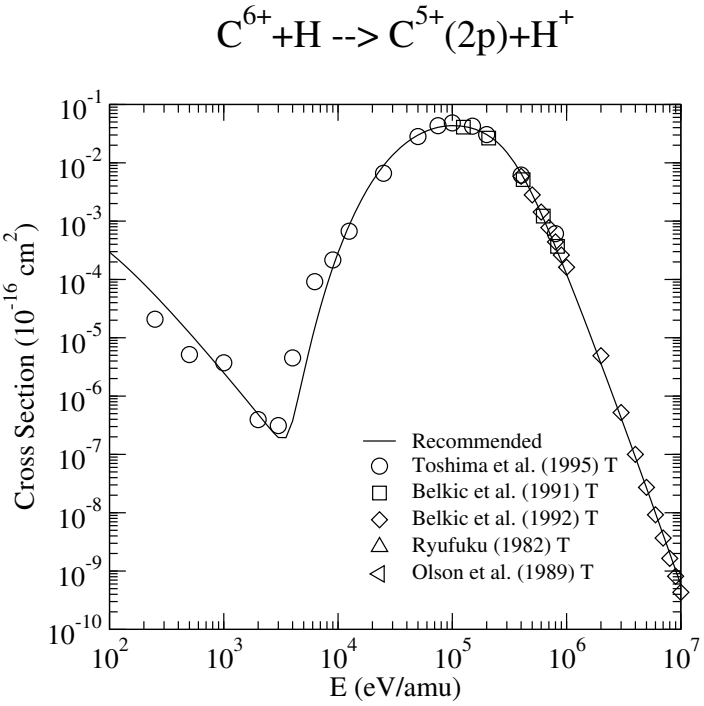

FIG. 141: Cross section for charge exchange.

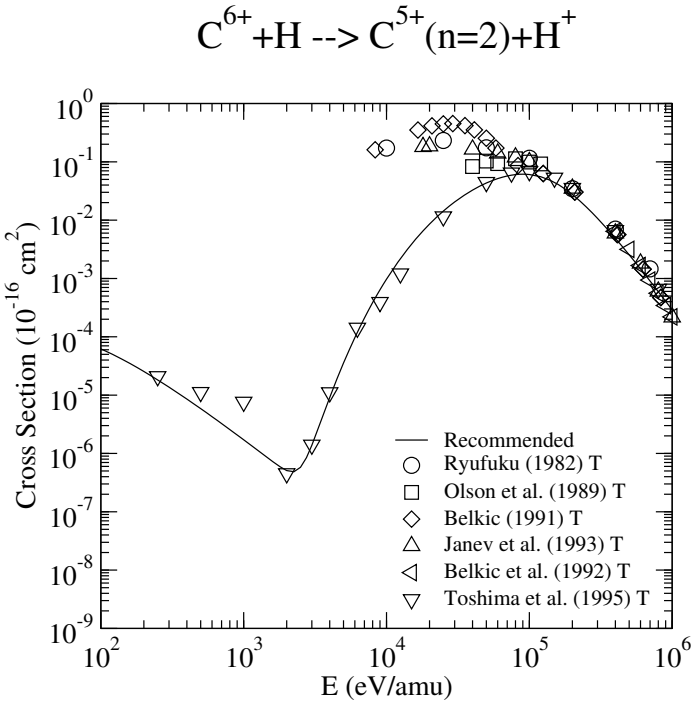

FIG. 142: Cross section for charge exchange.

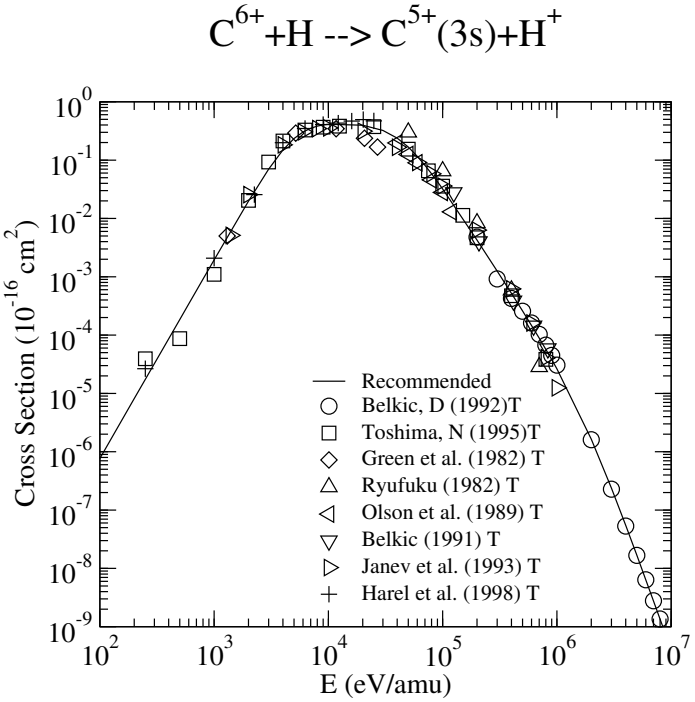

FIG. 143: Cross section for charge exchange.

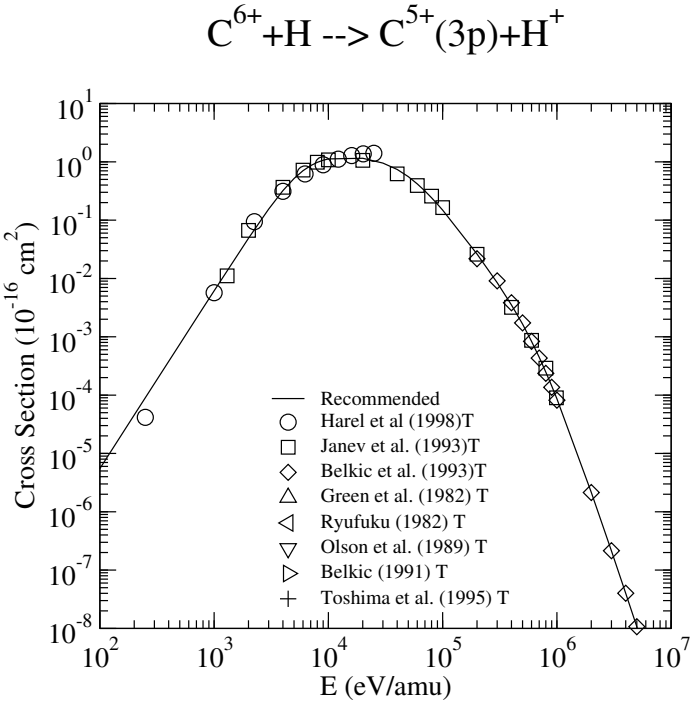

FIG. 144: Cross section for charge exchange.

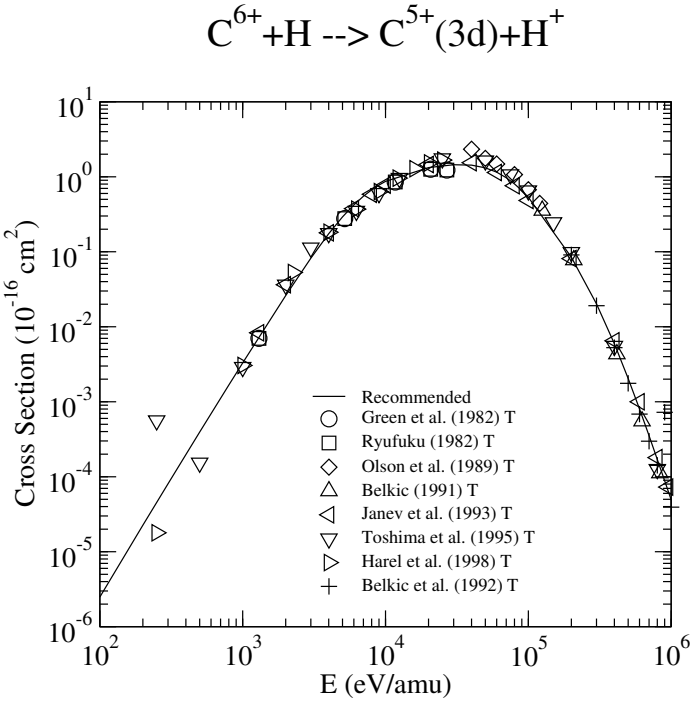

FIG. 145: Cross section for charge exchange.

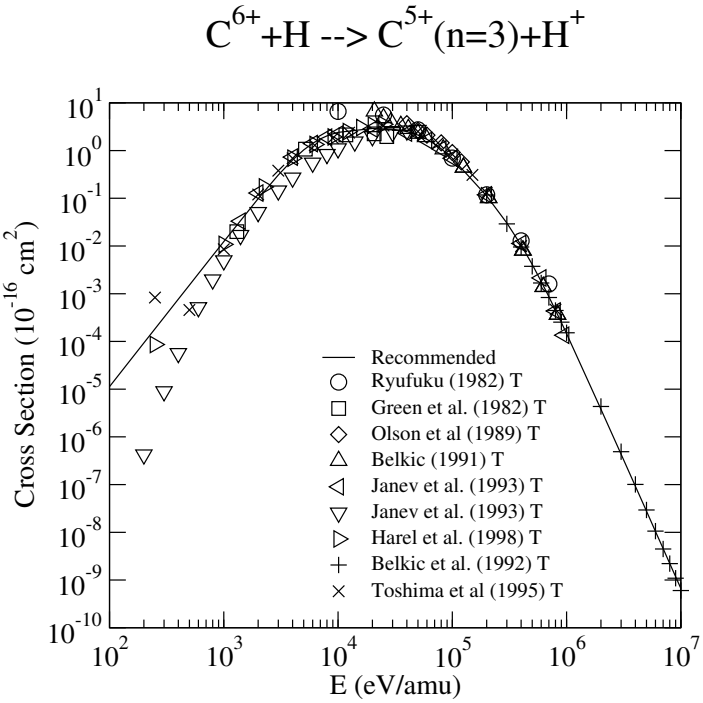

FIG. 146: Cross section for charge exchange.

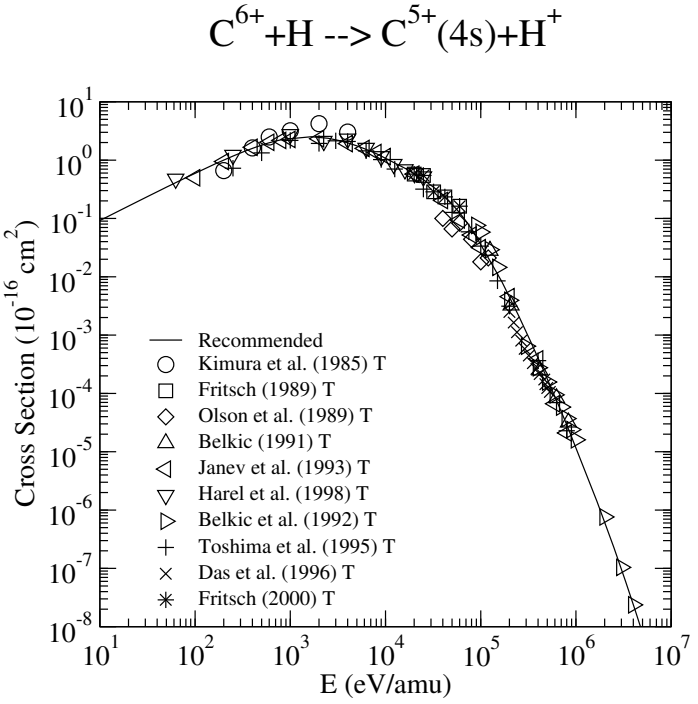

FIG. 147: Cross section for charge exchange.

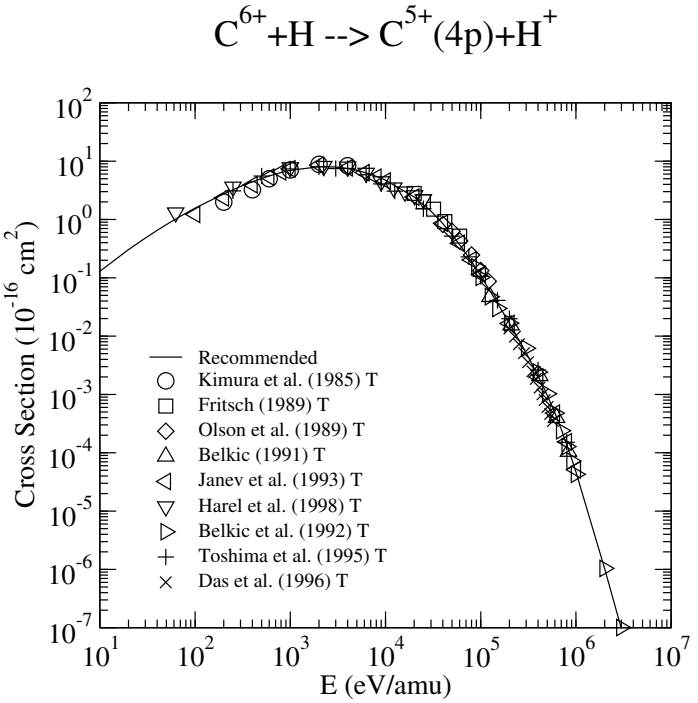

FIG. 148: Cross section for charge exchange.

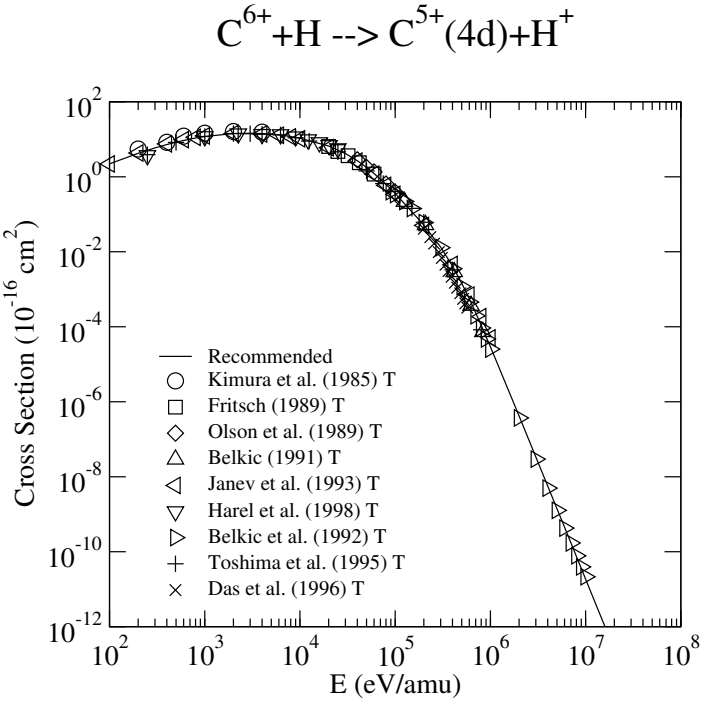

FIG. 149: Cross section for charge exchange.

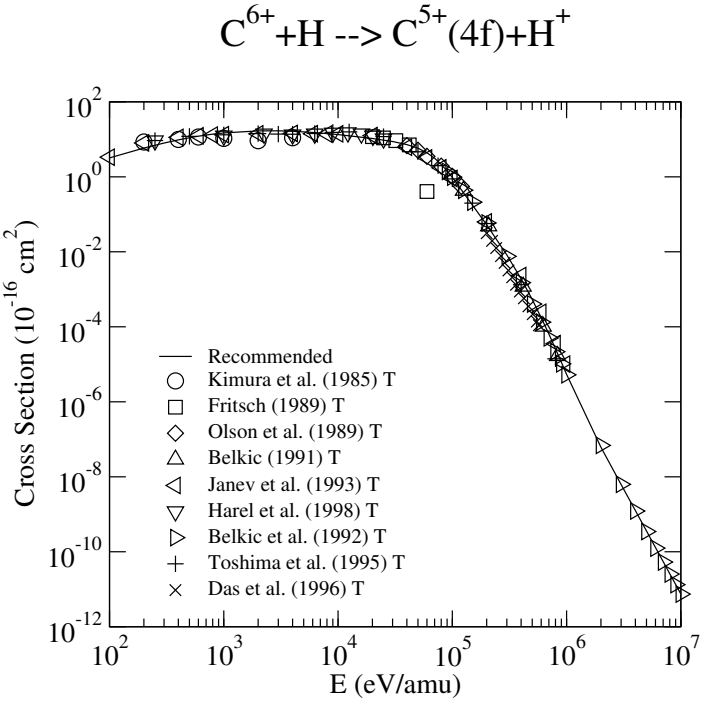

FIG. 150: Cross section for charge exchange.

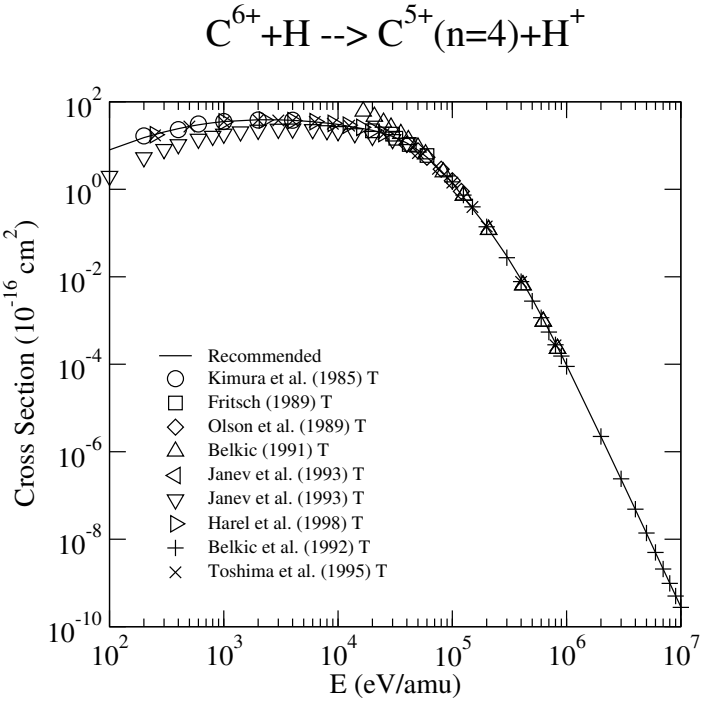

FIG. 151: Cross section for charge exchange.

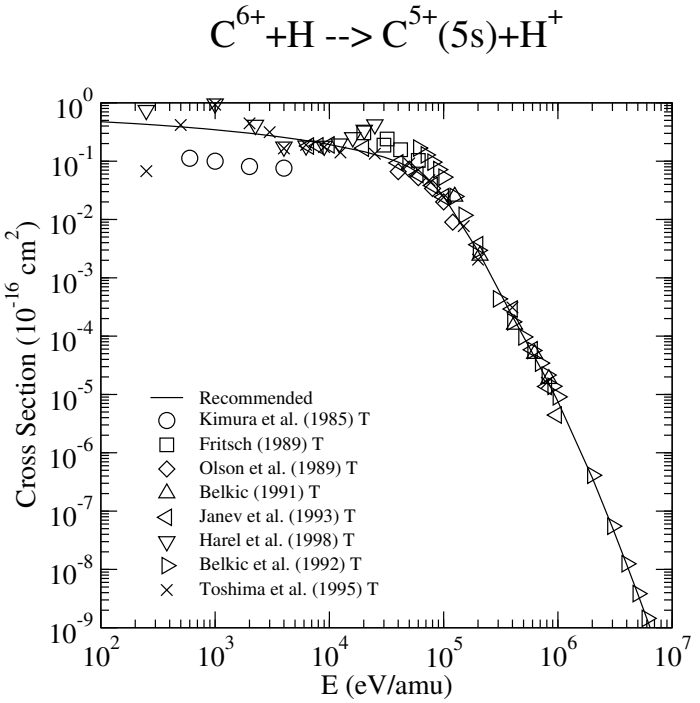

FIG. 152: Cross section for charge exchange.

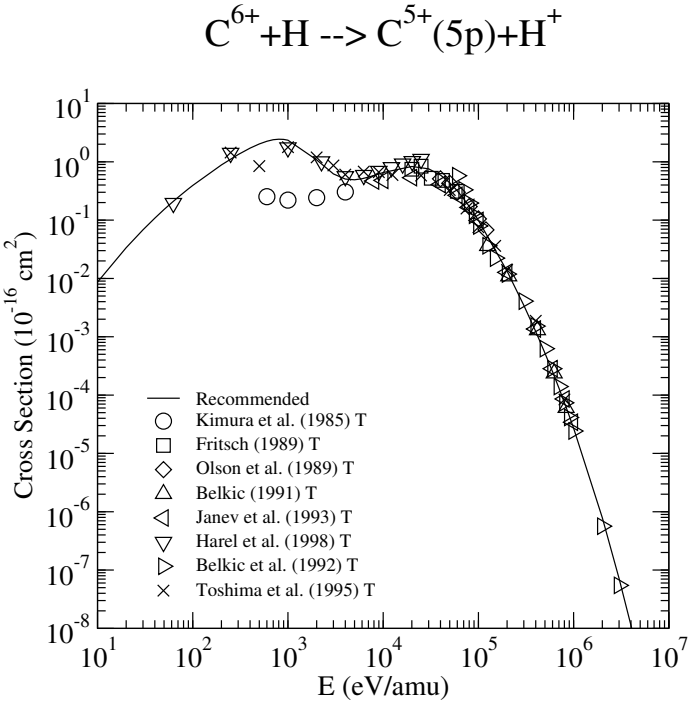

FIG. 153: Cross section for charge exchange.

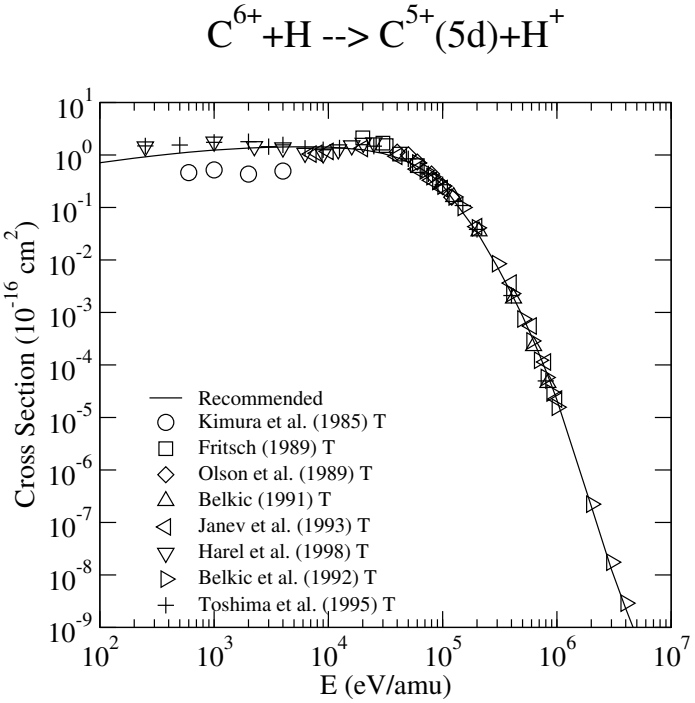

FIG. 154: Cross section for charge exchange.

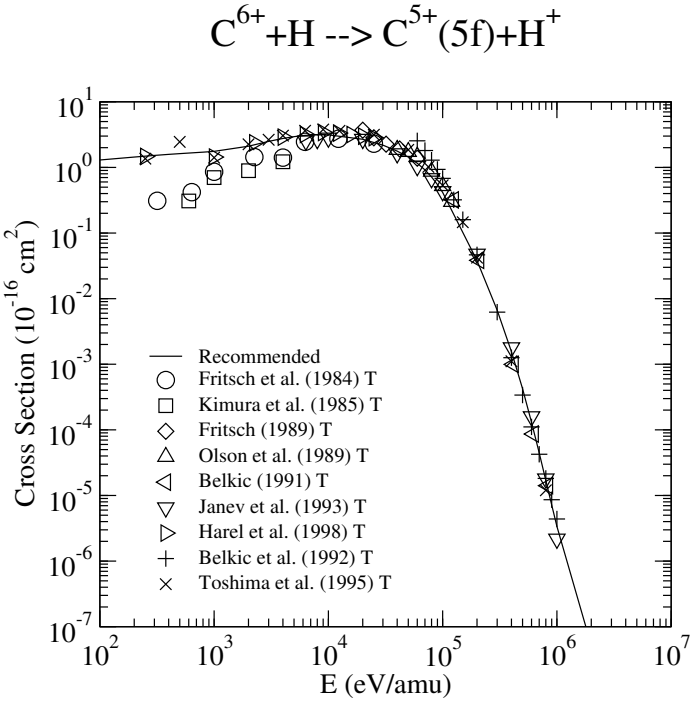

FIG. 155: Cross section for charge exchange.

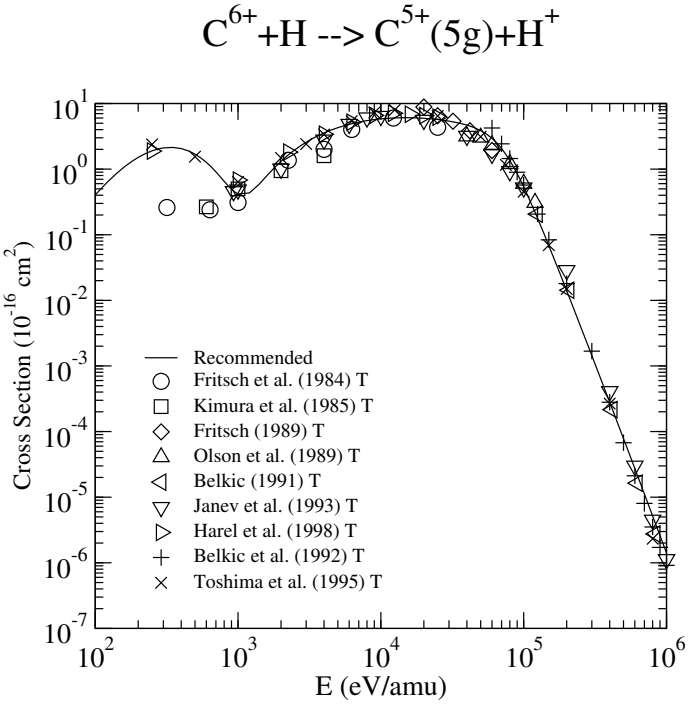

FIG. 156: Cross section for charge exchange.

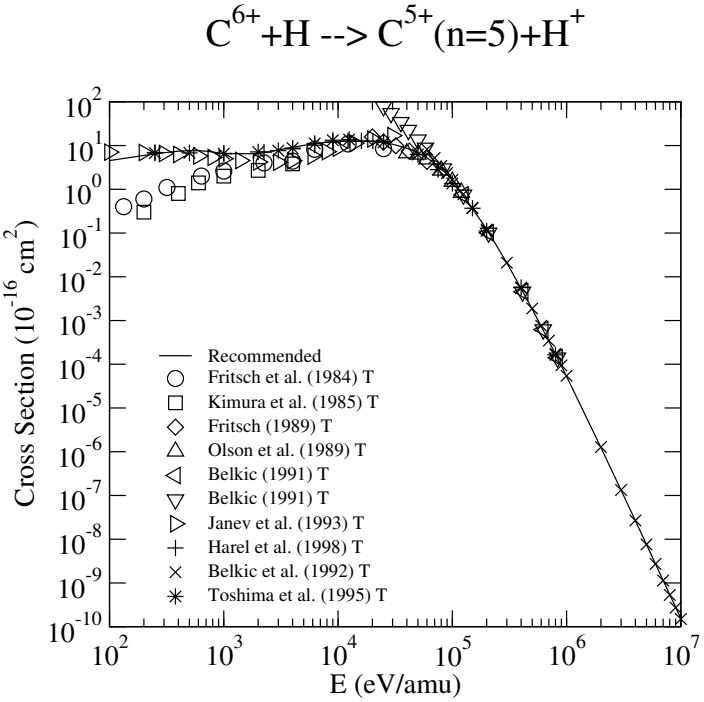

FIG. 157: Cross section for charge exchange.

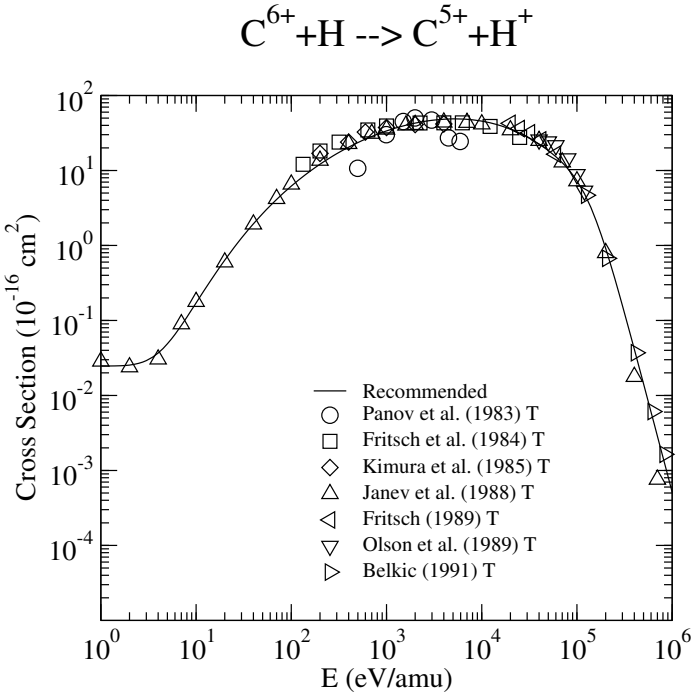

FIG. 158: Cross section for charge exchange.

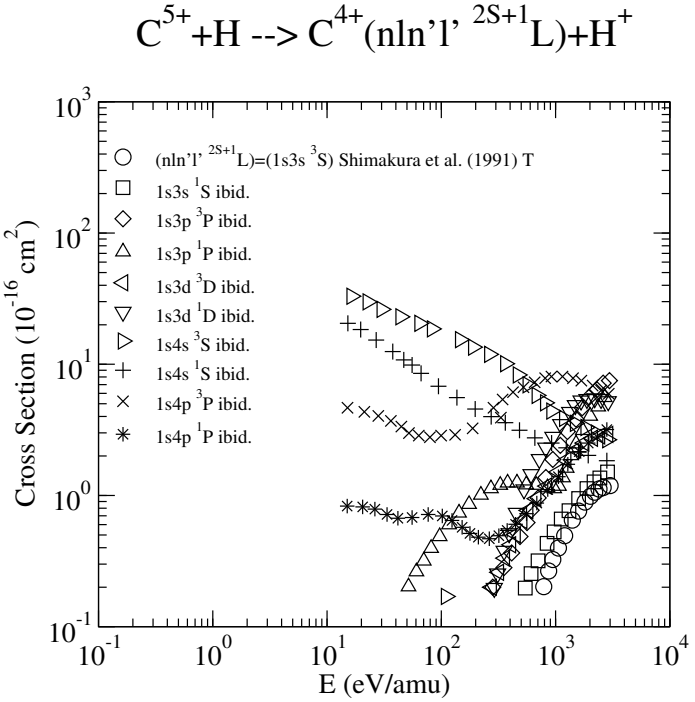

FIG. 159: Cross section for charge exchange.

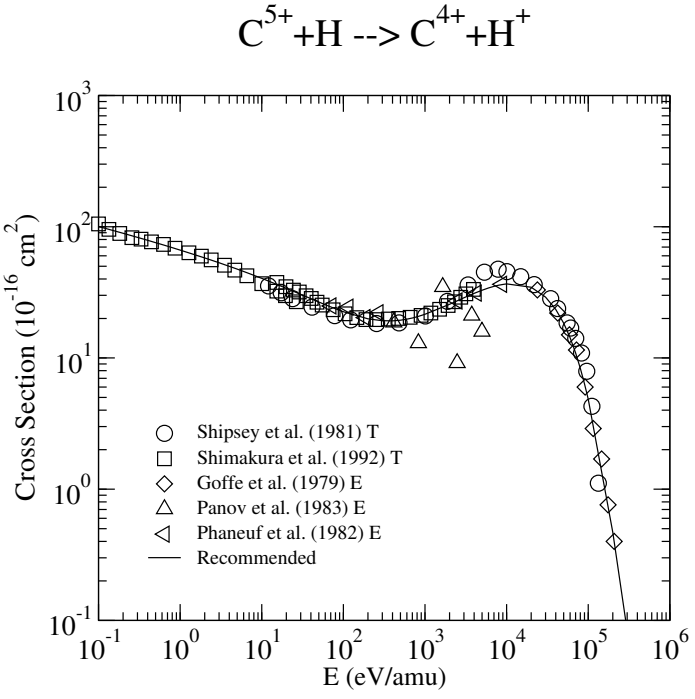

FIG. 160: Cross section for charge exchange.

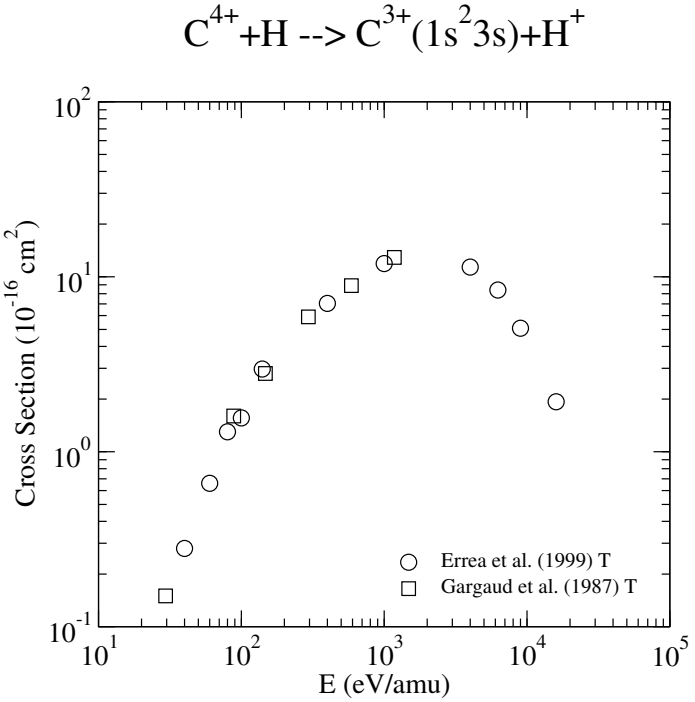

FIG. 161: Cross section for charge exchange.

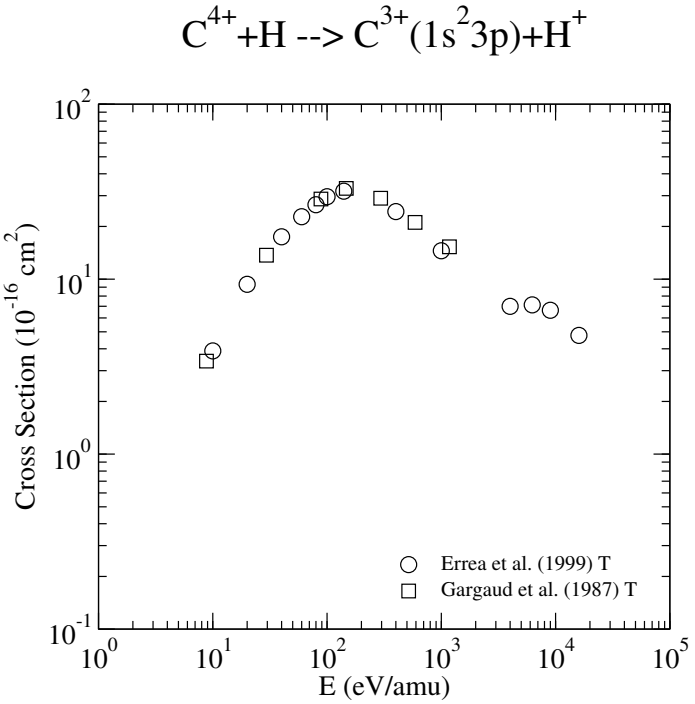

FIG. 162: Cross section for charge exchange.

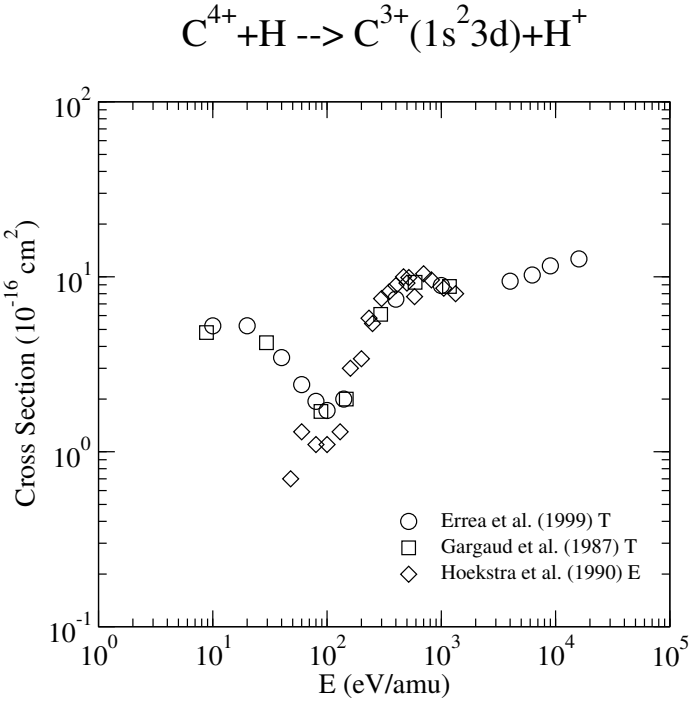

FIG. 163: Cross section for charge exchange.

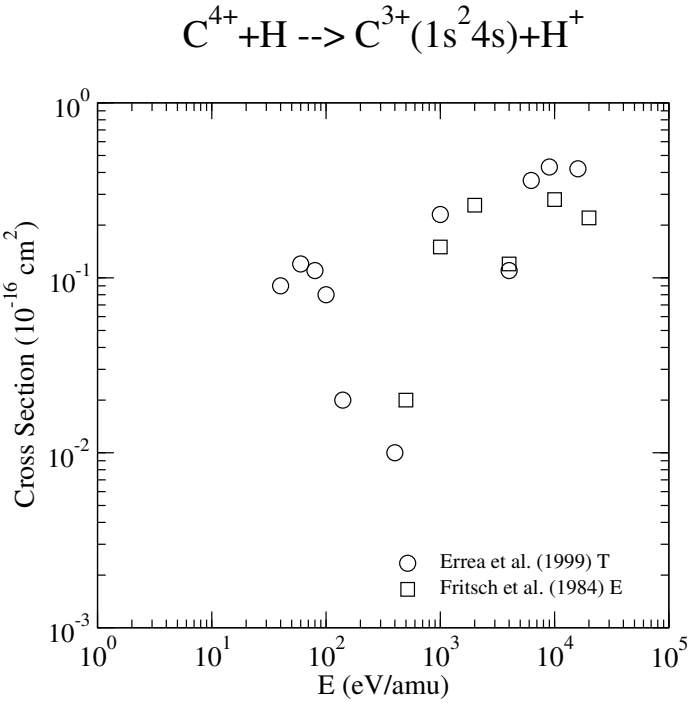

FIG. 164: Cross section for charge exchange.

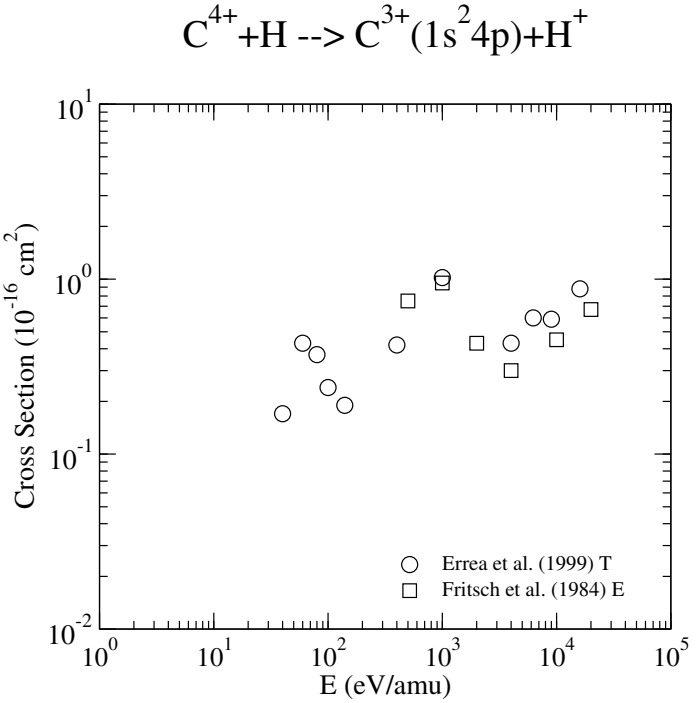

FIG. 165: Cross section for charge exchange.

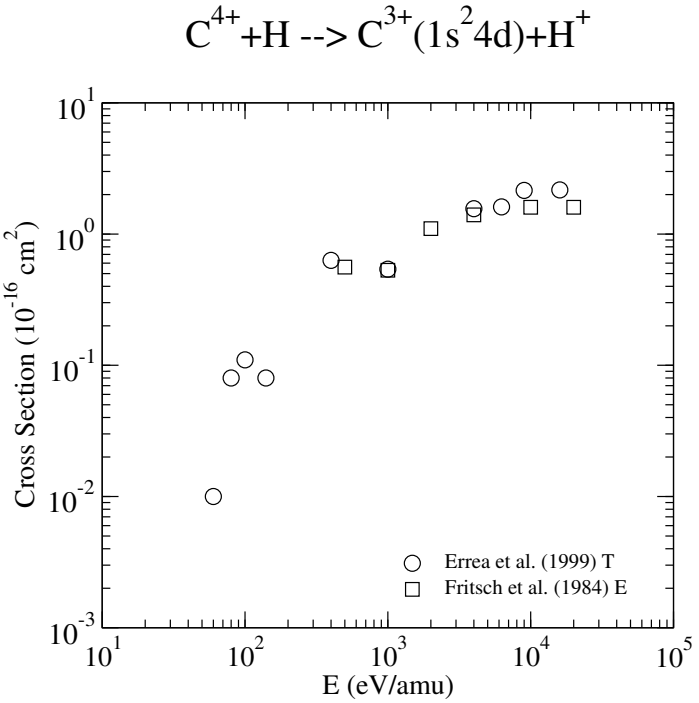

FIG. 166: Cross section for charge exchange.

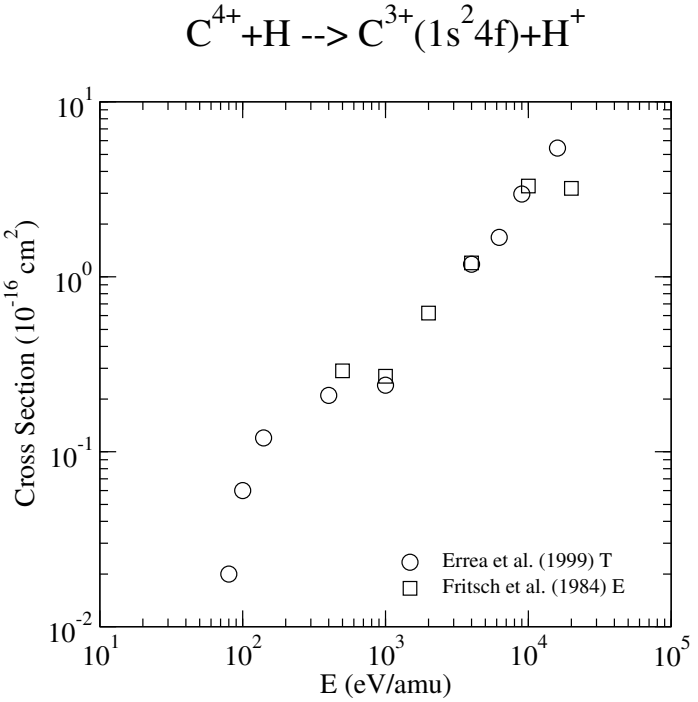

FIG. 167: Cross section for charge exchange.

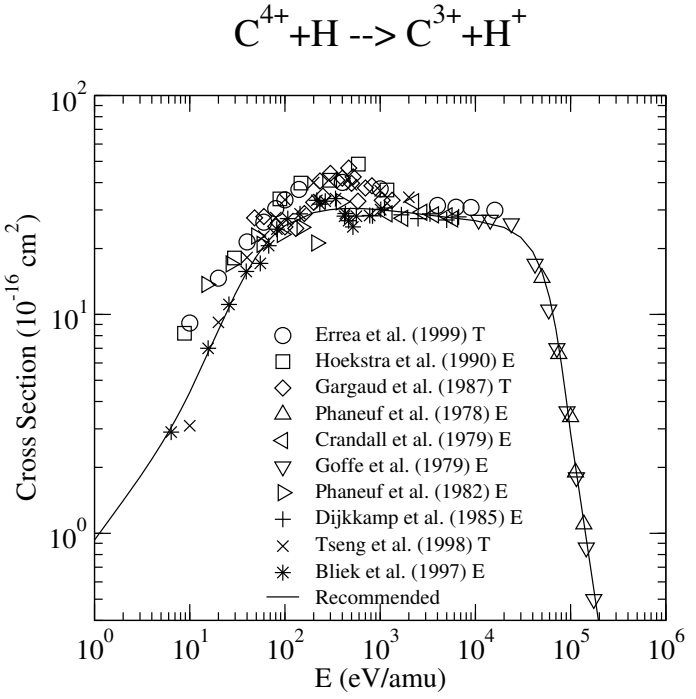

FIG. 168: Cross section for charge exchange.

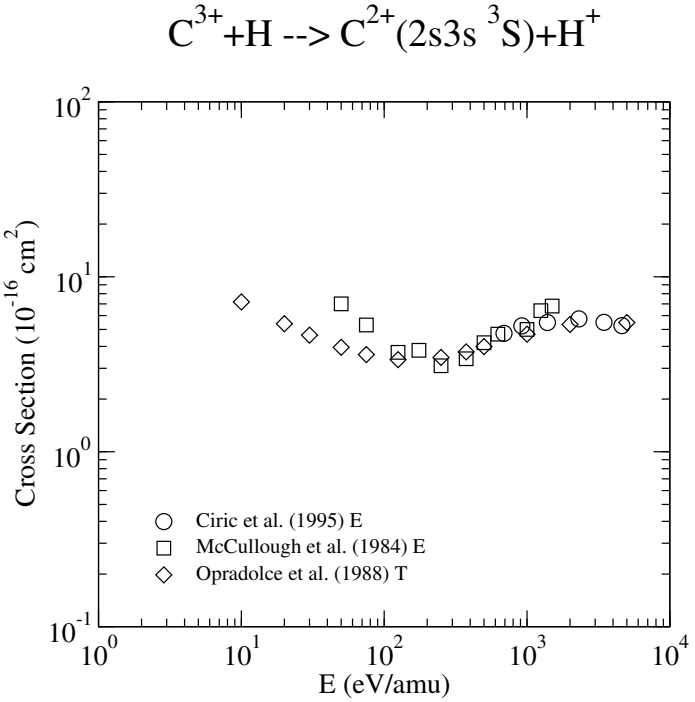

FIG. 169: Cross section for charge exchange.

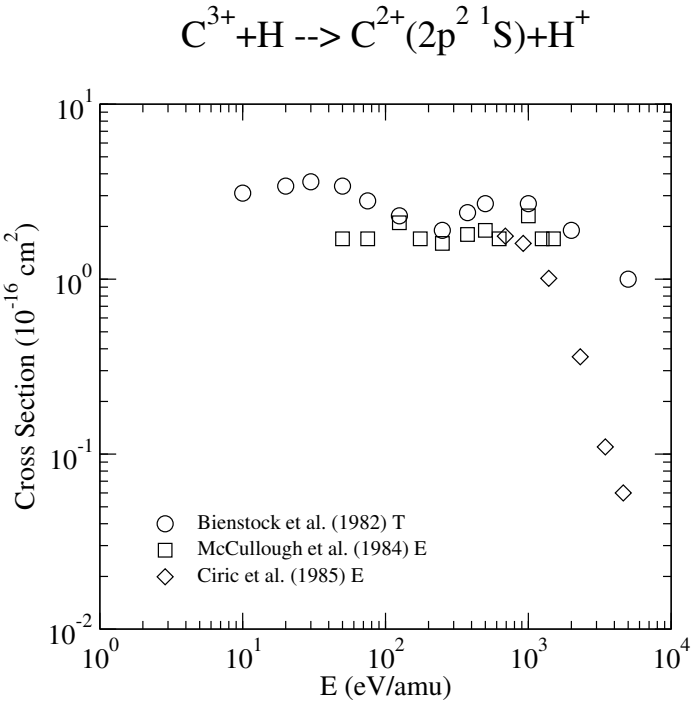

FIG. 170: Cross section for charge exchange.

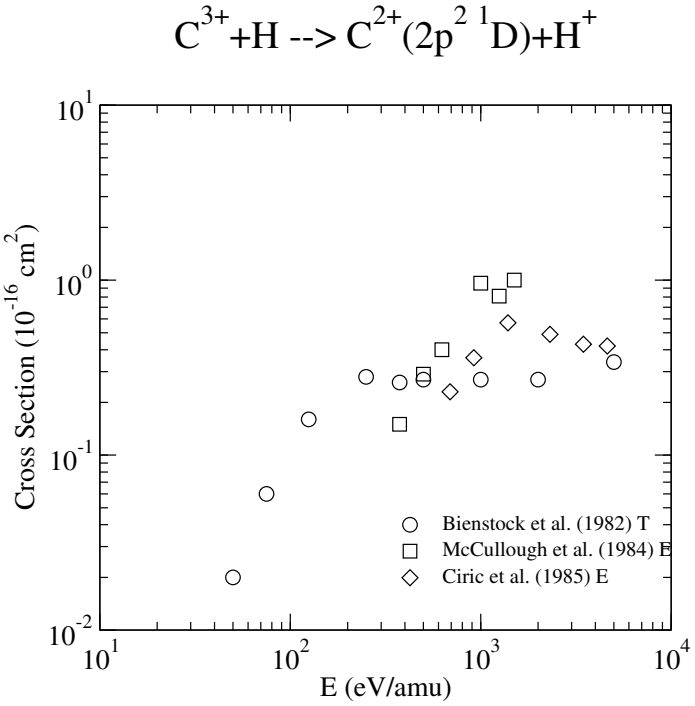

FIG. 171: Cross section for charge exchange.

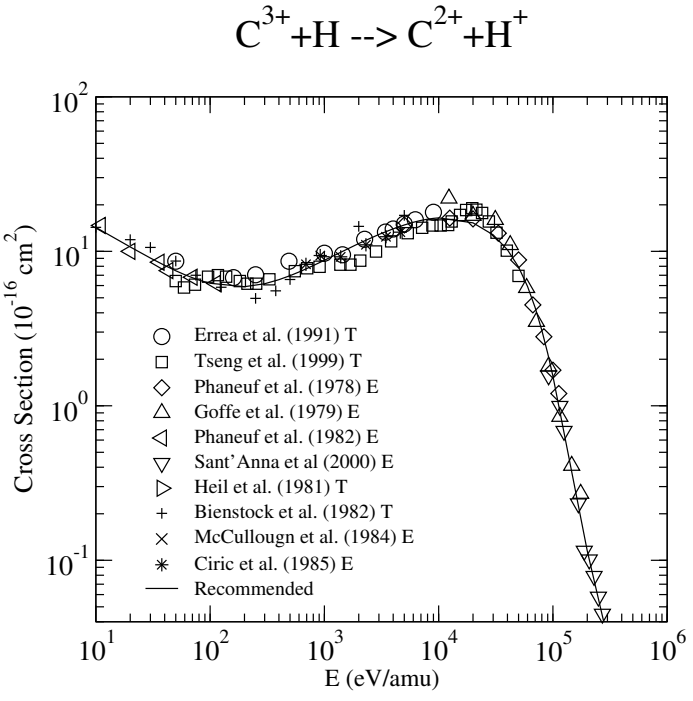

FIG. 172: Cross section for charge exchange.

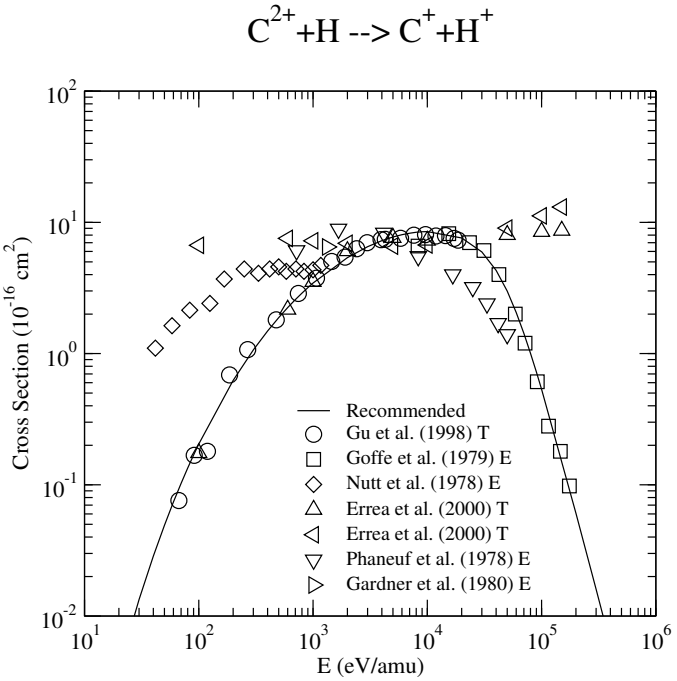

FIG. 173: Cross section for charge exchange.

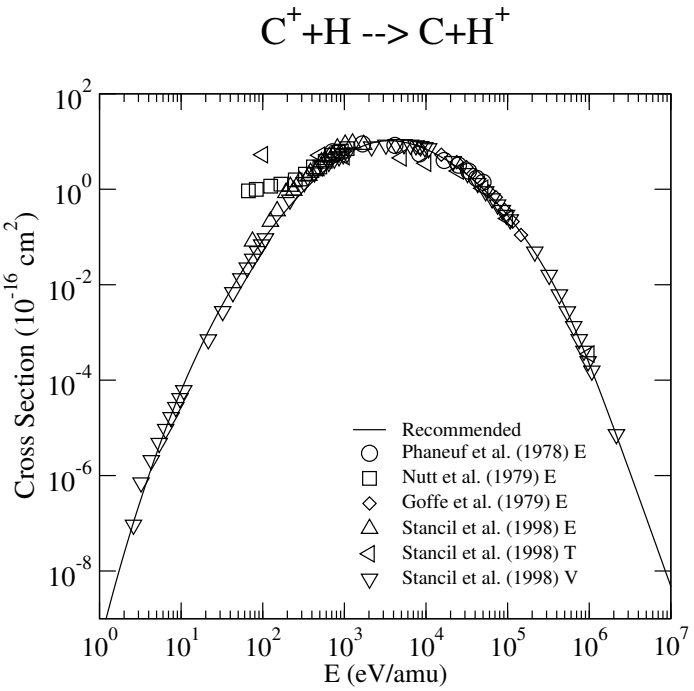

FIG. 174: Cross section for charge exchange.